



**Your Safety • Your Mobility  
Your Economic Opportunity**

**RP 235**

**Calibration of the AASHTOWare Pavement ME  
Design Performance Models for Flexible  
Pavements in Idaho**

By

Fouad Bayomy

Ahmed Muftah

Emad Kassem

University of Idaho

Prepared for

Idaho Transportation Department

Research Program, Contracting Services

Division of Engineering Services

<http://itd.idaho.gov/alt-programs/?target=research-program>

June 2018

**IDAHO TRANSPORTATION DEPARTMENT  
RESEARCH REPORT**

### **Standard Disclaimer**

This document is disseminated under the sponsorship of the Idaho Transportation Department and the United States Department of Transportation in the interest of information exchange. The State of Idaho and the United States Government assume no liability of its contents or use thereof.

The contents of this report reflect the view of the authors, who are responsible for the facts and accuracy of the data presented herein. The contents do not necessarily reflect the official policies of the Idaho Transportation Department or the United States Department of Transportation.

The State of Idaho and the United States Government do not endorse products or manufacturers. Trademarks or manufacturers' names appear herein only because they are considered essential to the object of this document.

***This report does not constitute a standard, specification, or regulation.***

1. Report No. FHWA-ID-18-235	2. Government Accession No.	3. Recipient's Catalog No.	
4. Title and Subtitle Calibration of the AASHTOWare Pavement ME Design Performance Models for Flexible Pavements in Idaho		5. Report Date June 2018	
		6. Performing Organization Code KLK572	
7. Author(s) Fouad Bayomy, Ahmed Muftah, Emad Kassem, Fahmid Tousef, and Hamza Alkuime		8. Performing Organization Report No.	
9. Performing Organization Name and Address University of Idaho Department of Civil Engineering 875 Perimeter Drive MS 1022 Moscow, ID 83844-1022		10. Work Unit No. (TRAIS)	
		11. Contract or Grant No. UI-15-04	
12. Sponsoring Agency Name and Address Idaho Transportation Department (SPR) Division of Highways, Resource Center, Research Program PO Box 7129 Boise, ID 83707-7129		13. Type of Report and Period Covered Final Report 01/01/2016 - 6/30/2018	
		14. Sponsoring Agency Code ITD Report: RP 235	
15. Supplementary Notes Project performed in cooperation with the Idaho Transportation Department and the U.S. Department of Transportation, Federal Highway Administration.			
16. Abstract This project aims at developing local calibration factors for the AASHTOWare Pavement Mechanistic-Empirical Design (PMED) software. The performance models included in the software as released by AASHTO are calibrated from national Long-Term Pavement Performance (LTPP) pavement sites. Hence, the models calibration factors represent averages of national sites across the nation. For specific local conditions, the performance predicted by the models may deviate from the actual performance observed in the pavements due to varied material, climate, traffic and site conditions. Therefore, the Idaho Transportation Department (ITD), in its efforts to implement the new AASHTO pavement design software, launched series of research projects to prepare the required design inputs including materials, traffic and climatic data as required by the new PMED. To calibrate the software for more accurate prediction of asphalt pavement performance in Idaho, local calibration of the models was needed. In this project, researchers of the University of Idaho in cooperation with ITD engineers, identified 32 pavement sites across the state. The sites are selected to represent different geographical, climate and traffic conditions that are mostly prevailing in the state road network. Structural, material and traffic data for all these pavement sites were accumulated and prepared in accordance to the PMED software inputs. Actual performance data were collected from ITD Transportation Asset Management System (TAMS) and from ITD video logs of the selected pavements. The performance predicted by the software was then compared to the actual performance observed in the field as recorded in TAMS over the pavement service lives. With massive amount of software runs and statistical analysis of the results, local calibration factors are developed to represent the best case scenario for performance prediction of asphalt pavements in Idaho. The developed factors were validated using additional nine LTPP sites in Idaho. Furthermore, as part of this project, material testing was performed to populate the ITD material database with creep compliance and indirect tensile properties at low temperatures that were missing in the database. An updated and completed ITD database is developed as well. The information in the database is stored in formats that make it easily accessible and usable by the PMED software.			
17. Key Words Mechanistic-empirical pavement design, asphalt pavements, pavement performance, local calibration, cracking and rutting.		18. Distribution Statement Copies available online at <a href="http://itd.idaho.gov/alt-programs/?target=research-program">http://itd.idaho.gov/alt-programs/?target=research-program</a>	
19. Security Classification (of this report) Unclassified	20. Security Classification (of this page) Unclassified	21. No. of Pages 125	22. Price

**FHWA Form F 1700.7**

## METRIC (SI\*) CONVERSION FACTORS

APPROXIMATE CONVERSIONS TO SI UNITS					APPROXIMATE CONVERSIONS FROM SI UNITS				
Symbol	When You Know	Multiply By	To Find	Symbol	Symbol	When You Know	Multiply By	To Find	Symbol
<u>LENGTH</u>					<u>LENGTH</u>				
in	inches	25.4	millimeters	mm	mm	millimeters	0.039	inches	in
ft	Feet	0.3048	meters	m	m	meters	3.28	feet	ft
yd	yards	0.914	meters	m	m	meters	1.09	yards	yd
mi	miles (statute)	1.61	kilometers	km	km	kilometers	0.621	Miles (statute)	mi
<u>AREA</u>					<u>AREA</u>				
in <sup>2</sup>	square inches	645.2	millimeters squared	cm <sup>2</sup>	mm <sup>2</sup>	millimeters squared	0.0016	square inches	in <sup>2</sup>
ft <sup>2</sup>	square feet	0.0929	meters squared	m <sup>2</sup>	m <sup>2</sup>	meters squared	10.764	square feet	ft <sup>2</sup>
yd <sup>2</sup>	square yards	0.836	meters squared	m <sup>2</sup>	km <sup>2</sup>	kilometers squared	0.39	square miles	mi <sup>2</sup>
mi <sup>2</sup>	square miles	2.59	kilometers squared	km <sup>2</sup>	ha	hectares (10,000 m <sup>2</sup> )	2.471	acres	ac
ac	Acres	0.4046	hectares	ha					
<u>MASS (weight)</u>					<u>MASS (weight)</u>				
oz	ounces (avdp)	28.35	grams	g	g	grams	0.0353	ounces (avdp)	oz
lb	pounds (avdp)	0.454	kilograms	kg	kg	kilograms	2.205	pounds (avdp)	lb
T	short tons (2000 lb)	0.907	megagrams	mg	mg	megagrams (1000 kg)	1.103	short tons	T
<u>VOLUME</u>					<u>VOLUME</u>				
fl oz	fluid ounces (US)	29.57	milliliters	mL	mL	milliliters	0.034	fluid ounces (US)	fl oz
gal	Gallons (liq)	3.785	liters	liters	liters	liters	0.264	Gallons (liq)	gal
ft <sup>3</sup>	cubic feet	0.0283	meters cubed	m <sup>3</sup>	m <sup>3</sup>	meters cubed	35.315	cubic feet	ft <sup>3</sup>
yd <sup>3</sup>	cubic yards	0.765	meters cubed	m <sup>3</sup>	m <sup>3</sup>	meters cubed	1.308	cubic yards	yd <sup>3</sup>
Note: Volumes greater than 1000 L shall be shown in m <sup>3</sup>									
<u>TEMPERATURE (exact)</u>					<u>TEMPERATURE (exact)</u>				
°F	Fahrenheit temperature	5/9 (°F-32)	Celsius temperature	°C	°C	Celsius temperature	9/5 °C+32	Fahrenheit temperature	°F
<u>ILLUMINATION</u>					<u>ILLUMINATION</u>				
fc	foot-candles	10.76	lux	lx	lx	lux	0.0929	foot-candles	fc
fl	foot-lamberts	3.426	candela/m <sup>2</sup>	cd/cm <sup>2</sup>	lx	lux	0.2919	foot-lamberts	fl
<u>FORCE and PRESSURE or STRESS</u>					<u>FORCE and PRESSURE or STRESS</u>				
lbf	pound-force	4.45	newtons	N	N	newtons	0.225	pound-force	lbf
psi	pound-force per square inch	6.89	kilopascals	kPa	kPa	kilopascals	0.145	pound-force per square inch	psi

---

## Acknowledgements

This project is funded by Idaho Transportation Department (ITD) from SPR funds. It is performed in cooperation with ITD. The authors would like to acknowledge all members of the research project Technical Advisory Committee (TAC) for their valuable feedback and cooperation all over the project tasks. The authors would like to thank many professionals at ITD for their technical help and feedback. The authors also would like to acknowledge the work and support of many individuals at the University of Idaho who participated in the completion of this project. Graduate students Hamza Alkuime, Fahmid Tousif and Mumtahn Hasnat worked on the laboratory testing of creep compliance and Indirect Tension tests, Video Logs data analysis and the development of the performance database. Their efforts are acknowledged and greatly appreciated. The authors also acknowledge and appreciate all the support provided by the administrative staff at the National Institute of Advanced Transportation Technology (NIATT) at the University of Idaho.

The cooperation and support provided by the Washington State University (WSU) is also acknowledged. Major part of Task 4 (Development of Creep Compliance Data) was performed at WSU by Mr. Amir Bahadori, a graduate student, under the supervision of Professor Haifang Win. Their cooperation and timely delivery is greatly appreciated.

At last, but not least, special thanks are due to Dr. Linda Pierce for her critical review and invaluable suggestions and feedback. Dr. Pierce not only served as the peer reviewer of the report, but also contributed significantly to the technical editing of the report. The authors greatly appreciate her efforts and timely review.

## Technical Advisory Committee

Each research project is overseen by a technical advisory committee (TAC), which is led by an ITD project sponsor and project manager. The Technical Advisory Committee (TAC) is responsible for monitoring project progress, reviewing deliverables, ensuring that study objective are met, and facilitating implementation of research recommendations, as appropriate. ITD's Research Program Manager appreciates the work of the following TAC members in guiding this research study.

**Project Sponsor** – John Bilderback, P.E.

**Project Manager** – Mike Santi, P.E.

### **TAC Members**

John Arambarri, P.E.

Chad Clawson, P.E.

James Poorbaugh, P.E.

Mark Wheeler, P.E.

**FHWA-Idaho Advisor** – Kyle Holman, P.E.



---

# Table of Contents

Executive Summary.....	xiii
Introduction.....	xiii
Research Methodology.....	xiii
Key Findings.....	xiii
Recommendations.....	xiv
Chapter 1 Introduction.....	1
Background.....	1
Problem Statement .....	1
Scope of Research and Project Tasks .....	2
Report Organization .....	4
Chapter 2 Review of the PMED Distress Prediction Models for Flexible Pavements .....	7
Performance Indicators .....	7
Alligator Cracking (Bottom-Up Cracking) .....	7
Longitudinal Cracking (Top-down Cracking) .....	7
Thermal Transverse Cracking.....	7
Transverse Reflection Cracking.....	8
Rutting.....	8
International Roughness Index (IRI).....	8
Performance Models in the PMED Software.....	8
AC Rutting Prediction Model .....	9
Rutting Prediction Model for Unbound Materials and Subgrade Soil .....	10
Load Associated Cracking Prediction Models .....	12
Non-Load Associated Transverse Cracking Prediction Model .....	17
Reflection Cracking in AC Overlays .....	18
Smoothness Prediction Model.....	19
PMED Calibration and Implementation Efforts by State DOTs .....	20
Arizona .....	21
California.....	22
Montana.....	22
Nevada .....	23
Oregon .....	23
Utah.....	24

---

Washington.....	25
Wyoming.....	26
State DOT PMED Implementation Summary.....	27
Chapter 3 Development of PMED Calibration Coefficients for Idaho.....	33
Procedures of the MEPDG Guide for Local Calibration.....	34
Idaho Local Calibration Procedures.....	36
Hierarchical Input Level Selection for Each Input Parameter.....	36
Develop Local Experimental Plan and Sampling Template (Matrix).....	44
Estimate Sample Size for Specific Distress Prediction Models.....	45
Roadway Segments Selection.....	47
Extract and Evaluate Distress Project Data.....	50
Conduct Field and Forensic Investigations.....	54
Assess Local Bias: Validation of Global Calibration Values to Local Conditions, Polices, and Materials.....	56
Eliminate Local Bias of Distress and IRI Prediction Models.....	58
Assess the Standard Error of the Estimate.....	58
Reduce Standard Error of the Estimate.....	59
Results of Calibration of Performance Models.....	59
Rutting Models.....	59
Longitudinal (Top-Down) Cracking Model.....	64
Alligator (Bottom-Up) Cracking Model.....	65
Thermal (Transverse) Cracking Model.....	65
International Roughness Index Model.....	65
Chapter 4 Validation of the Developed Calibration Coefficients.....	69
Chapter 5 Summary, Conclusions, and Recommendations.....	77
Summary.....	77
Conclusions.....	78
Recommendations.....	79
References.....	81
Appendix A Updated PMED Database to Include Creep Compliance and IDT Data (e-file).....	85
Appendix B Performance Database.....	105



---

## List of Tables

Table 1 Arizona Local Calibration Coefficients <sup>(14)</sup> .....	22
Table 2 Montana Local Calibration Coefficients <sup>(16)</sup> .....	23
Table 3 Oregon Local Calibration Coefficients <sup>(21)</sup> .....	24
Table 4 Utah Local Calibration Coefficients <sup>(22)</sup> .....	25
Table 5 Washington State Local Calibration Coefficients <sup>(23)</sup> .....	26
Table 6 Wyoming Local Calibration Coefficients <sup>(6)</sup> .....	27
Table 7 Summary of Local Calibration Coefficients for Rutting .....	28
Table 8 Summary of Calibration Coefficients for Fatigue Cracking .....	29
Table 9 Summary of Local Calibration Coefficients for Transverse Cracking.....	30
Table 10 Summary of Local Calibration Coefficients for IRI.....	31
Table 11 Required Flexible Pavement Input Parameters <sup>(3,5)</sup> .....	37
Table 12 Example of Sensitivity Analysis Effective Binder Content and Distress Prediction.....	39
Table 13 Summary of Very Significant to Significant Key Design Input Parameters for New Flexible Pavements <sup>(4)</sup> .....	40
Table 14 Summary of Received Field Cores Based on Mix Type and Asphalt Binder .....	43
Table 15 Creep Compliance Test Results for Mix (KN13823),(1/psi) .....	44
Table 16 IDT Test Results for Mix (KN13823),(psi).....	44
Table 17 Local Experimental Plan and Sampling Template .....	45
Table 18 Minimum Recommended Number of Pavement Sections for Local Calibration .....	47
Table 19 List of the Roadway Segments Selected for Local Calibration .....	48
Table 20 Asphalt and Rigid Pavement Cracking Types Collected in Idaho .....	50
Table 21 Comparison between ITD and PMED Flexible Pavement Distresses .....	51
Table 22 Cracks Types, Extent, and Severity Level .....	52
Table 23 Summary of Statistical Analysis of Predicted vs. Measured Distress Using the Global Calibration Coefficients .....	57
Table 24 Calibration Parameters to Adjust to Eliminate Bias <sup>(3,5)</sup> .....	58
Table 25 Calibration Parameters to Adjust to Reduce the Standard Error <sup>(3,5)</sup> .....	59
Table 26 Calibration Coefficients for AC Layer Rutting.....	60

---

Table 27 Calibration Coefficients for Base Layer Rutting.....	61
Table 28 Calibration Coefficients for Subgrade Rutting.....	62
Table 29 Calibration Coefficients for Rutting.....	63
Table 30 Calibration Coefficients for Longitudinal Cracking.....	65
Table 31 Calibration Coefficients for Alligator Cracking .....	66
Table 32 Calibration Coefficients for Thermal Cracking .....	67
Table 33 Calibration Coefficients for IRI .....	68
Table 34 Local Calibration Coefficients for AC Rutting .....	70
Table 35 Local Calibration Coefficients for Base Layer Rutting .....	71
Table 36 Local Calibration Coefficients for Subgrade Rutting .....	71
Table 37 Local Calibration Coefficients for Total Rutting .....	72
Table 38 Local Calibration Coefficients for Alligator Cracking.....	73
Table 39 Local Calibration Coefficients for Longitudinal Cracking.....	73
Table 40 Local Calibration Coefficients for Thermal Cracking .....	74
Table 41 Calibration Coefficients for IRI .....	75
Table 42 Summary of Calibration Coefficients Before and After Local Calibration.....	77

---

## List of Figures

Figure 1 AC Rutting Prediction Model .....	9
Figure 2 Rutting Prediction Equations for Unbound Materials and Subgrade Soil.....	10
Figure 3 Comparison of Measured and Predicted Total Rutting Resulting from Global Calibration <sup>(11)</sup> .....	11
Figure 4 Standard Error Equations for the Rutting Models .....	11
Figure 5 PMED Equations for the Allowable Number of Traffic Repetitions to Fatigue Damage.....	12
Figure 6 PMED Equation for the Damage Ratio.....	13
Figure 7 Bottom-Up Cracking Transfer Function .....	13
Figure 8 Comparison of Cumulative Fatigue Damage and Measured Alligator Cracking Resulting from Global Calibration Process <sup>(11)</sup> .....	14
Figure 9 Comparison of Cumulative Fatigue Damage and Measured Alligator Cracking Resulting from Global Calibration Process <sup>(11)</sup> .....	14
Figure 10 Top-Down Transfer Function .....	15
Figure 11 Standard Error Equations for Bottom-Up and Top-Down Cracking.....	15
Figure 12 Fatigue Cracking Prediction Model for CTB Layers.....	16
Figure 13 CTB Layer Damaged Modulus Equation.....	17
Figure 14 PMED Thermal Cracking Model .....	17
Figure 15 Standard Error Equations for the Thermal Cracking.....	17
Figure 16 Paris Law for Crack Propagation .....	18
Figure 17 Reflection Cracking Model in AC Overlays.....	19
Figure 18 Smoothness Prediction Model.....	20
Figure 19 Summary of Agency PMED Implementation <sup>(12)</sup> .....	21
Figure 20 Target Analogy for Precision and Accuracy <sup>(32)</sup> .....	33
Figure 21 Improvement of Bias and Precision through Local Calibration <sup>(34)</sup> .....	34
Figure 22 Summary of Sensitivity Analysis and Input Effect on Rutting .....	40
Figure 23 Example of Road Segment Input Data .....	42
Figure 24 Estimation of Minimum Sample Size .....	46
Figure 25 Geographical Locations of the Selected Road Segments for Local Calibration .....	49
Figure 26 Example of Extracted Images of the Video-Based Distress Data Collection.....	53

---

Figure 27 Example of Data Sheet for Cracking Analysis Using PathView Video Images.....	54
Figure 28 Plan of SH008 Trench Locations.....	55
Figure 29 Trench Side View.....	55
Figure 30 Example of Trench Rut Depth Measurements on SH008 .....	56
Figure 31 Distress Indictors (Rutting and IRI) with the Null Hypothesis Test .....	57
Figure 32 Measured vs. Predicted AC Rutting Using Global Calibration Coefficients .....	60
Figure 33 Measured vs. Predicted AC Rutting Using Local Calibration Coefficients.....	60
Figure 34 Measured vs. Predicted Granular Base Rutting Using Global Calibration Coefficients .....	61
Figure 35 Measured vs. Predicted Granular Base Rutting Using Local Calibration Coefficients .....	61
Figure 36 Measured vs. Predicted Subgrade Rutting Using Global Calibration Coefficients.....	62
Figure 37 Measured vs. Predicted Subgrade Rutting Using Local Calibration Coefficients.....	62
Figure 38 Measured vs. Predicted Total Rutting Using Global Calibration Coefficients.....	63
Figure 39 Measured vs. Predicted Total Rutting Using Local Calibration Coefficients.....	63
Figure 40 Measured vs. Predicted Longitudinal Cracking Using Global Calibration Coefficients.....	64
Figure 41 Measured vs. Predicted Longitudinal Cracking Using Local Calibration Coefficients.....	64
Figure 42 Measured vs. Predicted Alligator Cracking Using Global Calibration Coefficients .....	66
Figure 43 Measured vs. Predicted Alligator Cracking Using Local Calibration Coefficients .....	66
Figure 44 Measured vs. Predicted Transverse Cracking Using Global Calibration Coefficients .....	67
Figure 45 Measured vs. Predicted Transverse Cracking Using Local Calibration Coefficients .....	67
Figure 46 Measured vs. Predicted IRI Using Global Calibration Coefficients .....	68
Figure 47 Measured vs. Predicted IRI using Local Calibration Coefficients .....	68
Figure 48 Measured vs. Predicted AC Using Local Calibration Coefficients .....	70
Figure 49 Measured vs. Predicted Base Layer Rutting Using Local Calibration Coefficients.....	70
Figure 50 Measured vs. Predicted Subbase Layer Rutting Using Local Calibration Coefficients.....	71
Figure 51 Measured vs. Predicted Total Rutting Using Local Calibration Coefficients.....	72
Figure 52 Measured vs. Predicted Alligator Cracking Using Local Calibration Coefficients .....	72
Figure 53 Measured vs. Predicted Longitudinal Cracking Using Local Calibration Coefficients.....	73
Figure 54 Measured vs. Predicted Thermal Cracking Using Local Calibration Coefficients.....	74
Figure 55 Measured vs. Predicted IRI Using Local Calibration Coefficients.....	74

---

## List of Acronyms

AADT	Annual average daily traffic
AADTT	Annual average daily truck traffic
AASHO	American Association of State Highway Officials
AASHTO	American Association of State Highway and Transportation Officials
AC	Asphalt concrete
CBR	California Bearing Ratio CBR
CC	Creep compliance
CI	Cracking Index
DOT	Department of Transportation
E*	Dynamic Modulus
EICM	Enhanced integrated climatic model
ESAL	Equivalent single axle load
FHWA	Federal Highway Agency
HMA	Hot mix asphalt
IDT	Indirect tensile test
ITD	Idaho Transportation Department
IRI	International Roughness Index
JMF	Job mix formula
JPCP	Jointed plain concrete pavement
LTPP	Long Term Pavement Performance
MAF	Monthly adjustment factor
ME	Mechanistic-empirical
MEPDG	Mechanistic-Empirical Pavement Design Guide
MR	Resilient modulus
NCHRP	National Cooperative Highway Research Program
NMAS	Nominal maximum aggregate size
PG	Performance grade
PMED	AASHTOWare Pavement ME Design™ software
PPMIS	ITD Pavement Performance Management Information System
S <sub>e</sub>	Standard Error
SP-#	Superpave Mix-#
TAMS	Transportation Asset Management System
VCD	Vehicle class distribution
VFA	Voids filled with asphalt
VMA	Voids in mineral aggregate
WIM	Weigh-in-motion



# Executive Summary

## Introduction

This report summarizes findings from research conducted for the Idaho Transportation Department (ITD). The study objective included developing a detailed, statistically sound, and practical experimental plan for validating, and potentially calibrating, the AASHTOWare Pavement ME Design™ (PMED) asphalt pavement performance models to Idaho conditions. The validation and calibration process involved laboratory testing to determine the asphalt Concrete materials properties, conducting PMED analysis based on globally-calibrated performance prediction models, and comparing the results to local performance observations. A statistical comparison of results indicated the PMED asphalt pavement performance models, using the global calibration coefficients, did not reflect Idaho conditions. Therefore, recalibration was recommended and local calibration coefficients were determined.

## Research Methodology

The PMED is a comprehensive tool for the analysis and design of new and rehabilitated flexible and rigid pavement structures based on mechanistic-empirical (ME) principles. The PMED pavement performance prediction models are based on globally-calibrated models and may not necessarily reflect pavement performance in Idaho. Therefore, it is essential to evaluate, validate, and if necessary calibrate, the PMED pavement performance prediction models to local conditions. In 2009, ITD initiated a major effort toward the implementation of the PMED. The main focus of the implementation was to establish a comprehensive material, traffic, and climatic input database. Under a separate study, an implementation plan and design guide to help ITD personnel with implementing the PMED was developed. The research effort discussed in this report is the last phase toward successful implementation of the PMED based on Idaho conditions. The calibration and validation of the performance models was conducted per the American Association of State Highway and Transportation Officials (AASHTO) *Guide for the Local Calibration of the Mechanistic-Empirical Pavement Design Guide*<sup>(3)</sup> and the *Road Map for Implementing The AASHTO Pavement ME Design Software for the Idaho Transportation Department, ITD project RP211A*.<sup>(5)</sup>

## Key Findings

- The globally-calibrated PMED rutting model overestimates the total (accumulated) rutting as compared to field-measured values. The rutting model was locally-calibrated to improve the prediction, with less bias and errors.
- The globally-calibrated alligator (bottom-up) cracking model provides reasonable predictions for Idaho conditions.

- The globally-calibrated longitudinal (top-down) cracking model provides poor predictions with high bias and standard error. The locally-calibrated coefficients reduced the bias and the error; however, there is still a statistically significant difference between the observed and predicted cracking. Many studies recommend that the longitudinal cracking model should only be used for experimental/informational purposes, the longitudinal cracking model is currently undergoing refinement as part of National Highway Research Cooperative (NCHRP) Project 1-52, *A Mechanistic-Empirical Model for Top-Down Cracking of Asphalt Pavement Layers*.
- The globally-calibrated thermal cracking model under predicts thermal cracking as compared to field-measured values. Therefore, the thermal cracking model was calibrated, and the results showed significant improvement in the model prediction with less bias and error.
- The reflective cracking model was not calibrated due to lack of data on field-measured reflective cracking.
- The semi-rigid fatigue cracking model was not calibrated in this study. All pavement sections selected for the calibration effort excluded AC over jointed plain concrete pavement (JPCP) sections. Also, for sections with cement treated base, there was no field-observed fatigue cracking. For these reasons, the research team was unable to calibrate the semi-rigid fatigue cracking model.

## Recommendations

- The calibration of the PMED pavement performance prediction models is a continual process. The local calibration effort should result in models with reasonable bias between predicted and observed models. As additional years of performance data are obtained, and as new models are added and existing models are revised, recalibration may be warranted.
- Ongoing and future work that examines and assesses PMED pavement performance prediction models and software updates should continue to be monitored. The pavement performance database developed in this study provides the needed data to evaluate future PMED performance prediction model updates.
- At this time, the PMED longitudinal (top-down) cracking model should only be used for experimental or informational purposes.
- Some of the challenges identified in this study were the lack of observed pavement distress, limited range of distress values, and shorter pavement service life. Therefore, the research team recommends monitoring the sections used in the calibration effort until the next major rehabilitation project.
- ITD, through preventive maintenance, applies seal coats on many major pavement sections. The seal coat application limits the observation of distresses in the field, which may lead to an inaccurate



assessment of pavement performance on these sections. Thus, pavement sections with seal coats should be excluded from use with future calibration efforts.

- One of the future tools that may be provided in the PMED software is automation of the local calibration process. The local calibration tool will require a database that contains sections with pavement performance information. Emphasizing the importance of the developed database and the vital role it will play in providing accurate and precise data for the performance of the flexible pavements under Idaho conditions. Therefore, continual population and maintenance of the performance database is strongly recommended.



# Chapter 1

## Introduction

### Background

The American Association of State Highway Officials (AASHO) developed its first pavement design guide in 1961.<sup>(1)</sup> The guide was a result of experiments at the AASHO test road during the 1950-1960s. This empirical-based design method had a number of limitations, including a single climatic region (Ottawa, Illinois), limited traffic loads (vehicle type and weight), as well as, a limited range of materials (e.g., one asphalt binder type, one base type, one subgrade soil type). With advancements in material characterization and pavement performance evaluation, the American Association of State Highway and Transportation Officials (AASHTO) developed the *Mechanical Empirical Pavement Design Guide, A Manual of Practice* (MEPDG), and accompanying software, through the National Cooperative Highway Research Program (NCHRP) Project 01-37A, *Development of the 2002 Guide for the Design of New and Rehabilitated Pavement Structures: Phase II*.<sup>(2)</sup> The accompanying software has received multiple updates and revisions and is now available as AASHTOWare Pavement ME Design™ (PMED).

In the mechanistic-empirical (ME) design process, cumulative pavement distresses are calculated based on pavement response (e.g., stress, strain, deflection) and empirical distress performance models that relate pavement response to observed distress. Various distresses can be predicted, such as, rutting in each layer, bottom-up and top-down cracking, reflective cracking, thermal cracking, and roughness (characterized by the International Roughness Index [IRI]). The performance models used in the PMED were globally-calibrated using data obtained from in-service pavements, primarily from the Long Term Pavement Performance (LTPP) program.

Accordingly, the globally-calibrated models should be evaluated to determine whether they accurately predict field performance, if not, the models should be calibrated to local conditions. Otherwise, some pavements may be overdesigned and others under designed, resulting in either excessive costs or shortened pavement life. AASHTO highly recommends that each agency conduct an analysis of the PMED results to determine if the globally-calibrated performance models accurately predict field performance.<sup>(3)</sup>

### Problem Statement

The Idaho Transportation Department (ITD) maintains more than 12,200 lane-miles of roads. With a large roadway system and a limited budget, it is essential that proper pavement structures are designed and constructed to withstand anticipated traffic loads and climate conditions over the intended design life. In 2010, ITD developed a plan to assist with the implementation of the PMED.<sup>(4,5,6)</sup> The implementation plan included developing traffic inputs, characterizing material properties for asphalt mixes, unbound aggregate layers, and subgrade soils. In addition, a user's guide was developed to assist

ITD personnel with the implementation of the PMED. One of the final steps for PMED implementation includes validating, and if needed, locally calibrating the PMED pavement performance models.

## Scope of Research and Project Tasks

The scope of this project includes developing the local calibration coefficients for asphalt pavement performance models specific to Idaho conditions. This project was divided into the following tasks:

**Task 1:** Review the PMED pavement performance prediction models for flexible pavements. The distress and IRI prediction models, as well as the global calibration coefficients, shall be reviewed. Trial runs will be performed with the most current PMED version.

**Task 2:** Evaluate the required PMED design inputs. In this task, the research team will study and evaluate the inputs required to run the latest PMED version. In addition, the level of input for each required parameter will be determined based on previous literature studies, as well as ITD available data.

**Task 3:** Identify and select the pavement sections for calibration. In addition to the LTPP projects available in Idaho, the research team, in coordination with ITD, will identify and select roadway sections representative of the different districts in Idaho. The pavement sections shall cover a reasonable range of climate conditions, traffic levels, and subgrade strength. The selected pavement sections shall have all required PMED inputs and sufficient field-measured performance data (both to be provided by ITD). Requested data includes, but not limited to:

- Project location (latitude and longitude).
- Construction year and month.
- As-built pavement structure (layer type and thickness of each layer).
- AC, base, subbase, and subgrade material properties.
- Ground water table level.
- Traffic volume and axle load spectra data in the required PMED format.
- Performance data (rutting, longitudinal cracking, alligator fatigue cracking, transverse cracking, and IRI) since original construction.
- Maintenance history.

Based on the research teams experience with ITD data for in-service pavement sections, level 1 input data will be difficult to obtain for most of the required inputs. Therefore, level 2 and 3 input data will be used when level 1 data is unavailable. Previous outcomes of ITD Project RP 193 (KLK557), *Implementation of the MEPDG for Flexible Pavements in Idaho*, will play a vital role in the characterization of the material, traffic, and climate of the selected pavement sections.

Selected pavement sections should have in-service lives of more than 5 years. Pavement sections close to receiving major rehabilitation activities are preferred since their condition tends to include a variety of distress types and severities. Selected pavement sections also need to include Superpave asphalt mixes to utilize the materials database developed under RP 193.

The total number of required pavement sections, including the Idaho LTPP flexible pavement sections, will be determined by the research team in coordination with ITD.

**Task 4:** Conduct creep compliance and indirect tensile (IDT) strength testing. Thermal cracking is a predominant distresses in the Northern U.S. Based on results from NCHRP Project 01-40, *Facilitating the Implementation of the Guide for the Design of New and Rehabilitated Pavement Structures*, thermal cracking prediction is very sensitive to IDT creep compliance and IDT strength.<sup>(7,8,9)</sup> Similar to AC dynamic modulus, a material library and prediction model calibration coefficients for IDT creep compliance and strength need to be completed to characterize local materials. Tentatively, all six classes of ITD mixes are included in this study. Each class will include three mixes, pending the availability of materials. It is desired that the three mixes of each class have different performance grade (PG) binders. In total, there will be 18 mixes included in this study. Field cores will be delivered to the Washington State University for testing. The cores shall be taken from new pavement sections. IDT creep compliance and strength tests will be conducted in accordance with AASHTO T322, *Standard Method of Test for Determining the Creep Compliance and Strength of Hot Mix Asphalt (HMA) Using the Indirect Tensile Test Device*.

**Task 5:** Develop a performance database of the identified pavement sections. The performance database required for local calibration of the PMED performance models shall come from two sources. For LTPP pavement sections, the data will be obtained from the LTPP database. Since the PMED distress and roughness models were globally-calibrated using the more than 90 LTPP pavement sections distributed across the U. S., the LTPP performance data is consistent with the definitions included in the PMED. For the Idaho pavement sections, performance data will be obtained from the ITD Pavement Performance Management Information System (PPMIS). The PPMIS data will be evaluated for accuracy, reasonableness, outliers, and anomalies.

Review of ITD cracking (alligator, longitudinal, and transverse) measurement methods (severity and extent for each type of crack) indicated that ITD cracking data are collected and measured differently from the LTPP cracking evaluation method. The research team, in cooperation with the ITD Construction and Materials Engineers, will study the feasibility of processing and converting ITD cracking to be consistent with the LTPP cracking data. Thus, cracking prediction models in the PMED can be evaluated and calibrated using both LTPP and ITD data.

The PMED predicts rutting within each layer and sums all layer rutting to calculate total rutting. On the other hand, ITD and LTPP only measure the total pavement rutting at the surface of the

asphalt concrete (AC) layer. Thus, for rutting model calibration, the focus will be on total rut-depth. Percentages of the sub-layer rutting, based on engineering reasonableness, as well as the globally-calibrated rutting models will be assumed.

**Task 6:** Run the PMED using the globally-calibrated models with the developed database. The PMED will be run and the predicted performance compared to the field-measured performance. Precision and bias of the globally-calibrated performance models will be assessed. This will warrant whether or not the globally-calibrated models need to be locally calibrated.

**Task 7:** Develop Idaho calibration coefficients. In this task, using the outcomes of Task 5, the PMED will be run using different trial sets of calibration coefficients for each performance model to determine the best combination of calibration coefficients. The set of local calibration coefficients that produce a higher precision and lower bias for each distress model, as compared to the globally-calibrated models, will be selected. The IRI model will be calibrated after the distress models since it is dependent on the predicted rutting and cracking, as well as other factors. Finally, the resulting goodness of fit and bias of the locally-calibrated models will be statistically validated.

**Task 8:** Summary of findings and recommendations. Before completing the final report and developing the training workshop, a summary of findings and draft calibration coefficients will be developed and submitted to ITD for review. ITD review comments and recommendations will be incorporated in the final report and the training workshop.

**Task 9:** Prepare and conduct training workshop. The IDT PMED User Manual will be reviewed and updated to reflect the new findings from this project. A workshop to demonstrate and train ITD personnel on the new software will be performed at a suitable location where access to the software will be available.

**Task 10:** Final report. A draft report will be edited by a professional editor and reviewed by an external expert. The edited and reviewed draft report will be submitted to ITD for comments before submission of the final report.

## **Report Organization**

This report presents the research work completed for the validation and calibration of the PMED to Idaho conditions. The report is organized into five chapters as described below:

**Chapter 1** provides the introduction of this research project, presents the problem statement, research objectives, and project description.

**Chapter 2** presents a literature review of the PMED pavement performance prediction models for flexible pavements, and summarizes other State Department of Transportation (DOT) PMED implementation efforts.

**Chapter 3** presents the local calibration process, results, and analysis of the development of Idaho-specific local calibration coefficients.

**Chapter 4** presents the validation process of the determined local calibration coefficients to Idaho conditions.

Finally, **Chapter 5** summarizes the key findings from this research and presents recommendations for future work for ITD consideration.





## Chapter 2

# Review of the PMED Distress Prediction Models for Flexible Pavements

This chapter presents a summary of the asphalt pavement performance prediction models included in the PMED and a review of PMED implementation efforts conducted by other state DOTs. The purpose of the state DOT review is to learn what activities need to be performed to overcome the challenges with local calibration and successful implementation of the PMED. Summary of the implementation plans of the surrounding agencies, and their developed local calibration coefficients is also presented below.

### Performance Indicators

PMED analyzes pavement' performance over its design life. Pavement distress is determined using transfer functions and structural response models. The response models compute critical pavement stresses, strains, and deflections through mechanistic models and empirical transfer functions relate these critical pavement responses to performance indicators. The following discusses each of the distress models within the PMED.

#### Alligator Cracking (Bottom-Up Cracking)

Alligator cracking develops through repeated wheel loading and is defined as a series of interconnected cracks due to AC fatigue or stabilized base (characteristically with an "alligator hide" pattern). Alligator cracks initiate at the bottom of the AC layer and propagate to the surface. They initially show up as multiple short, longitudinal, or transverse cracks in the wheel path, becoming interconnected with continued truck loading. Alligator cracking is calculated as a percent of total lane area.<sup>(10,11)</sup>

#### Longitudinal Cracking (Top-down Cracking)

Longitudinal cracking is a load-related distress, occurring within the wheel paths, that primarily runs parallel to the pavement centerline. Longitudinal cracking initiates at the surface of the AC layer due to high localized tensile stresses from tire-pavement interaction.<sup>(11)</sup> Longitudinal cracking initially shows up as short cracks that become connected with continued truck loadings. Raveling or crack deterioration may occur along the edges of these cracks but they do not form an alligator cracking pattern. The PMED calculates longitudinal cracking as total feet per mile (includes both wheel paths).<sup>(11)</sup>

#### Thermal Transverse Cracking

Thermal (transverse) cracking is non-wheel load-related cracking that appears perpendicular to the pavement centerline and is caused by low temperatures. The PMED calculates transverse cracking as total feet per mile.

## Transverse Reflection Cracking

Transverse reflection cracking is a non-wheel load crack that is induced by transverse joints or cracks in the underlying pavement. Transverse reflection cracking is calculated in the PMED as the percent lane area (area cracked = linear ft of crack × 1 ft width, where crack width = 1 ft).<sup>(11)</sup>

## Rutting

Rutting is a surface depression in the wheel path caused by plastic or permanent deformation in each pavement layer. The rut depth represents the maximum vertical difference in elevation between the transverse profile of the pavement surface and a wire-line across the lane width. The PMED calculates rut depth in inches, and represents the maximum mean rut depth in both wheel paths. The PMED calculates total rutting and rutting in each pavement layer (AC, unbound aggregate layers, and subgrade).<sup>(11)</sup>

## International Roughness Index (IRI)

The PMED predicts the incremental change in smoothness over the entire design period. The IRI model uses the predicted distresses (rutting, bottom-up/top-down fatigue cracking, and thermal cracking), initial IRI, subgrade condition, site factors, and climatic factors to predict IRI over the design period.

## Performance Models in the PMED Software

The PMED predicts pavement distress by dividing the pavement structural layers into thinner sublayers. The thickness of the sublayers depends upon the layer thickness, layer type, and depth within the pavement structure. The JULEA program calculates the critical responses (stress and strain) in each sublayer.<sup>(2)</sup> For load related distresses, the AC dynamic modulus ( $E^*$ ) is calculated as a function of time at mid-depth of the AC layer. This is done by dividing the hourly temperatures of the AC sublayers over a given analysis period (2 weeks to 1 month) into five sub-seasons. For each sub-season, the temperature of AC sublayer represents 20 percent of the pavement temperature distribution frequency. This sub-season similarly represents these conditions when 20 percent of the monthly traffic takes place. This is done by computing pavement temperatures corresponding to standard normal deviations of -1.2816, -0.5244, 0, 0.5244 and 1.2816. These values correspond to accumulated frequencies of 10, 30, 50, 70 and 90 percent within a given month. The software uses these five quintile temperatures to calculate the dynamic modulus ( $E^*$ ) at the mid-depth of each AC sublayer taking into account the effect of loading rate (vehicle speed) and temperature variation through the analysis period.  $E^*$  is used for permanent deformation and fatigue damage calculations.<sup>(2,4)</sup> For transverse cracking, the Enhanced Integrated Climatic Model (EICM) processes the AC temperatures on an hourly basis. The hourly temperatures are used to predict AC creep compliance and IDT strength to compute the tensile strength of the surface AC layer. The following sections present the computational steps used in the PMED to estimate distress, and the local calibration coefficients that need to be determined for each distress prediction model.

(2,4,10,11)

### AC Rutting Prediction Model

PMED uses two different models to predict rutting, one for AC layers, and the other for unbound base and subgrade layers. The model for the AC layer is shown below.

$$\Delta_{p(AC)} = \beta_{1r} k_z \varepsilon_{r(AC)} 10^{k_{1r}} n^{k_{2r}} \beta_{2r} T^{k_{3r}} \beta_{3r} h_{AC}$$

where:

- $\Delta_{p(AC)}$  = Accumulated permanent or plastic vertical deformation in the AC layer/sublayer, in.
- $\varepsilon_{p(AC)}$  = Accumulated permanent or plastic axial strain in the AC layer/sublayer, in./in.
- $\varepsilon_{r(AC)}$  = Resilient or elastic strain calculated by the structural response model at the mid-depth of each AC sublayer, in./in.
- $h_{(AC)}$  = Thickness of the AC layer/sublayer, in.
- $n$  = Number of axle-load repetitions.
- $T$  = Mix or pavement temperature, °F
- $k_z$  = Depth confinement factor
- $k_{1r,2r,3r}$  = Global field calibration parameters ( $k_{1r} = -3.35412$ ,  $k_{2r} = 1.5606$ ,  $k_{3r} = 0.4791$ )
- $\beta_{1r}, \beta_{2r}, \beta_{3r}$  = Local or mixture field calibration constants; for the global calibration, these constants were all set to 1.0

**Figure 1 AC Rutting Prediction Model**

## Rutting Prediction Model for Unbound Materials and Subgrade Soil

PMED uses a modified version of the Tseng and Lytton model to determine the unbound aggregate and subgrade layer plastic vertical deformation.<sup>(4,10,11)</sup>

$$\Delta_{p(soil)} = \beta_{s1} k_{s1} \epsilon_v h_{soil} \left( \frac{\epsilon_0}{\epsilon_r} \right) e^{-\left(\frac{\rho}{n}\right)^\beta}$$

$$\text{Log} \beta = -0.61119 - 0.017638(Wc)$$

$$\rho = 10^9 \left( \frac{C_0}{(1 - (10^9)^\beta)} \right)^{\frac{1}{\beta}}$$

$$C_0 = \text{Ln} \left( \frac{a_1 M_r^{b_1}}{a_9 M_r^{b_9}} \right)$$

where:

- $\Delta_{p(soil)}$  = Permanent or plastic deformation for the layer/sublayer, in.
- $n$  = Number of axle-load applications
- $\epsilon_0$  = Intercept determined from laboratory repeated load permanent deformation tests, in./in.
- $\epsilon_r$  = Resilient strain imposed in laboratory test to obtain material properties  $\epsilon_0$ ,  $b$ , and  $\rho$ , in./in.
- $\epsilon_v$  = Average vertical resilient or elastic strain in the layer/sublayer and calculated by the structural response model, in./in.
- $h_{soil}$  = Thickness of the unbound layer/sublayer, in.
- $k_{s1}$  = Global calibration coefficients;  $k_{s1} = 2.03$  for granular materials and 1.35 for fine-grained materials
- $\beta_{s1}$  = Local calibration constant for the rutting in the unbound layers; the local calibration constant was set to 1.0 for the global calibration effort
- $Wc$  = Water content, percent
- $M_r$  = Resilient modulus of the unbound layer or sublayer, psi
- $a_{1,9}, b_{1,9}$  = Regression constants;  $a_1 = 0.15$  and  $a_9 = 20.0$

**Figure 2 Rutting Prediction Equations for Unbound Materials and Subgrade Soil**

Figure 3 shows a comparison of the measured versus predicted total rut depth. The total rut depth standard error ( $s_e$ ), is calculated as the sum of the standard error for each individual layers and is a function of the average predicted rut depth.

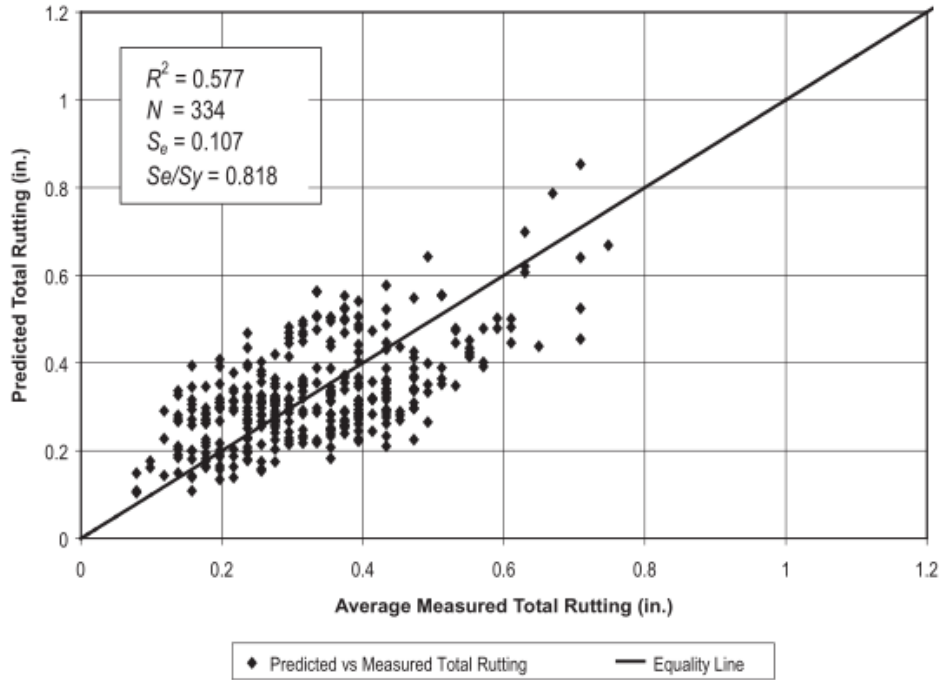


**Figure 3 Comparison of Measured and Predicted Total Rutting Resulting from Global Calibration <sup>(11)</sup>**

The standard error calculation for the individual layers AC and granular (coarse) and fine-grained unbound aggregates and soils are shown below.

$$S_{e(HMA)} = 0.24(\Delta_{AC})^{0.8026} + 0.001$$

$$S_{e(Gran)} = 0.1235(\Delta_{Gran})^{0.5012} + 0.001$$

$$S_{e(Fine)} = 0.1477(\Delta_{Fine})^{0.6711} + 0.001$$

where:

$\Delta_{AC}$  = Plastic deformation in the AC layers, in.

$\Delta_{Gran}$  = Plastic deformation in the aggregate and coarse-grained layers, in.

$\Delta_{Fine}$  = Plastic deformation in the fine-grained layers and soils, in.

**Figure 4 Standard Error Equations for the Rutting Models**

### Load Associated Cracking Prediction Models

The PMED calculates two types of load-related fatigue cracking, bottom-up (alligator) cracking and top-down (longitudinal) cracking. Once  $E^*$  and critical tensile strains at the critical locations are computed (for a given analysis period, traffic load, and environmental location), the allowable number of repetitions to (alligator or longitudinal) fatigue cracking failure ( $N_f$ ) is calculated using the following equations:

$$N_{f-AC} = k_{f1}(C)(C_H)\beta_{f1}(\epsilon_t)^{k_{f2}\beta_{f2}}(E_{AC})^{k_{f3}\beta_{f3}}$$

$$C = 10^M$$

$$M = 4.84 \left( \frac{V_{be}}{V_a + V_{be}} - 0.69 \right)$$

where:

- $N_{f-AC}$  = Allowable number of axle-load applications for a flexible pavement and AC overlays
- $\epsilon_t$  = Tensile strain at critical locations and calculated by the structural response model, in./in.
- $E_{AC}$  = Dynamic modulus of the AC measured in compression, psi
- $k_{f1}, k_{f2}, k_{f3}$  = Global field calibration coefficients ( $k_{f1} = 0.007566$ ,  $k_{f2} = +3.9492$ , and,  $k_{f3} = +1.281$ )
- $\beta_{f1}, \beta_{f2}, \beta_{f3}$  = Local or mixture specific field calibration constants; for the global calibration effort, these constants were set to 1.0.
- $V_{be}$  = Effective asphalt content by volume, percent
- $V_a$  = Percent air voids in the AC mixture
- $C_H$  = Thickness correction term, dependent on type of cracking

For bottom-up or alligator cracking:

$$C_H = \frac{1}{0.000398 + \frac{0.003602}{1 + e^{(11.02 - 3.49H_{AC})}}}$$

For top-down or longitudinal cracking:

$$C_H = \frac{1}{0.01 + \frac{12.00}{1 + e^{(15.676 - 2.8186H_{AC})}}}$$

**Figure 5 PMED Equations for the Allowable Number of Traffic Repetitions to Fatigue Damage**

The accumulative alligator and longitudinal fatigue damage ( $\Sigma D$ ) is calculated as the linear sum (Miner's hypothesis) of the ratio of the predicted to the allowable number of traffic repetitions in a specific environmental condition as shown below. This is done within a specific time increment and axle load interval for each axle type in the analysis.

$$DI = \sum (\Delta DI)_{j,m,l,p,T} = \sum \left( \frac{n}{N_{f-AC}} \right)_{j,m,l,p,T}$$

where:

- n = Actual number of axle-load applications within a specific time period
- j = Axle-load interval
- m = Axle-load type (single, tandem, tridem, or quad)
- l = Truck type using the truck classification groups included in PMED
- p = Month
- T = Median temperature for the five temperature intervals or quintiles used to subdivide each month, °F

**Figure 6 PMED Equation for the Damage Ratio**

The alligator cracking model does not consider an endurance limit. The fatigue damage is transformed into bottom-up alligator fatigue cracking by using the equation given below.

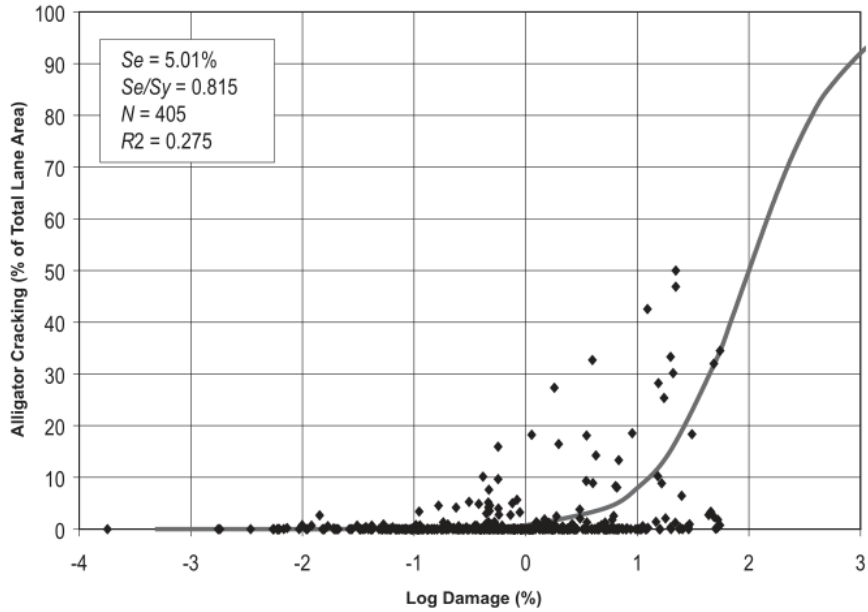
$$FC_{Bottom} = \left( \frac{1}{60} \right) \left( \frac{C_4}{1 + e^{(C_1 C_1^* + C_2 C_2^* \text{Log}(DI_{Bottom} * 100))}} \right)$$

where:

- $FC_{Bottom}$  = Area of alligator cracking that initiates at the bottom of the AC layers, percent of total lane area
- $DI_{Bottom}$  = Cumulative damage index at the bottom of the AC layers
- $C_{1,2,4}$  = Transfer function regression constants;  $C_4 = 6,000$ ;  $C_1 = 1.00$ ; and  $C_2 = 1.00$
- $C_1^* = -2C_2^*$
- $C_2^* = -2.40874 - 39.748(1 + H_{AC})^{-2.856}$

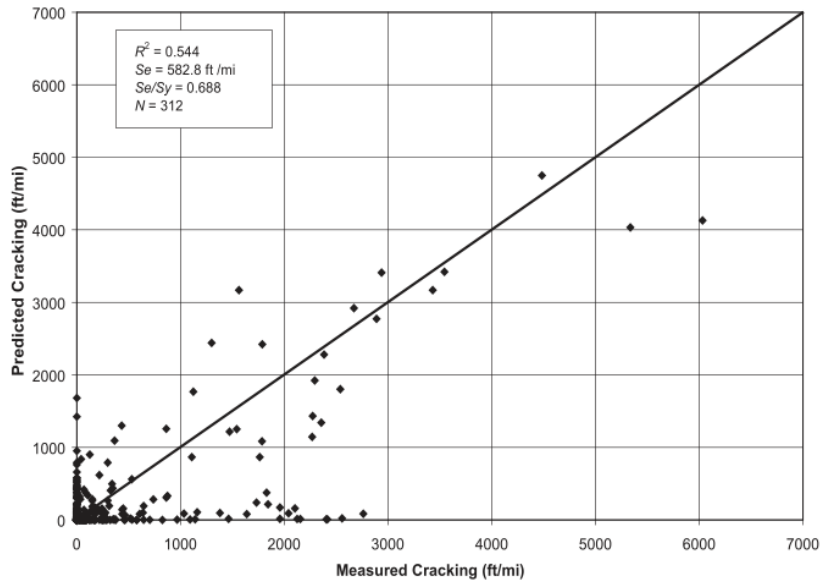
**Figure 7 Bottom-Up Cracking Transfer Function**

Figure 8 illustrates the comparison of the cumulative fatigue damage and measured alligator cracking.



**Figure 8 Comparison of Cumulative Fatigue Damage and Measured Alligator Cracking Resulting from Global Calibration Process<sup>(11)</sup>**

Figure 9 below shows a comparison between the measured and predicted lengths of longitudinal cracking (top-down cracking).



**Figure 9 Comparison of Cumulative Fatigue Damage and Measured Alligator Cracking Resulting from Global Calibration Process<sup>(11)</sup>**



Fatigue damage associated with longitudinal cracking is determined from the following equation:

$$FC_{Top} = 10.56 \left( \frac{C_4}{1 + e^{(C_1 - C_2 \text{Log}(DI_{Top}))}} \right)$$

where:

- $FC_{Top}$  = Length of longitudinal cracks that initiate at the top of the AC layer, ft/mi
- $DI_{Top}$  = Cumulative damage index near the top of the AC surface
- $C_{1,2,4}$  = Transfer function regression constants; C 1 = 7.00; C 2 = 3.5; and C 4 = 1,000

**Figure 10 Top-Down Transfer Function**

The standard error, for the alligator cracking prediction equation is a function of the average predicted area of alligator cracks.

$$S_{e(Alligator)} = 1.13 + \frac{13}{1 + e^{7.57 - 15 \text{Log}(FC_{Bottom} + 0.0001)}}$$

The standard error, for the longitudinal cracking prediction equation is a function of the average predicted length of the longitudinal cracks.

$$S_{e(Long)} = 200 + \frac{2300}{1 + e^{1.072 - 2.1654 \text{Log}(FC_{Top} + 0.0001)}}$$

**Figure 11 Standard Error Equations for Bottom-Up and Top-Down Cracking**

For the cement treated base (CTB) layers, PMED uses the models shown below to predict the fatigue behavior of these layers.

$$N_{f-CTB} = 10^{\left[ \frac{k_{c1}\beta_{c1}\left(\frac{\sigma_t}{M_R}\right)}{k_{c2}\beta_{c2}} \right]}$$

$$FC_{CTB} = C_1 + \frac{C_2}{1 + e^{(C_3 - C_4 \text{Log}(DI_{CTB}))}}$$

where:

- $N_{f-CTB}$  = Allowable number of axle-load applications for a semi-rigid pavement
- $\sigma_t$  = Tensile stress at the bottom of the CTB layer, psi
- $M_R$  = 28-day modulus of rupture for the CTB layer, psi
- $DI_{CTB}$  = Cumulative damage index of the CTB or cementitious layer and determined in accordance with Eq. 14
- $k_{c1,c2}$  = Global calibration coefficients—Undefined because prediction equation was never calibrated; these values are set to 1.0 in the software. From other studies,  $k_{c1} = 0.972$  and  $k_{c2} = 0.0825$
- $\beta_{c1,c2}$  = Local calibration constants; these values are set to 1.0 in the software
- $FC_{CTB}$  = Area of fatigue cracking, ft<sup>2</sup>
- $C_{1,2,3,4}$  = Transfer function regression constants; C 1 =1.0, C 2 =1.0, C 3 =0, and C 4 =1,000. To date, this transfer function has not been calibrated and these values will change when it is calibrated

### Figure 12 Fatigue Cracking Prediction Model for CTB Layers

The computational analysis of incremental fatigue cracking for a semi-rigid pavement uses the damaged modulus approach. In summary, the elastic modulus of the CTB layer decreases as the damage index,  $DI_{CTB}$ , increases. The equation below is used to calculate the damaged elastic modulus within each season or time period for the CTB and other pavement layers. One may notice that the equation below has not been globally calibrated due to the difficulty associated with obtaining field section design input and performance data.

$$E_{CTB}^{D(t)} = E_{CTB}^{Min} + \left( \frac{E_{CTB}^{Max} - E_{CTB}^{Min}}{1 + e^{(-4+14(DI_{CTB}))}} \right)$$

where:

- $E_{CTB}^{D(t)}$  = Equivalent damaged elastic modulus at time t for the CTB layer, psi
- $E_{CTB}^{Min}$  = Equivalent elastic modulus for the total destruction of the CTB layer, psi
- $E_{CTB}^{Max}$  = 28-day elastic modulus of the intact CTB layer, no damage, psi

**Figure 13 CTB Layer Damaged Modulus Equation**

### Non-Load Associated Transverse Cracking Prediction Model

The extent of transverse cracking expected in a pavement system is predicted by relating the crack depth to the amount of cracking (crack frequency) by the equation shown below.

$$TC = \beta_{t1} N \left[ \frac{1}{\sigma_d} \text{Log} \left( \frac{C_d}{H_{AC}} \right) \right]$$

where:

- TC = Observed amount of thermal cracking, ft/mi
- $\beta_{t1}$  = Regression coefficient determined through global calibration (400)
- $N_{[z]}$  = Standard normal distribution evaluated at [z]
- $\sigma_d$  = Standard deviation of the log of the depth of cracks in the pavement (0.769), in.
- $C_d$  = Crack depth, in.
- $H_{AC}$  = Thickness of AC layers, in.

**Figure 14 PMED Thermal Cracking Model**

The MEPDG manual of practice includes a comparison between the measured and predicted cracking for each hierarchical input level.<sup>(4,10,11)</sup> The standard error for the transverse cracking prediction equations include:

$$S_e(\text{Level 1}) = -0.1468(TC + 65.027)$$

$$S_e(\text{Level 2}) = -0.2841(TC + 55.462)$$

$$S_e(\text{Level 3}) = -0.3972(TC + 20.422)$$

**Figure 15 Standard Error Equations for the Thermal Cracking**

For a given thermal cooling cycle, Paris law is used to estimate the crack propagation as shown below.

$$\Delta C = A(\Delta K)^n$$

$$A = k_t \beta_t 10^{[4.389 - 2.52 \text{Log}(E_{AC} \sigma_m^n)]}$$

$$\eta = 0.8 \left( 1 + \frac{1}{m} \right)$$

where:

$\Delta C$  = Change in the crack depth due to a cooling cycle

$\Delta K$  = Change in the stress intensity factor due to a cooling cycle

$A, n$  = Fracture parameters for the AC mixture

$k_t$  = Coefficient determined through global calibration for each input level (Level 1 = 1.5; Level 2 = 0.5; and Level 3 = 1.5)

$E_{AC}$  = AC indirect tensile modulus, psi

$\sigma_m$  = Mixture tensile strength, psi

$m$  = Derived from the indirect tensile creep compliance curve measured in the laboratory

$\beta_t$  = Local or mixture calibration coefficient

$$K = \sigma_{tip} [0.45 + 1.99(C_o)^{0.56}]$$

$\sigma_{tip}$  = Far-field stress from pavement response model at depth of crack tip, psi

$C_o$  = Current crack length, ft

**Figure 16 Paris Law for Crack Propagation**

### Reflection Cracking in AC Overlays

For the AC over existing flexible and AC over rigid pavements overlay options PMED uses a simple empirical model, based on field observations, for the prediction of reflective cracking. This model predicts the percentage of cracks that propagate through the overlay as a function of time and AC overlay thickness using the equations shown below.

$$RC = \frac{100}{1 + e^{a(c)+bt(d)}}$$

$$CA_m = \frac{100}{1 + e^{6-(6DI_m)}}$$

$$TRA_m = \sum_{i=1}^m RC_t(\Delta CA_i)$$

where:

- RC = Percent of cracks reflected. [Note: The percent area of reflection cracking is output with the width of cracks being 1 ft.]
- t = Time, yr
- a,b = Regression fitting parameters defined through calibration process
- c,d = User-defined cracking progression parameters
- a =  $3.5+0.75(H_{eff})$
- b =  $-0.688684-3.37302(H_{eff})^{-0.915469}$
- DI<sub>m</sub> = Damage index for month m
- ΔDI<sub>i</sub> = Increment of damage index in month i
- TRA<sub>m</sub> = Total reflected cracking area for month m
- RC<sub>t</sub> = Percent cracking reflected for age t (in years), refer to Eq. 24
- ΔCA<sub>i</sub> = Increment of fatigue cracking for month i

**Figure 17 Reflection Cracking Model in AC Overlays**

### Smoothness Prediction Model

For new AC and AC overlays of flexible pavements, PMED predicts IRI, over time, as a function of the initial pavement IRI and site factors, and predicted values for fatigue cracking, transverse cracking, and average rut depth. The equation for IRI is shown below.<sup>(10,11)</sup>

$$IRI = IRI_o + C_1(RD) + C_2(FC_{Total}) + C_3(TC) + C_4(SF)$$

$$SF = Age^{1.5} \{ \ln[(precip + 1)(FI + 1)_{p02}] \} + \{ \ln[(precip + 1)(PI + 1)_{p200}] \}$$

where:

- IRI<sub>o</sub> = Initial IRI after construction, in/mi
- SF = Site factor.
- FC<sub>Total</sub> = Area of fatigue cracking (combined wheel path alligator, longitudinal, and reflection cracking), percent of total lane area (transverse width of crack is assumed to be 1-ft wide)
- TC = Length of transverse cracking (including transverse reflection cracks in existing AC pavements), ft/mi
- RD = Average rut depth, in.
- C<sub>1,2,3,4</sub> = Calibration coefficients; C<sub>1</sub> = 40.0, C<sub>2</sub> = 0.400, C<sub>3</sub> = 0.008, C<sub>4</sub> = 0.015.
- Age = Pavement age, yr
- PI = Percent plasticity index of the soil
- FI = Average annual freezing index, °F days
- Precip = Average annual precipitation or rainfall, in.
- p<sub>02</sub> = Percent passing the 0.02 mm sieve
- p<sub>200</sub> = Percent passing the 0.075 mm sieve

**Figure 18 Smoothness Prediction Model**

## PMED Calibration and Implementation Efforts by State DOTs

A number of state DOTs have implemented or plan to implement the PMED. There are also several DOT's who have no PMED implementation plans at this time. In a recent agency summary, conducted by the AASHTO Pavement ME National User Group, 13 DOTs have implemented the PMED, 35 DOTs, including Idaho, are planning to implement within the next five years, and 5 DOTs disclosed no plans for implementation (Figure 19).<sup>(12)</sup>

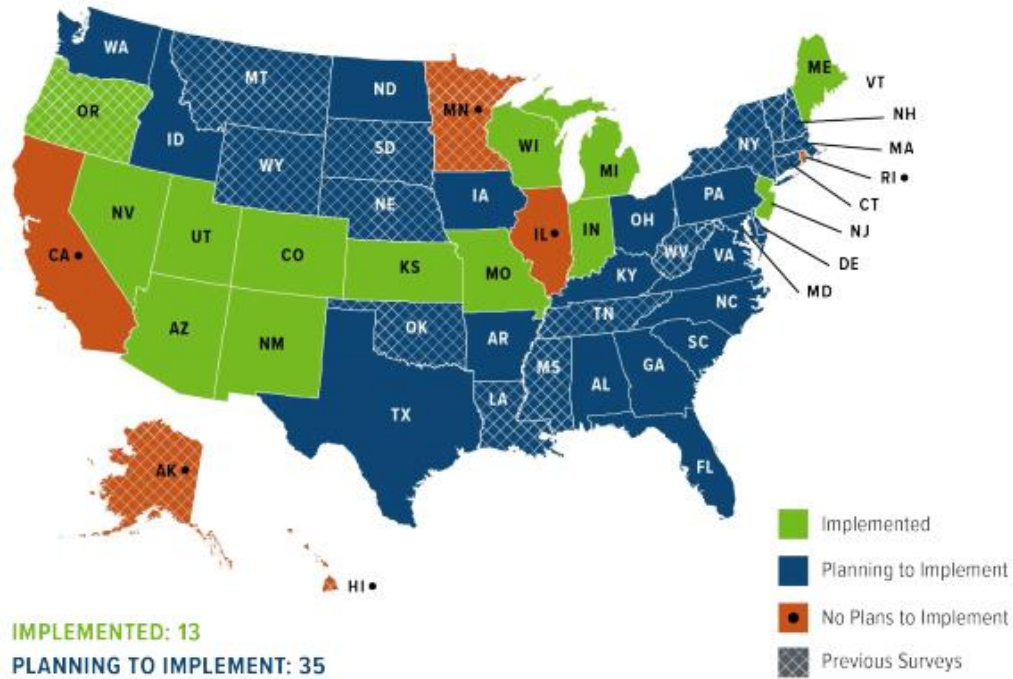


Figure 19 Summary of Agency PMED Implementation<sup>(12)</sup>

### Arizona

The Arizona DOT is one of the lead states for PMED implementation. Working with the Arizona State University, Arizona DOT initiated a long-term research project beginning in 1999. The main project objective was to develop performance-related specifications for asphalt pavements in Arizona based on the PMED.<sup>(13)</sup> This research project focused on development of Arizona-specific PMED inputs for asphalt binders and mixtures, unbound base materials and subgrade soils, climate, and traffic characteristics.

In addition, a research effort was conducted to develop local calibration coefficients for asphalt rutting, load-related alligator and longitudinal cracking, and IRI of new flexible pavements. A total of 22, 25, and 37 pavement sections, respectively, with performance and material characterization data were obtained from LTPP and Arizona DOT databases.<sup>(14)</sup> A trial and error method was used to determine local calibration coefficients that resulted in the least squared error and zero sum of standard error between PMED predicted and field-measured values. The recommended calibration coefficients for Arizona are summarized in Table 1.

**Table 1 Arizona Local Calibration Coefficients<sup>(14)</sup>**

<b>Distress Model</b>	<b>Distress Type/Layer</b>	<b>Calibration Coefficient</b>
<b>Rutting</b>	AC, ( $\beta_{r1}$ , $\beta_{r2}$ , $\beta_{r3}$ )	3.63, 1.10, 0.70
	Granular Base, ( $\beta_{B1}$ )	0.111
	Subgrade, ( $\beta_{s1}$ )	1.38
<b>Fatigue Cracking</b>	Fatigue Model, ( $\beta_{f1}$ , $\beta_{f2}$ and $\beta_{f3}$ )	0.729, 0.800, 0.800
	Bottom-Up Transfer Function (C1, C2)	0.732, 0.732
	Top-Down Transfer Function (C1, C2)	1.607, 0.803
<b>IRI</b>	Smoothness (C1, C2, C3, C4)	5.455, 0.354, 0.008, 0.015

**California**

In 2005, California Department of Transportation (Caltrans) approved the adoption of PMED for concrete pavements only using globally-calibrated coefficients.<sup>(15)</sup> Asphalt pavements are characterized using CalME, a Caltrans-developed ME design procedure.

**Montana**

For Montana, the PMED implementation effort was divided into three phases. Phase I included identifying test sections and preliminary data (e.g., pavement structure, materials, performance) needed for calibration.<sup>(11)</sup> Phase II involved data collection and analysis of the PMED performance prediction models for climate, materials, and design strategies in Montana. Phase III included additional data collection efforts for updating the calibration coefficients<sup>(16,17,18)</sup> In the Montana DOT study, results from NCHRP 1-40B, *User Manual and Local Calibration Guide for the Mechanistic-Empirical Pavement Design Guide and Software*, were used to determine bias and standard error and compared to the standard error from the original calibration process completed under NCHRP Project 1-37A. Bias was found for most of the distress transfer functions. Global calibration coefficients included in PMED v0.9 were initially used to predict the distresses and IRI of the Montana test sections and to determine model bias. These runs were considered a part of the validation process, similar to the process used under NCHRP Project 1-40B and NCHRP Project 9-30, *Experimental Plan for Calibration and Validation of HMA Performance Models for Mix and Structural Design*. Table 2 includes the local calibration coefficients for Montana.



**Table 2 Montana Local Calibration Coefficients<sup>(16)</sup>**

<b>Distress Model</b>	<b>Distress Type/Layer</b>	<b>Calibration Coefficient</b>
<b>Rutting</b>	AC, ( $\beta_{r1}$ , $\beta_{r2}$ , $\beta_{r3}$ )	7.0, 0.7, 1.13
	Granular Base, ( $\beta_{B1}$ )	0.3
	Subgrade, ( $\beta_{s1}$ )	0.3
<b>Fatigue Cracking</b>	Fatigue Model, ( $\beta_{f1}$ , $\beta_{f2}$ and $\beta_{f3}$ )	13.21, 1.00, 1.25
	Bottom-Up Transfer Function (C1, C2)	Default
	Top-Down Transfer Function (C1, C2)	Default
<b>IRI</b>	Smoothness (C1, C2, C3, C4)	default

### **Nevada**

Nevada DOT has recently finished a study on characterization of unbound base and subgrade soils to develop resilient modulus models for new design and rehabilitation projects to be used in the PMED.<sup>(19)</sup> The study recommends two different resilient modulus models, one for new pavement design and the second for rehabilitation pavement design. The results indicated that the design resilient modulus of the subgrade layer for both new and rehabilitation projects can be estimated based on the unconfined compressive strength properties or R-value. However, the design resilient modulus of the base layers can only be estimated based on the R-value. This concludes that the unconfined compressive strength is not a good indicator of the strength properties of the base layers, thus a confined compressive strength should be measured. In the meantime, another study from University of Nevada at Reno, showed a preliminary set of local calibration coefficients based on 45 projects. PMED v2.1 was used in this effort.<sup>(20)</sup> The local calibration coefficients were developed for AC rutting and bottom-up cracking; global calibration coefficients are used for IRI.

### **Oregon**

The Oregon DOT conducted a study to calibrate the PMED models associated with pavement rehabilitation. Forty-four pavement sections, across the state were selected. A detailed comparison of measured and predictive distresses was prepared. The results indicated that PMED v1.1 over predicted total rutting compared to the measured total rutting, with most of the predicted rutting associated with the subgrade.<sup>(21)</sup> For bottom-up and thermal cracking, PMED v1.1 significantly underestimates the amount of cracking as compared to field observations. Finally, there was a high-level of variability between predicted and measured values for longitudinal (top-down) cracking. Therefore, it was determined that local calibration to Oregon conditions was warranted.

The models included in the Oregon DOT local calibration for flexible pavement overlays included: rutting, bottom- up (alligator), top-down (longitudinal), and thermal cracking. The locally-calibrated models for rutting, alligator cracking, and longitudinal cracking provided better predictions with lower standard error and bias than the globally-calibrated models. However, there was a high degree of variability between the measured and predicted distresses, particularly for longitudinal and transverse cracking, even after local calibration. It is assumed that there is a substantial lack-of-fit modeling error for the occurrence of longitudinal cracks. The study recommended the PMED v1.1 calibrated models for rutting and alligator cracking be implemented. However, it was recommended that further sites be established and involved in the future calibration efforts to increase the accuracy of the prediction models.<sup>(21)</sup> Table 3 summaries the local calibration coefficients for Oregon.

**Table 3 Oregon Local Calibration Coefficients<sup>(21)</sup>**

<b>Distress Model</b>	<b>Distress Type/Layer</b>	<b>Calibration Coefficient</b>
<b>Rutting</b>	AC, ( $\beta r1$ , $\beta r2$ , $\beta r3$ )	1.48, 1, 0.9
	Granular Base, ( $\beta B1$ )	0
	Subgrade, ( $\beta s1$ )	0
<b>Fatigue Cracking</b>	Fatigue Model, ( $\beta f1$ , $\beta f2$ and $\beta f3$ )	default
	Bottom-Up Transfer Function (C1, C2)	0.560, 0.225
	Top-Down Transfer Function (C1, C2)	1.453, 0.097
<b>IRI</b>	Smoothness (C1, C2, C3, C4)	default

## Utah

The Utah DOT initiated a PMED implementation project consisting of two phases.<sup>(22)</sup> Phase I included 1) determination of LTPP data to be used for PMED validation and local calibration, 2) sensitivity analysis, 3) comparison of the PMED to the existing Utah DOT pavement design methods, and 4) preparation of a scope of future work needed for full PMED implementation. Phase II focused on the validation of the PMED globally-calibrated performance prediction models using data from both LTPP and Utah DOT’s pavement management system. In addition, local calibration coefficients were developed. It should be mentioned that PMED v0.8 was used during Phase I, while PMED v1.0 was used for Phase II. A total of 18 new AC, and 8 AC over AC rehabilitation projects were used for all the calibration and validation of the performance models. Level 2 truck volume and truck axle load spectra data and Level 3 tire pressure, truck speed, and truck wander data were used in the analysis. Most of the AC, base/subbase, and foundation material characterization data were Level 3 inputs and few material characterization were

available at Level 2. The Natural Resources Conservation Service was used for subgrade soil characterization. Data included in the PMED for Utah and surrounding states was used to create virtual site-specific climatic information. The Utah DOT calibration study showed, for new flexible pavements and AC over AC rehabilitation design, the globally-calibrated alligator cracking model predictions were relatively good for low to moderate cracking. There were no pavement sections in Utah with significant alligator cracking to verify severe cracking model predictions. The globally-calibrated transverse cracking model predictions were adequate for newly constructed pavements with Superpave binders. Good agreement was found between measured and predicted IRI using the PMED globally-calibrated IRI prediction model. Only the rutting prediction models needed to be calibrated to reflect Utah conditions.<sup>(22)</sup> Table 4 presents the Utah’s local calibration coefficients.

**Table 4 Utah Local Calibration Coefficients<sup>(22)</sup>**

<b>Distress Model</b>	<b>Distress Type/Layer</b>	<b>Calibration Coefficient</b>
<b>Rutting</b>	AC, ( $\beta r1$ , $\beta r2$ , $\beta r3$ )	0.560, 1.00, 1.00
	Granular Base, ( $\beta B1$ )	0.604
	Subgrade, ( $\beta s1$ )	0.4
<b>Fatigue Cracking</b>	Fatigue Model, ( $\beta f1$ , $\beta f2$ and $\beta f3$ )	default
	Bottom-Up Transfer Function (C1, C2)	default
	Top-Down Transfer Function (C1, C2)	default
<b>IRI</b>	Smoothness (C1, C2, C3, C4)	default

**Washington**

The flexible pavement distress models, excluding the IRI model, were successfully calibrated to Washington State conditions using MEPDG version 1.0.<sup>(23)</sup> The final local calibration coefficients for Washington State are shown in Table 5. Based on the outcome of the calibration process, the developed coefficients were found to be reasonable, and applicable to more than 90 percent of WSDOT flexible pavements Recommendations for PMED implementation and improvement include:

1. Local agencies need to balance the accuracy of inputs and costs.
2. Local calibration, along with implementation, is a continual process. Users need to allow sensible bias between local observations and model prediction. The final design should be within a reasonable range.
3. Agencies with similar materials and climates may combine data to increase the number of pavement sections for local calibration.

4. Ongoing and future work that inspects and evaluates the PMED performance prediction models and software function should continue to be monitored.<sup>(23)</sup>

**Table 5 Washington State Local Calibration Coefficients<sup>(23)</sup>**

<b>Distress Model</b>	<b>Distress Type/Layer</b>	<b>Calibration Coefficient</b>
<b>Rutting</b>	AC, ( $\beta r1$ , $\beta r2$ , $\beta r3$ )	1.05, 1.109, 1.1
	Granular Base, ( $\beta B1$ )	Default
	Subgrade, ( $\beta s1$ )	0
<b>Fatigue Cracking</b>	Fatigue Model, ( $\beta f1$ , $\beta f2$ and $\beta f3$ )	0.96, 0.97, 1.03
	Bottom-Up Transfer Function (C1, C2)	1.071, 1.0
	Top-Down Transfer Function (C1, C2)	6.42, 3.596
<b>IRI</b>	Smoothness (C1, C2, C3, C4)	Could not locally calibrate due to software bug

### Wyoming

Wyoming DOT has been actively working toward the implementation of the Mechanistic-Empirical design. Their plan consists of two phases: Phase 1 includes development of the database, and Phase 2 focuses on data analyses, recommendations, trial designs and examples, design comparisons, design guidelines, and implementation.<sup>(24,25)</sup> The traffic and climate inputs have been characterized and the DOT is focusing on a comprehensive field and laboratory test program for subgrade soils. To efficiently store the results from the field and laboratory testing results, an electronic database (WYOMEP) was developed in Microsoft Access 2013. Specific data or inputs requested by user are efficiently and easily sorted, filtered, and queried in the database. Wyoming DOT will continue to populate the database with future construction projects. A set of preliminary local calibration coefficients, primarily for primary and secondary roadways were developed in 2012.<sup>(6,24)</sup> The local calibration coefficients for Wyoming and are shown in Table 6.

**Table 6 Wyoming Local Calibration Coefficients<sup>(6)</sup>**

<b>Distress Model</b>	<b>Distress Type/Layer</b>	<b>Calibration Coefficient</b>
<b>Rutting</b>	AC, ( $\beta_{r1}$ , $\beta_{r2}$ , $\beta_{r3}$ )	1.0896, 1.0, 1.0
	Granular Base, ( $\beta_{B1}$ )	0.9475
	Subgrade, ( $\beta_{s1}$ )	0.6897
<b>Fatigue Cracking</b>	Fatigue Model, ( $\beta_{f1}$ , $\beta_{f2}$ and $\beta_{f3}$ )	1.00, 1.00, 1.00
	Bottom-Up Transfer Function (C1, C2)	0.4951,1.469
	Top-Down Transfer Function (C1, C2)	Default
<b>Thermal Cracking</b>	Thermal Fracture (K1,K2)	7.5,7.5
<b>IRI</b>	Smoothness (C1, C2, C3, C4)	20.53,0.4094,0.00179,0.015

## State DOT PMED Implementation Summary

Based on review of DOT PMED calibration and implementation activities, successful PMED implementation is accomplished with comprehensive material and traffic characterization. Development of accompanying database (library) will greatly enhance future calibration efforts. Distress prediction models may require local calibration to improve prediction accuracy and reduce bias. Understanding the sensitivity of each input and establishing reasonable ranges for key design inputs are extremely important.

In a study conducted by the Federal Highway Administration (FHWA), agency recommendations for local calibration include evaluating measured distress data and ensuring it is consistent with the distress definitions in the PMED.<sup>(26)</sup> In addition, material, traffic, and climate parameters should be reviewed to determine if changes to default inputs are necessary to model pavement sections accurately. Some of the other challenges identified were the lack of distress or pavement material information, limited ranges of distress values and pavement service life, and fewer sites than needed to conduct statistically meaningful calibration.

Pavement performance data measured accurately over time in a manner consistent with PMED requirements is essential for implementation and local calibration.<sup>(4,5,10)</sup> Many DOTs (including ITD) collect cracking data in a format inconsistent with the PMED recommended method. Therefore, to conduct the local calibration, cracking data may require additional analysis to format to the PMED method. Additional agencies calibration coefficients were obtained from the literature and included in the summary tables that follow.<sup>(27,28,29,30,31)</sup> A summary of the local calibration coefficients for rutting,

fatigue cracking (alligator and longitudinal), thermal cracking, and IRI are shown in Table 7 through Table 10, respectively.

**Table 7 Summary of Local Calibration Coefficients for Rutting**

State		AC			Granular Base	Subgrade
		$\beta_{r1}$	$\beta_{r2}$	$\beta_{r3}$	$\beta_{B1}$	$\beta_{s1}$
Arizona		3.63	1.10	0.70	0.111	1.38
Montana		7	0.7	1.13	0.30	0.30
Oregon		1.48	1.00	0.9	0	0
Utah		0.56	1.00	1.00	0.604	0.40
Washington		1.05	1.109	1.10	1.00	0.00
Wyoming		1.0896	1.00	1.00	0.9475	0.6897
Arkansas		1.20	1.00	0.80	1.00	0.50
Kansas	Conventional	1.50	0.90	1.00	0.50	0.50
	PMA *	2.50	1.15	1.00	0.50	0.50
	Superpave	1.50	1.20	1.00	0.50	0.50
North Carolina		0.983	1.00	1.00	1.58	1.10

PMA\* = Polymer Modified Asphalt

**Table 8 Summary of Calibration Coefficients for Fatigue Cracking**

State		AC Fatigue Model			AC Bottom-Up Transfer function		AC Top-Down Transfer Function	
		$\beta_{f1}$	$\beta_{f2}$	$\beta_{f2}$	C1	C2	C1	C2
Arizona		0.729	0.8	0.8	0.732	0.732	1.607	0.803
Montana		13.21	1.00	1.25	1.00	1.00	7.00	3.50
Oregon		1.00	1.00	1.00	0.560	0.225	1.453	0.097
Utah		1.00	1.00	1.00	1.00	1.00	7.00	3.50
Washington		0.96	0.97	1.03	1.071	1.00	6.42	3.596
Wyoming		1.00	1.00	1.00	0.4951	1.469	7.00	3.50
Arkansas		1.00	1.00	1.00	0.688	0.294	3.016	0.216
Kansas	Conventional	0.05	1.00	1.00	1.00	1.00	7.00	3.50
	PMA*	0.005	1.00	1.00	1.00	1.00	7.00	3.50
	Superpave	0.0005	1.00	1.00	1.00	1.00	7.00	3.50
North Carolina		1.00	1.00	1.00	0.437	0.15	7.00	3.50

PMA\* = Polymer Modified Asphalt

**Table 9 Summary of Local Calibration Coefficients for Transverse Cracking**

State		Calibration Coefficient ( $\beta_{t1}$ )
Arizona		-
Montana		0.25
Oregon		-
Utah		-
Washington		-
Wyoming		7.5
Arkansas		-
Kansas	Conventional	2.00
	PMA*	2.00
	Superpave	3.50
North Carolina		-

PMA\* = Polymer Modified Asphalt



**Table 10 Summary of Local Calibration Coefficients for IRI**

Calibration Coefficients		$C_1$	$C_2$	$C_3$	$C_4$
Arizona		5.455	0.354	0.008	0.015
Montana		40	0.4	0.008	0.015
Oregon		40	0.4	0.008	0.015
Utah		40	0.4	0.008	0.015
Washington		40	0.4	0.008	0.015
Wyoming		20.53	0.4094	0.00179	0.015
Arkansas		40	0.4	0.008	0.015
Kansas	Conventional	40	0.4	0.008	0.015
	PMA*	40	0.4	0.008	0.015
	Superpave	40	0.4	0.008	0.015
North Carolina		40	0.4	0.008	0.015

PMA\* = Polymer Modified Asphalt



## Chapter 3

# Development of PMED Calibration Coefficients for Idaho

Calibration, as defined in the MEPDG, means to reduce the total error between the measured and predicted distresses by varying the appropriate model coefficients.<sup>(3,5)</sup> There are three important stages in the calibration process. The first stage is to conduct verification runs on pavement sections using the PMED global calibration coefficients. This step helps to identify the accuracy of the global calibration coefficients to local conditions. Figure 20 illustrates the difference between accuracy and precision. The second stage calibrates the performance prediction model coefficients to remove the bias and decrease the standard error between the measured and predicted distress. Figure 21 illustrates an example of improvement in bias and precision as a result of local calibration. Once the standard error is within the adequate level set by the user, the third stage of the process is validation. The validation process (conducted using pavement segments not included in local calibration) defines if the factors are appropriate and adequate for the construction, climate, materials traffic and other conditions that may be encountered within the system.<sup>(3)</sup>

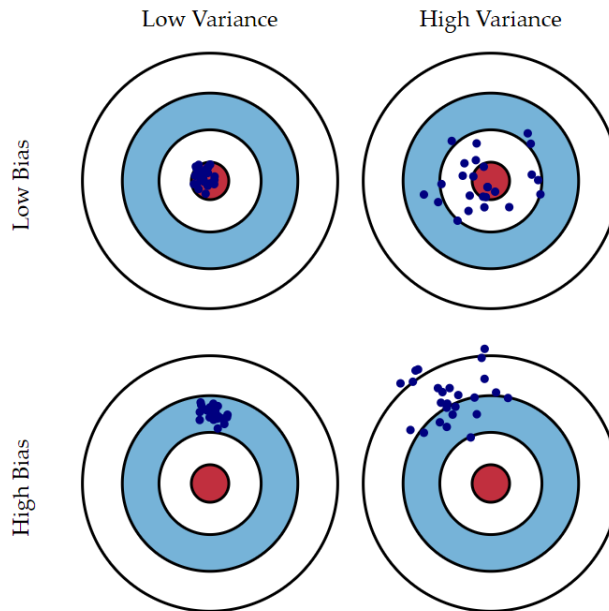


Figure 20 Target Analogy for Precision and Accuracy<sup>(32)</sup>

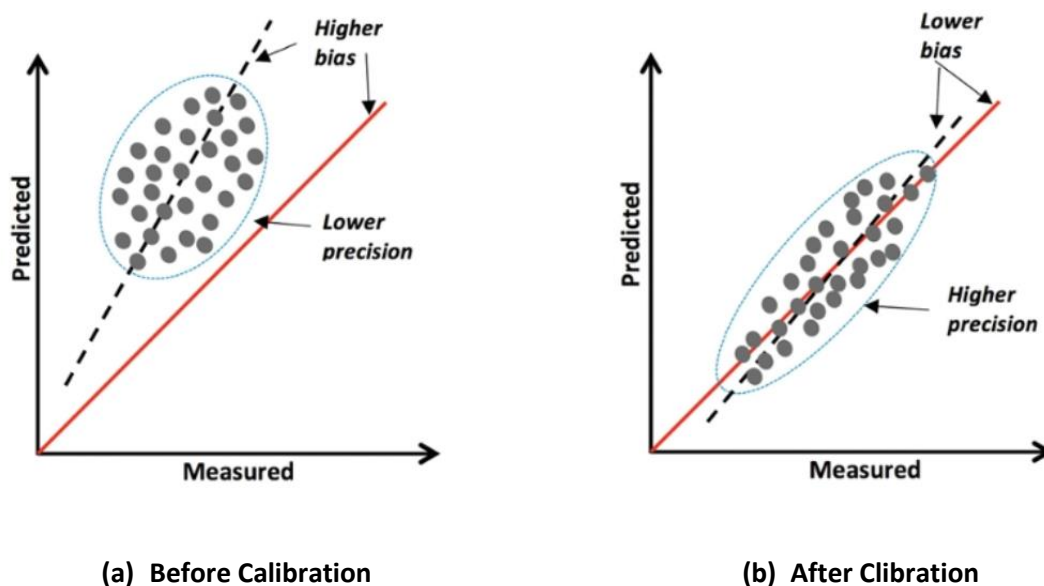


Figure 21 Improvement of Bias and Precision through Local Calibration<sup>(34)</sup>

As previously discussed, the PMED performance prediction models were globally-calibrated using primarily, LTPP pavement sections. A comparison of predicted to measured distress for selected pavement sections in Idaho showed that the global calibration coefficients yielded biased and inaccurate performance predictions, particularly for cracking. Therefore, to improve the PMED performance predictions, local calibration is required. Well-calibrated performance models result in improved performance prediction, minimized premature failure, and reduced overdesign of pavement sections, which may result in savings in construction and maintenance costs. This chapter presents the process of developing local calibration coefficients for flexible pavement prediction models for the State of Idaho.

## Procedures of the MEPDG Guide for Local Calibration

The *Guide for the Local Calibration of the Mechanistic-Empirical Pavement Design Guide*<sup>(3)</sup> recommended the following steps for local calibration:

**Step 1- Select Hierarchical Input Level for Each Input Parameter:** This step is an ITD policy decision likely influenced by current field and laboratory testing capabilities, material and construction specifications, and traffic data collection. This step is essential since it may have a significant influence on the final standard error of each distress prediction model.

**Step 2 - Develop Local Experimental Plan and Sampling Template:** The main objective of this step is to clarify the calibration of the PMED distress and IRI prediction models abased on local conditions, materials, and policies. The goals of this effort include determining if any local bias exists, defining the cause of any bias, and finally, computing the local calibration coefficients for each distress and IRI prediction models.

**Step 3 - Estimate Sample Size for Specific Distress Prediction Models:** This step is used to determine the sample size (number of roadway sections) to check the adequacy of the global calibration coefficients and determine the local calibration coefficients for each distress model, if needed.

**Step 4 - Select Roadway Segments:** This step is used to choose the roadway sections and evaluate the availability and adequacy of existing information and data. During this effort, pavement sections requiring minimal additional sampling and field testing are preferred to minimize costs.

**Step 5 - Extract and Evaluate Distress and Project Data:** After selecting the roadway sections, the next step is to collect all data and identify any missing data elements that are needed. All data should be entered into a calibration database.

**Step 6 - Conduct Field and Forensic Investigations:** This step is divided into three activities. First, develop a material sampling and testing plan to determine any missing data elements or to validate key inputs for selected pavement sections. Second, decide whether forensic investigations are required to confirm the assumptions embedded in the PMED. For instance, the percent of total rutting measured at the surface that can be assigned to each pavement layer and the location of crack initiation (bottom-up versus top-down, load-related cracking). Third, re-evaluate the number of roadway sections and data needed to execute the PMED. The main objective of this activity is to ensure that a sufficient number of pavement sections are available for the local validation-calibration effort.

**Step 7 - Assess Local Bias:** In this step, the PMED global calibration coefficients are used to estimate the performance indicators for each roadway segment (new pavement and rehabilitation strategies). To validate each distress prediction model, the predicted distress values are compared to the measured ones. Then, determine the standard error and bias of the estimate.

**Step 8 - Eliminate Local Bias of Distress and IRI Prediction Models:** This step is used to eliminate significant bias as specified by the agency.

**Step 9 - Assess the Standard Error of the Estimate:** Determine the difference between the standard error from the local calibration data set and the standard error derived from the global data set.

**Step 10 - Reduce Standard Error of the Estimate:** If the user decides that the standard error is too large, resulting in overly conservative designs at higher reliability levels, revisions to the local calibration coefficients of the transfer functions or statistical models may be needed. This step can be complicated and may require external revisions to the local calibration parameters or agency-specific values to improve prediction model precision.

**Step 11 - Interpretation of Results, Deciding on Adequacy of Calibration Parameters:** The local standard error of the estimate for each distress and IRI prediction model should be evaluated to determine the impact on the resulting designs at different reliability levels. A sampling template can be used to determine the design life of typical site features and pavement structures or rehabilitation

strategies for different reliability levels. An agency should review the expected pavement/rehabilitation design life within each cell of the sampling template.

## **Idaho Local Calibration Procedures**

The research team followed the guidelines of the MEPDG to perform the local calibration. The steps followed are described below:

### **Hierarchical Input Level Selection for Each Input Parameter**

PMED inputs are categorized into four general areas: project inputs, traffic inputs, climatic inputs, and pavement structure inputs. Project inputs include general information to identify the project, such as the type of design, construction and traffic opening dates, etc. These inputs also include information regarding the design criteria (threshold values for distresses and roughness) and reliability level for each distress selected in the criteria. Traffic, climate, and structure inputs must be completed to design/analysis a specific pavement structure. A brief listing of input parameters for flexible pavement design or analysis is presented in Table 11.<sup>(3,5)</sup> Appendix B includes a summary of all PMED required inputs for new and rehabilitated flexible pavements.

**Table 11 Required Flexible Pavement Input Parameters<sup>(3,5)</sup>**

Input Group		Input Parameter
Truck Traffic	Axle Load Distributions (Single, Tandem, Tridem, and Quad)	
	Truck Volume Distribution	
	Lane & Directional Truck Distribution	
	Tire Pressure	
	Axle Configuration, Tire Spacing	
	Truck Wander	
	Traffic Speed	
Climate		Temperature, Wind Speed, Cloud Cover, Precipitation, Relative Humidity
Material Properties	Unbound Layers & Subgrade Materials	Seasonally Adjusted Resilient Modulus – All Unbound Layers
		Classification & Volumetric Properties
		Coefficient of Lateral Pressure
		Plasticity index, Gradation Parameters, Effective Grain Sizes, Specific
		Gravity, Optimum Moisture Contents, Parameters to Define the Soil Water
		Characteristic Curve (SWCC)
	Bedrock	Elastic Modulus

**Table 11 Required Flexible Pavement Input Parameters (Cont.)**

Input Group		Input Parameter
Material Properties	Asphalt Concrete (AC), Recycled AC	Time-Temperature Dependent AC Dynamic Modulus
		AC Creep Compliance & Indirect Tensile Strength
		Volumetric Properties
		Asphalt Binder Viscosity (Stiffness) Characterization to Account for Aging
All Materials Except Bedrock		Unit Weight
		Poisson's Ratio
		Other Thermal Properties; Conductivity; Heat Capacity; Surface Absorptivity
Existing Pavement (In Case of Overlay Design)		Condition of Existing Layers

The PMED hierarchical input level feature provides the user flexibility in determining the required input parameters based on its importance and anticipated funding cost. For flexible pavements, the PMED includes three input levels for traffic and material properties. Inputs can consist of a mix of hierarchical levels. Hierarchical input levels include:

- Level 1 represents the highest level of accuracy and lowest level of input errors. Input parameters are measured directly either in the laboratory or in the field. This level of input has the highest cost in testing and data collection. It is important to note that Level 1 is more representative of agency or project specific traffic, materials, and climatic inputs.
- Level 2 represents an intermediate level of accuracy. Parameters are estimated from correlations based on limited routine laboratory test results or selected from an agency database.
- Level 3 represents the lowest level of accuracy. Usually, typical default values (best estimates) of input parameters are used in this level.

The research team studied and evaluated the inputs required to run the latest version of the PMED, and determined the level of input for each required parameter based on data availability. For the AC, ITD use six typical Superpave mixes (SP1 to SP6). These typical mixes were characterized and evaluated under RP193 project, and a database for these mixes' properties was developed. Thus, properties such as E\* and G\* were used from this database based on the mix type and use it in the software as level one.



Volumetric properties was determined from the Job Mix Formula (JMF), if such data is not available, level three was assumed. For the unbound layers and subgrade soils, data obtained from the ITD construction history and phase reports were used, most of the projects report R-value to characterize the strength of the layer. For this reason, level two was used, unless the modulus of resilience was determined. The annual daily truck traffic was determined from the projects design documents. However, there is no documentation for the vehicle class distribution and Axles per Tuck, thus for all projects, the traffic volume characteristics was determined based on the nearest Weigh-In-Motion (WIM) stations. Otherwise, Idaho default traffic distribution was assumed based on Idaho PMED User Guide.<sup>(6)</sup>

In addition, a sensitivity analysis was conducted to evaluate the effect of each parameter on the distresses prediction. Table 12, for example, presents the results of the sensitivity analysis on the impact of effective binder content on distress prediction. As shown, the increase of the effective binder content has a relatively low impact on IRI and rutting. However, it significantly reduced the bottom-up and top-down cracking. On the contrary, the thermal cracking increased with higher binder content.

**Table 12 Example of Sensitivity Analysis Effective Binder Content and Distress Prediction**

SP5-Mix#1					
Effective binder content (Vb%)	8	9	10	11	12
IRI (in/mile)	156	155	155	156	157
Bottom-up fatigue cracking%	4.7	2.7	2.3	2.0	1.9
Thermal cracking (ft/mile)	93	110	156	295	455
Top-down fatigue cracking (ft/mile)	4440	3801	3368	3057	2814
AC rutting (in)	0.60	0.61	0.62	0.63	0.64

Figure 22 shows the effect of different parameters on the rutting performance. As shown, the change in the higher binder grade has higher effect on rutting than the change in the binder content. AADTT and elevation of the road also have a strong contribution to the rutting accumulation.

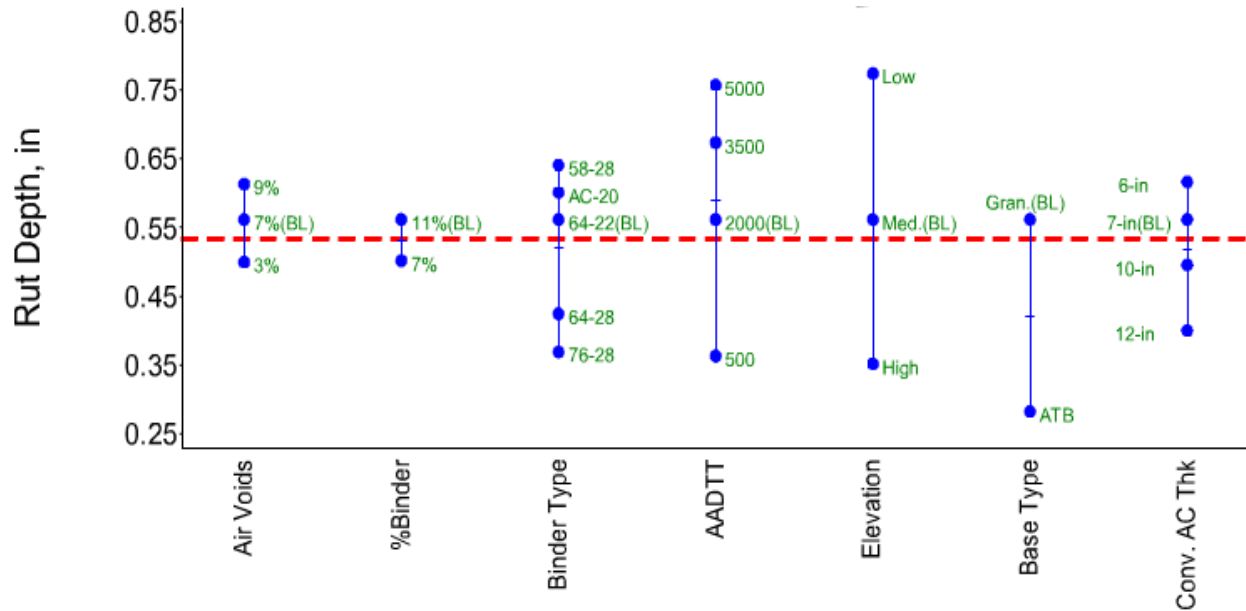


**Figure 22 Summary of Sensitivity Analysis and Input Effect on Rutting**

Many previous studies conducted sensitivity analyses to determine and study the inputs that have significant effect on the performance prediction of new flexible pavements. Table 13 represents the most significant design inputs based on many sensitivity analyses found in the literature.

**Table 13 Summary of Very Significant to Significant Key Design Input Parameters for New Flexible Pavements<sup>(4)</sup>**

Performance Indicators	Input Parameters/Predictors
<b>Longitudinal Cracking</b>	AADTT AC Layer Thickness AC Binder Grade Effective Asphalt Content AC Mixture In-Situ Air Voids AC Mixture Stiffness Foundation Quality Environmental Location
<b>Alligator Cracking</b>	AADTT AC Binder Grade Effective Asphalt Content AC Mixture In-Situ Air Voids AC Layer Thickness AC Mixture Stiffness (Insignificant at Very Thick AC Layers) Foundation Quality Environmental Location

**Table 13 Summary of Very Significant to Significant Key Design Input Parameters for New Flexible Pavements (Cont.)**

<b>Performance Indicators</b>	<b>Input Parameters/Predictors</b>
<b>AC Rutting</b>	AADTT AC Mixture Stiffness AC Layer Thickness AC Binder Grade AC Mixture In-Situ Air Voids Environmental Location
<b>Total Rutting</b>	AADTT Total Pavement Thickness GWT AC Binder Grade Foundation Quality Base Resilient Modulus Climatic Location
<b>Transverse Cracking</b>	AC Thickness AC Binder Grade AC Mixture In-Situ Air Voids AC Mixture Tensile Strength Environmental Location
<b>IRI</b>	Alligator Cracking Total Rutting Environmental Location Initial IRI

It was observed that, all input data obtained for each project contains a mix of input levels. Figure 23 shows an example of typical input data collected from the ITD construction history and material records. More data is provided in Appendix B.



Table 14 shows the matrix of received field cores based on mix design type (SP) and asphalt binder type. Each cell shows the available (blue shading) nominal maximum aggregate size (NMAS) for the combination of asphalt binder and mix type. For some cases more than one mix was available.

**Table 14 Summary of Received Field Cores Based on Mix Type and Asphalt Binder**

SP\PG	PG	PG	PG	PG	PG	PG	PG
	58-34	58-28	64-34	64-28	70-34	70-28	76-28
SP2							
SP3							
SP5							
SP6							

The nondestructive creep compliance test for each sample was conducted first at temperatures of -4 °F, 14 °F and 32 °F with loading duration of 100s, followed by IDT strength testing at 14 °F at a displacement rate of 0.1 inch/min. The deformation was continued until the load on the sample achieved a value of zero and the specimens completely split. The value of creep compliance and IDT strength were used to complete the ITD-MEPDG database. The data can be used as Level 1 inputs for the PMED thermal cracking model to predict mixture performance at low temperature. Table 15 and 16 show an example of the creep compliance and IDT results.

**Table 15 Creep Compliance Test Results for Mix (KN13823),(1/psi)**

Loading Time (Sec)	Low Temp (-4 deg F)	Mid Temp (14 deg F)	High Temp (32 deg F)
1s	2.44E-07	3.90E-07	5.27E-07
2s	2.46E-07	4.03E-07	5.97E-07
5s	2.68E-07	4.57E-07	7.21E-07
10s	3.07E-07	4.90E-07	8.63E-07
20s	3.08E-07	5.35E-07	1.09E-06
50s	3.52E-07	6.15E-07	1.57E-06
100s	3.83E-07	7.16E-07	2.08E-06

**Table 16 IDT Test Results for Mix (KN13823),(psi)**

Sample #	1	2	3	Average
IDT (psi) @ 14°F	613.42	611.49	697.23	640.7

The PMED inputs were mainly obtained from the ITD district material engineers. The structure of each section “as built,” material testing records, and quality control reports were provided. The database developed from the RP193 research project, containing Idaho asphalt mixes, materials, traffic, and climate was also a major source of data. If a specific input value was missing, the default value or its best estimate was entered considering its sensitivity level to the PMED predicted performance.

**Develop Local Experimental Plan and Sampling Template (Matrix)**

Based on the *Guide for the Local Calibration of the Mechanistic-Empirical Pavement Design Guide*, the sampling template, as much as possible, should be designed as fractional factorial matrix.<sup>(3)</sup> The matrix should cover different pavement structures, traffic loads, soil types, and rehabilitation techniques used by the agency. However, not all cells will likely be filled due to the limitations of covering all structure types. Also, each cell might be filled with or without replicate roadway segments. The matrix should be a balanced design that can be blocked for specific design features or site conditions for each agencies pavement and distress types.

In the process of identifying the road segments with ITD material engineers, it was challenging to develop the local experimental plan and sampling template with road sections covering all or most of the cells in the matrix. In Idaho’s case, the sections were identified on the availability of project and performance data. Table 17 below shows the sampling templates with selected pavement sections (blue shaded cells).

To reduce the number of pavement sections for calibration, it is allowable to use pavement section from earlier studies, such as LTPP sections. However, the research team recommended using less than half of the LPTT sites as calibration sites, due to the potential differences between the LTPP program and ITD’s operational policies.

**Table 17 Local Experimental Plan and Sampling Template**

Mix Type	Volume of Truck Traffic	Soil Type	Pavement Structure				
			New Design	Rehabilitation			FDR Stabilized With Cement
			Unbound Aggregate Base	AC Overlay		CIR	
Flexible	Rigid						
Neat Mixtures	Low	Coarse Grained					
		Low Plasticity					
		High Plasticity					
	High	Coarse Grained					
		Low Plasticity					
		High Plasticity					
Polymer Modified Asphalt	High	Coarse Grained					
		Low Plasticity					
		High Plasticity					

**Estimate Sample Size for Specific Distress Prediction Models**

According to recommended practice for PMED local calibration, cells of the sampling matrix should contain at least two replicate pavement sections to provide an estimate of the pure error. The estimated sample size is the total number of pavement sections based on the statistical confidence level of significance. A higher confidence level provides more reliable data, but requires a higher number of pavement sections. The level of significance, standard error, and threshold values affect the minimum recommended number of pavement sections required for local calibration. Estimation of samples size is provided in the following equations:

$$n \geq \left( \frac{tS_y}{e_t} \right)^2$$

$$\sigma^2 \geq (n - 1) \frac{S^2}{x_\alpha^2}$$

$$\frac{S_e}{S_y} \geq \left[ \frac{x_\alpha^2}{n - 1} \right]^{0.5}$$

where:

- n = Minimum number of sections required for each distress/IRI prediction model validation and local calibration
- $Z_{\alpha/2}$  = 1.601 for a 90 percent confidence interval
- $\sigma$  = Performance indicator threshold (design criteria)
- $e_t$  = Tolerable bias at 90 percent reliability
- $S_e$  = Standard error of estimate

#### Figure 24 Estimation of Minimum Sample Size

The *Guide for the Local Calibration of the Mechanistic-Empirical Pavement Design Guide* recommends the following minimum number of pavement sections for each distress:

- Total rutting: 20 roadway sections.
- Load-related cracking: 30 road sections.
- Non-load-related cracking: 30 roadway sections.
- Reflection cracking (AC surfaces only): 26 roadway sections.

Table 18 presents the assumptions used in the sample size computations. The threshold values and standard error of estimate for each distress/IRI model, shown in this table, are based on MEPDG recommendations.<sup>(3,5)</sup> The minimum sample size required for IRI model calibration is 79 pavement sections. In PMED, IRI is a function of the other distresses. Based on studies from other agencies, once cracking and rutting models are calibrated, the IRI model should yield reasonable predictions. Therefore, it is not necessary to use a large sample size to calibrate the IRI model.



**Table 18 Minimum Recommended Number of Pavement Sections for Local Calibration**

Performance Indicator	$\sigma$	$S_e$	n
Alligator Cracking (%)	20	7	8
Longitudinal Cracking (ft/mile)	2000	600	11
Transverse Cracking, (ft/mile)	700	250	8
Rutting (in.)	0.4	0.1	16
IRI (in/mile)	160	18	79

### Roadway Segments Selection

Based on the research teams experience with data available for in-service pavement sections in Idaho, level 1 input data is difficult to obtain for most of the required inputs. Thus levels 2 and 3 input data was used if level 1 data is unavailable. Previous outcomes of project RP193 (KLK557) played a vital role in the characterization of the material, traffic, and climate of the selected pavement section.

In addition to the Idaho LTPP sections, the research team, in coordination with ITD material engineers, identified and selected roadway sections from different districts in Idaho. These pavement sections covered reasonable range of environmental conditions, traffic levels, and subgrade strength. ITD provided the available project data, as well as the time series of measured field performance data of each project. These data include but are not limited to:

- Project location (latitude and longitude).
- Construction year and month.
- As-built pavement structure (layer type and thickness of each layer).
- AC/base/subbase/subgrade material properties.
- Traffic volume and axle load spectra data.
- Performance data (rutting, longitudinal cracking, alligator fatigue cracking, transverse cracking, and IRI) at different points of time.
- Maintenance history.

In order to have a reasonable performance record, pavement sections having more than 5 years of performance data is recommended.<sup>(5)</sup> Pavements nearing major rehabilitation activities were identified as better candidates since they tend to show a variety of distress types. However, selected pavement sections also needed to be restricted to those built with Superpave AC mixes to be able to utilize the materials database was developed under RP193.<sup>(4)</sup>

As described previously, ITD cracking data is collected in a format different from the PMED. Therefore, it was difficult to quantify the cracking severity level. For this reason, the research team used the video log files to redevelop the cracking data. The cracking observation was limited to a 3-year period for all pavement sections based on the availability of the video log files. Having three data points for each roadway section provides more reliable data than the severity level classification; moreover, each roadway section has same number of performance observations. Statistically, it would not be good practice to have some roadway segments with more observations than others, because segments that having more observations would have a greater influence on the validation and calibration process than the segments with less observations. Table 19 and Figure 25 shows the selected pavement sections and geographical locations, respectively.

**Table 19 List of the Roadway Segments Selected for Local Calibration**

District #	Construction Year	Route	Beg MP	End MP
D1	2008	US-95	403.5	408.75
	2004	US-95	411.84	415.83
	2002	US-95	415.5	421.3
	2006	SH-3	76.822	84.201
	2013	SH-3	103.15	111.38
	2013	US-95	477.1	486.36
D2	2008	SH006	100	104.5
	2004	SH008	0	1.76
	2003	US-95	344	344.57
	2003	US-95	366.59	373.03
	2007	US-95	319.88	337.67
	2008	SH003	5.00	8.5
	2011	SH013	11.257	18.711
	2010	SH013	18.68	25.378
D3	2005	US-95	277.28	279.1
	2012	SH 55	113.9	115.9
	2010	US 95	64.94	67.14
	2011	US 95	0	16.7
	2012	US 95	38.4	46.6
	2011	SH 55	66.1	80.63
	2010	SH 78	29.1	36.7
	2010	SH 78	0	11.5
	2011	SH 51	60	76.9
	2011	SH 55	63.2	66.1
	2011	SH 51	47.7	54.6
	2011	SH 78	60	76
	2012	SH 55	13.1	18
	2012	US 20/26	0	1.58
2012	US 95	47.58	60.87	

**Table 19 List of the Roadway Segments Selected for Local Calibration (Cont.)**

District #	Construction Year	Route	Beg MP	End MP
D3	2012	SH 16	0	13.392
	2013	SH 52	14.4	30.42
D4	2000	SH 77	18.5	23
D5	2005	US91	JCT-15	JCT US-91
	2011	SH34	Conda RD	Blackfoot RV
	2014	US30	328.6	330.7
D6	2012	US20	328.6	335.7
	2011	US20	377.08	387.03

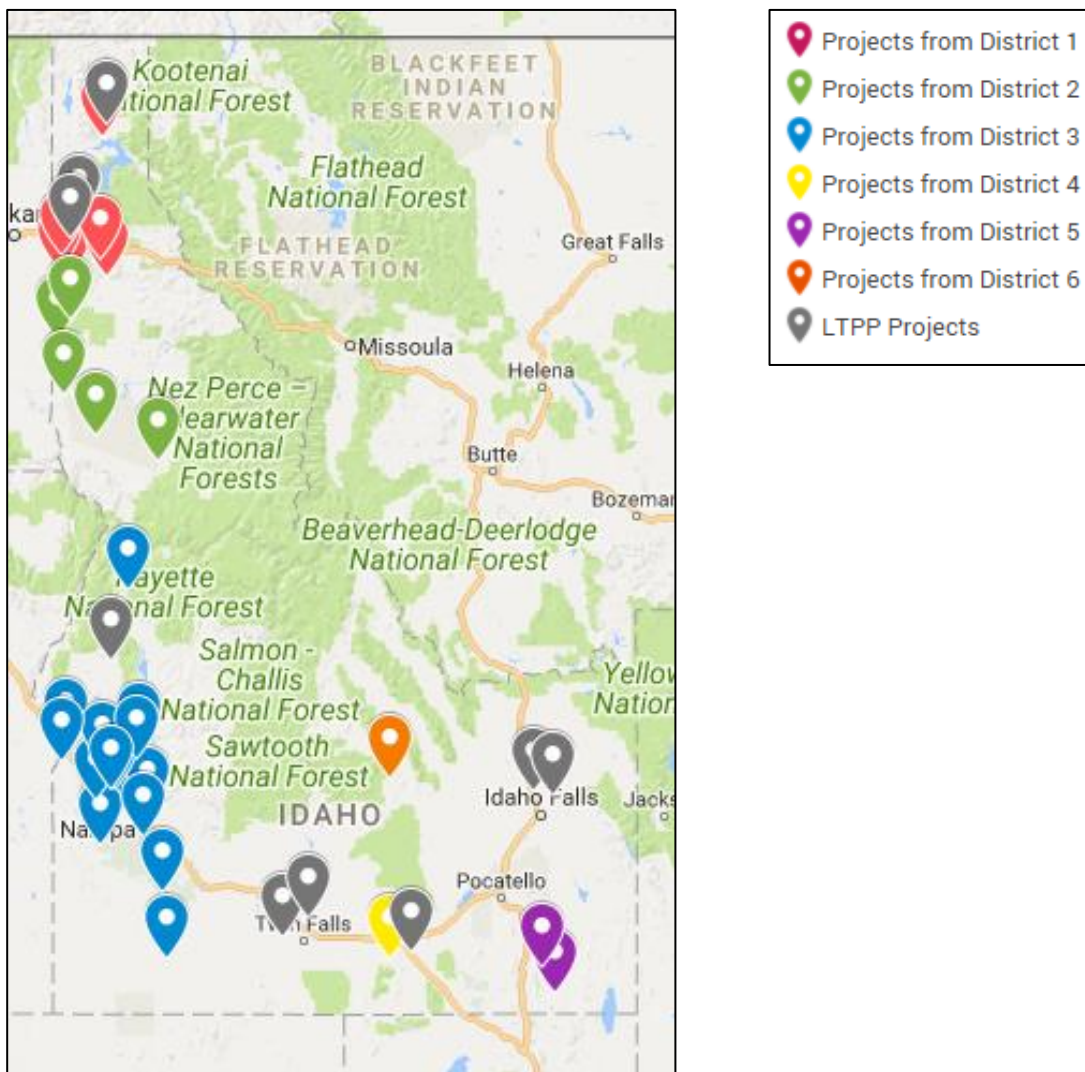


**Figure 25 Geographical Locations of the Selected Road Segments for Local Calibration**

**Extract and Evaluate Distress Project Data**

After selecting the roadway segments, the next step is to collect all data and identify any missing information. The collected data for the calibration can be divided into two main categories, input data (e.g., traffic, pavement structure, layer properties) and performance data. For AC pavements, PMED performance criteria includes rutting, load-related cracking (alligator and longitudinal), thermal cracking (transverse), reflective cracking in AC overlays, and IRI.

ITD only collects surface rut depth, however, PMED determines rutting in each pavement layer (AC, base, and subgrade). Collecting rut depth for each individual layer is expensive, time consuming, since trenches are needed to evaluate rutting at each layer, and requires lane closures which are disruptive to the traveling public. Therefore, the research team used the simple approach to determine the rut depth for each layer. This approach includes determining the percent of total rutting in each layer from the PMED output and multiplying that percent by the total measured rutting.

Table 20 shows the types of asphalt and rigid pavement cracking reported by ITD. Each crack type includes three severity levels; low, medium, and high. However, the PMED only predicts longitudinal (top down fatigue cracking), transverse (thermal cracking), and alligator (bottom-up fatigue cracking).

**Table 20 Asphalt and Rigid Pavement Cracking Types Collected in Idaho**

<b>Flexible (asphalt) cracking collected</b>	<b>Rigid (concrete) cracking collected</b>
Alligator	Transverse Slab
Block	Spalling
Edge	Scaling
Transverse	Meander
Longitudinal	Faulting
Patching/Potholes	Corner

Table 21 compares the current IDT distress report with those of the PMED.

**Table 21 Comparison between ITD and PMED Flexible Pavement Distresses**

<b>Distress Type</b>	<b>ITD</b>	<b>PMED</b>
Permanent deformation - total pavement	Total rut depth (inch)	Rut depth (inch)
Permanent deformation - AC only	Not reported	Rut depth (inch)
Bottom-up fatigue (alligator) cracking	Light/moderate/heavy extent Slight/moderate/heavy severity	Area percentage
Thermal (transverse) cracking	Light/moderate/heavy extent Slight/moderate/heavy severity	ft/mile
Top-down fatigue (longitudinal) cracking	Light/moderate/heavy extent Slight/moderate/heavy severity	ft/mile

In order to use the historic ITD performance data, the research team first quantified distresses according to the ITD pavement rating manual guide,<sup>(35,36)</sup> using the average or representative value for each distress rating. Table 22 shows the cracking severity and extent per the ITD manual. Cracking is reported as light, moderate, and heavy extent and slight, moderate, and heavy severity, which could be reproduced by assigning an average cracking value for each rating. However, the level of accuracy was very low, and the variability was high. It was also difficult to quantify the cracks based on the crack rating and severity level, especially, when the roadway section has the same rating for different years.

**Table 22 Cracks Types, Extent, and Severity Level**

<b>Crack type</b>	<b>Extent level</b>	<b>Severity Level</b>
<b>Longitudinal Cracking</b>	<b>Light extent</b> of cracking corresponds to 100 feet or less of cracking per 500 feet.	<b>Slight Severity:</b> Crack width is hairline up to 1/8"
	<b>Moderate extent</b> of cracking corresponds to 100- 500 feet of cracking per 500 feet.	<b>Moderate Severity:</b> Crack width is 1/8" - 1/4" or there is a dip 3" - 6" wide at the crack
	<b>Heavy extent</b> of cracking corresponds to more than 500 feet of racking in 500 feet.	<b>Heavy Severity:</b> Crack width is more than 1/4" or there is a distinct dip of 6" - 8" wide or there is visible vegetation in the crack.
<b>Transverse Cracking</b>	<b>Light extent</b> of cracking corresponds to 1-4 cracks per 500 feet.	<b>Slight Severity:</b> Crack width is hairline up to 1/8"
	<b>Moderate extent</b> of cracking corresponds to 4-10 cracks per 500 feet.	<b>Moderate Severity:</b> Crack width is 1/8" - 1/4" or there is a dip 3" - 6" wide at the crack
	<b>Heavy extent</b> of cracking corresponds to more than 10 in 500 feet, or less than 50 feet in between cracks.	<b>Heavy Severity:</b> Crack width is more than 1/4" or there is a distinct dip of 6" - 8" wide or there is visible vegetation in the crack.
<b>Alligator Cracking</b>	<b>Light extent</b> of cracking corresponds to 10% of less of the total evaluation section having cracking.	<b>Slight Severity:</b> Large alligator cracking, 3 feet or more in size.
	<b>Moderate extent</b> of cracking corresponds to 10-40% of the total evaluation section having cracking.	<b>Moderate Severity:</b> Alligator cracking 1 foot to 2 feet in size
	<b>Heavy extent</b> of cracking corresponds to more than 40% of the total evaluation section having cracking	<b>Heavy Severity:</b> Alligator cracking smaller than 1 foot in size

As an alternative approach, the research team used the video log data files and analyze each photo manually to collect the cracking data. Figure 26 shows an example of the photos from the video log.

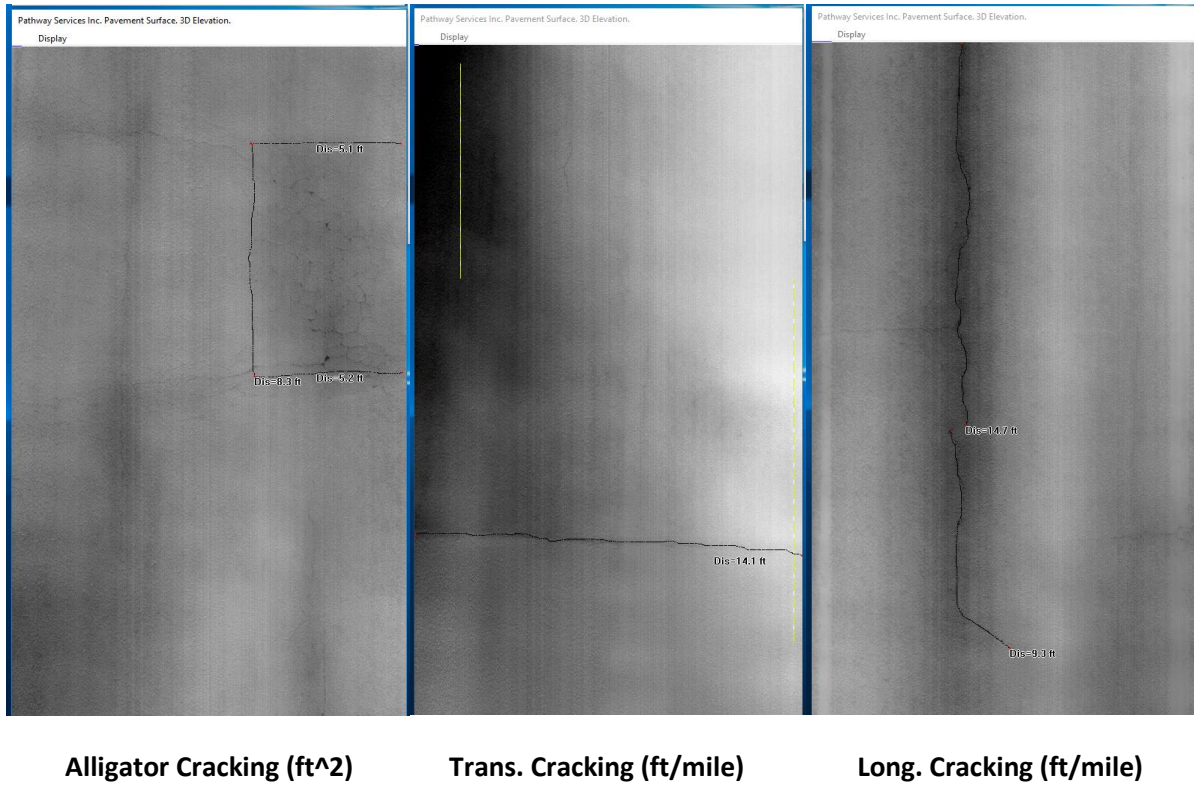


**Figure 26 Example of Extracted Images of the Video-Based Distress Data Collection**

The cracking data observation was limited to a 3 year period (2014 to 2016) for all pavement section. The procedure was to track each roadway section using PathView software provided by ITD, and quantify the amount of alligator, longitudinal, and thermal cracking. Each photo has a dimension that represent 13.6 ft. wide and 26.4 feet long. The alligator cracking was measured as an area in square feet, and longitudinal and thermal cracking were measured in ft. using a measurement tool available in the PathView software. Cracks were recorded for each photo. The data was tabulated for 200 photos, representing 1-mile (Figure 27). Vendor software can analyze images automatically; however, it was not available to the research team, and based on communications with the software vender, the automated tool does not provide the accuracy level needed for PMED calibrated. For these reason, the research team conduct crack measurement manually.

SH078-2013				
Tracking# 22	Year 2013	Mile Post 0.00 - 1.00	Total # of 200 images	Section Area = 71808 ft <sup>2</sup>
<b>Summary of Section results</b>				
<b>Distress type</b>		<b>Alligator Cracking (%)</b>	<b>Trans. Cracking (ft/mile)</b>	<b>Long. Cracking (ft/mile)</b>
<b>Totals</b>		<b>0.022</b>	<b>22.59</b>	<b>43.85</b>
<b>Image Analysis</b>				
<b>Image #</b>	<b>Distance (ft)</b>	<b>Alligator Cracking (ft<sup>2</sup>)</b>	<b>Trans. Cracking (ft)</b>	<b>Long. Cracking (ft)</b>
1	26.4			
2	52.8			
3	79.2			
4	105.6			
	↓		↓	
198	5227.2			
199	5253.6			
200	5280			

**Figure 27 Example of Data Sheet for Cracking Analysis Using PathView Video Images**

ITD collects all other inputs, such as traffic, climate, and materials, in the same process as the PMED.

**Conduct Field and Forensic Investigations**

Since, the research team obtained the video log data for the selected road sections, there was sufficient data to observe crack propagation over the three year period. However, for rutting, it was impossible to determine if the rutting happened in the AC layer alone or in all layers of the roadway section. For this reason, the research team conducted a field investigation on one heavily loaded roadway section, State Highway 8, located in district two (SH008). This roadway section developed rut depths, and was one of the best sections to conduct a forensic investigation. Figure 28 shows the roadway section plan and trench locations.



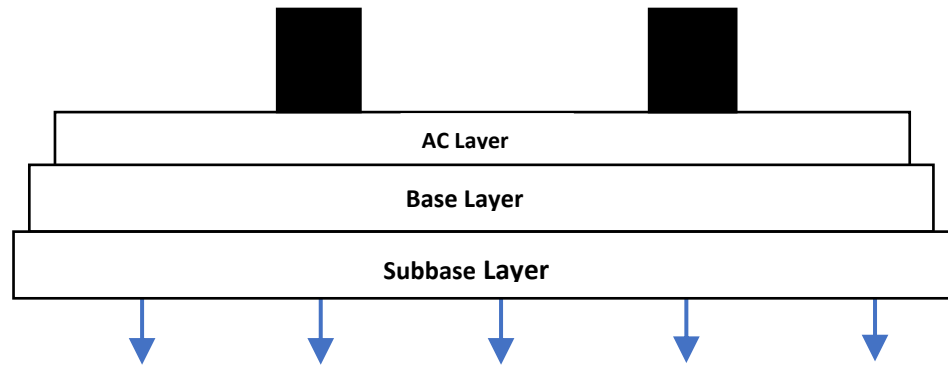


**Figure 28 Plan of SH008 Trench Locations**

The AC layer rutting was less than the total rutting for all trenches. This concludes the measured rutting happened in all layers. Which is in support of the assumption used to calculate rutting in each layer. Figure 29 and 30 show a pavement cross section and rut measurements taken during the investigation.



**Figure 29 Trench Side View**



Rut Depth (in.)	Left Edge	Left wheel path	Center of the lane	Right wheel path	Right Edge
<b>Total rutting ( surface)</b>	0	0.48,0.49	0	0.33, 0.28	0
<b>AC layer thickness</b>	4.8, 4.92,4.83	4.26,4.28, ,4.30	4.73,4.75,4.78	4.62,4.69,4.63	4.79,4.83,4.82
<b>Base layer thickness</b>	3.67	3.63	3.58	3.55	3.59
<b>Subbase layer thickness</b>	17.3	16.5	16.5	16.5	16.5

**Figure 30 Example of Trench Rut Depth Measurements on SH008**

**Assess Local Bias: Validation of Global Calibration Values to Local Conditions, Polices, and Materials**

Bias is defined as consistent under or over prediction of distress/IRI and can be determined using statistical methods. A significance level,  $\alpha$ , of 0.05 or 5 percent, was assumed for all hypothesis testing described explained:

**Hypothesis 1:** Perform a paired t-test to test:

- i.  $H_0$ : Mean measured distress/IRI = mean predicted distress/IRI.
- ii.  $H_A$ : Mean measured distress/IRI  $\neq$  mean predicted distress/IRI.

If the hypothesis is accepted, local calibration is not required and the global calibration coefficients are robust and produce accurate predictions of pavement distress. Rejecting the null hypothesis ( $p$ -value < 0.05) implies the measured and predicted PMED distress/IRI are from different populations. This indicates that for the range of distress/IRI used in the analysis, the PMED results in biased predictions. When the null hypothesis is rejected, adjustments need to be made to the calibration coefficients due to the significant differences found between the predicted and measured performance. It will also be necessary to determine which calibration coefficients are causing these differences so appropriate adjustments can be made. A full factorial is not needed for local calibration, but replication within some

cells is needed when a partial or fractional factorial is used. The experimental plan and sampling matrix is developed around the hypothesis that there is no significant bias and no error between the measured and predicted performance.<sup>(3,5)</sup> Figure 31 shows an example of rutting and IRI distress indicators and the null hypothesis test.

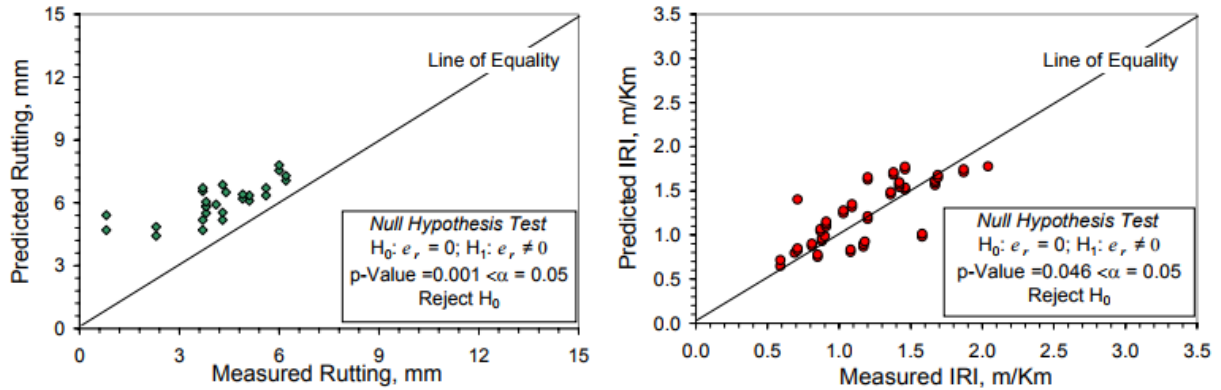


**Figure 31 Distress Indicators (Rutting and IRI) with the Null Hypothesis Test**

After collecting all the data for the selected pavement sections, the research team ran the PMED. Table 23 presents the statistical analysis of the selected roadway sections using the globally-calibrated coefficients. As can be seen, distresses with a p-value less than 0.05 indicates significant difference between the measured and predicted distress. Therefore, local calibration should be conducted to reduce the bias and the sum of standard errors.

**Table 23 Summary of Statistical Analysis of Predicted vs. Measured Distress Using the Global Calibration Coefficients**

Performance Indicator	N	Bias $e_{r(\text{mean})}$	Standard Error (Se)	Sy	Se/Sy	R <sup>2</sup> , %	p-value (t-test)
Total Rutting (in)	113	-0.0686	0.093	0.034	2.783	3.7%	<0.0001
Alligator Cracking (%)	101	-0.412	1.103	0.202	5.467	0.4%	<0.0001
Longitudinal Cracking (ft/mile)	96	-455.87	841.047	63.193	13.309	28.65%	<0.0001
Transverse Cracking (ft/mile)	118	63.559	207.160	197.325	1.050	1.95%	<0.0001
IRI (in/mile)	128	-16.805	34.310	51.188	0.670	35%	<0.0001

**Eliminate Local Bias of Distress and IRI Prediction Models**

The cause of the local bias should be identified and removed in this step. Elimination of the bias should consider traffic conditions, climate, and material characteristics. Performance prediction may be improved by adjusting calibration coefficients, rerunning the PMED, and analyzing the results. Table 24 shows the recommended calibration coefficients that can be modified to eliminate bias.<sup>(5)</sup>

**Table 24 Calibration Parameters to Adjust to Eliminate Bias<sup>(3,5)</sup>**

Distress		Eliminate Bias
Total Rutting	AC and Unbound Materials Layers	$K_{r1}, \beta_{s1}, \beta_{r1}$
Load Related Cracking	Alligator Cracking	$C_2, K_{f1}$
	Longitudinal Cracking	$C_2, K_{f1}$
	Semi-Rigid Pavements	$C_2, \beta_{c1}$
Non-Load Related Cracking	Transverse Cracking	$\beta_{f3}$
Roughness, IRI		$C_4$

**Assess the Standard Error of the Estimate**

After eliminating the bias, coefficient of determination ( $R^2$ ) and standard error of the estimate (SEE) are computed using the developed local calibration coefficients to evaluate the new calibrated models goodness of fit. The calibrated model's  $R^2$  and SEE are compared to the PMED global calibration  $R^2$  and SEE. Engineering judgment and diagnostic statistics can be used to determine the reasonableness of goodness of fit. Models exhibiting a low  $R^2$  (i.e., less than 50 percent) or excessive SEE are deemed as having a poor goodness of fit.

### Reduce Standard Error of the Estimate

If the standard error is too large, which results in very conservative pavement designs at higher reliability levels, the local calibration coefficients should be re-adjusted. Recommendations calibration parameters to be adjusted to reduce the standard error are given in Table 25.

**Table 25 Calibration Parameters to Adjust to Reduce the Standard Error<sup>(3,5)</sup>**

Distress		Reduce Standard Error
Total Rutting	AC and Unbound Materials Layers	$K_{r2}$ , $K_{r3}$ , and $\beta_{r2}$ , $\beta_{r3}$
Load Related Cracking	Alligator Cracking	$K_{f2}$ , $K_{f3}$ , and $C_1$
	Longitudinal Cracking	$K_{f2}$ , $K_{f3}$ , and $C_1$
	Semi-Rigid Pavements	$C_1$ , $C_2$ , $C_4$

## Results of Calibration of Performance Models

### Rutting Models

Only total rutting is reported in the ITD database; therefore, the research team used the proportional rutting percent of each layer based on the PMED prediction using the global calibration coefficients. Once the rutting of each layer (AC, base, and subgrade) was determined, the rutting model for each layer was calibrated separately. The comparison of predicted and measured rutting before and after local calibration for all pavement sections are shown in Figures 32 through 47 and global and local calibration coefficients are summarized in Tables 26 through 33.

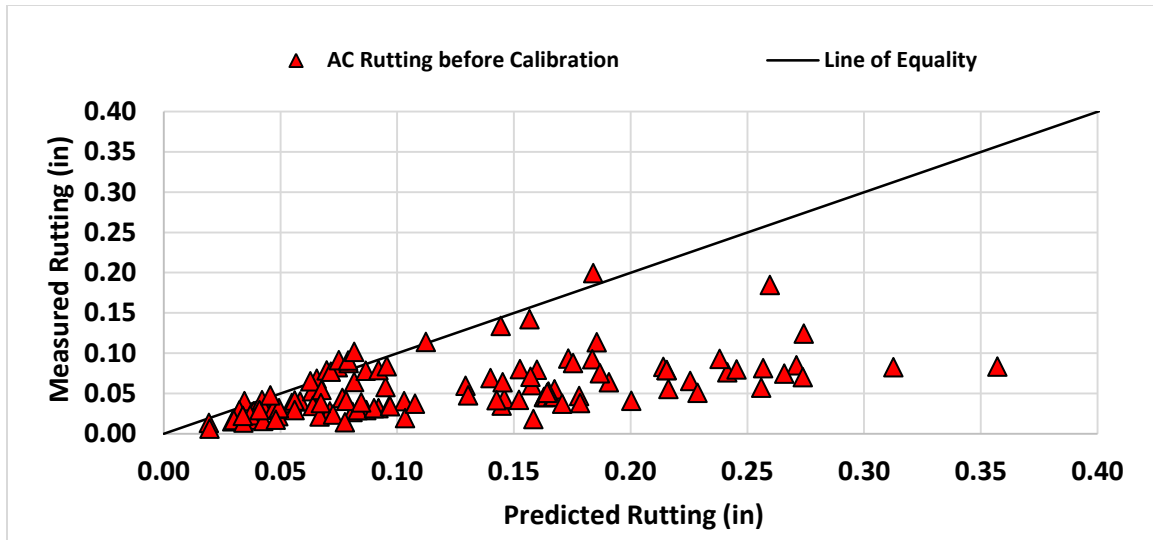


Figure 32 Measured vs. Predicted AC Rutting Using Global Calibration Coefficients

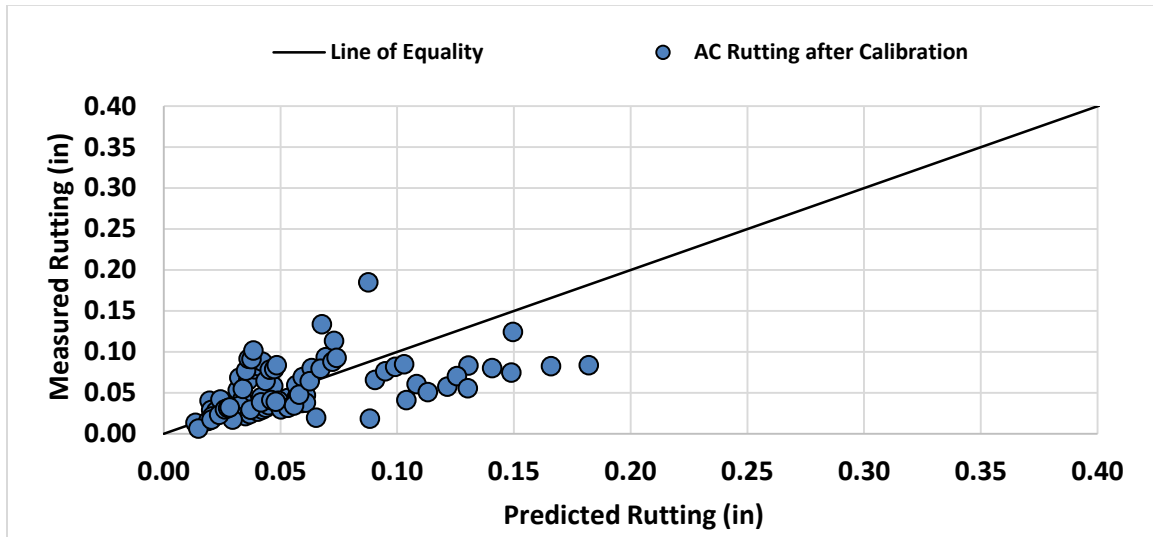


Figure 33 Measured vs. Predicted AC Rutting Using Local Calibration Coefficients

Table 26 Calibration Coefficients for AC Layer Rutting

Calibration Coefficients	$\beta_{1r}$	$\beta_{2r}$	$\beta_{3r}$	N	Bias, $e_{r(\text{mean})}$	Standard Error, Se	Se/Sy	R <sup>2</sup> , %	p-value (Paired t-test)
Global	1.00	1.00	1.00	113	-0.0293	0.040	1.707	29.5	6.79E-21
Local	3.00	1.00	0.661	113	-9E-05	0.021	0.888	47.8	0.132

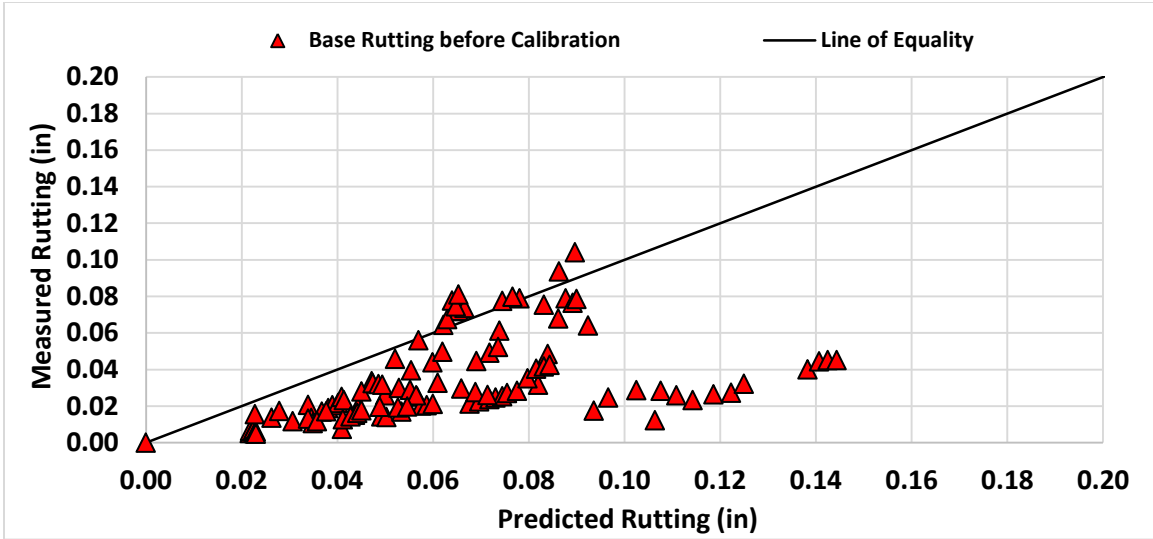


Figure 34 Measured vs. Predicted Granular Base Rutting Using Global Calibration Coefficients

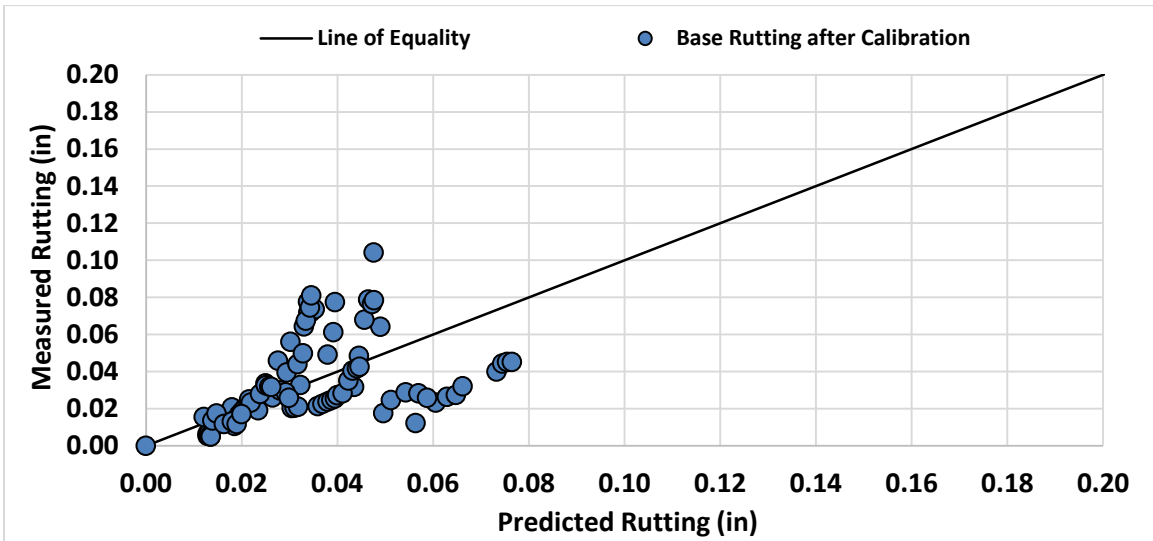


Figure 35 Measured vs. Predicted Granular Base Rutting Using Local Calibration Coefficients

Table 27 Calibration Coefficients for Base Layer Rutting

Calibration Coefficient	$\beta_{1s}$ (Coarse)	N	Bias, $e_{r(\text{mean})}$	Standard Error, Se	Se/Sy	$R^2$ , %	p-value (Paired t-test)
Global	1.00	113	-0.08955	0.120	2.571	23.9	7.62E-21
Local	0.53	113	-4.43E-05	0.046	0.987	48.5	0.482

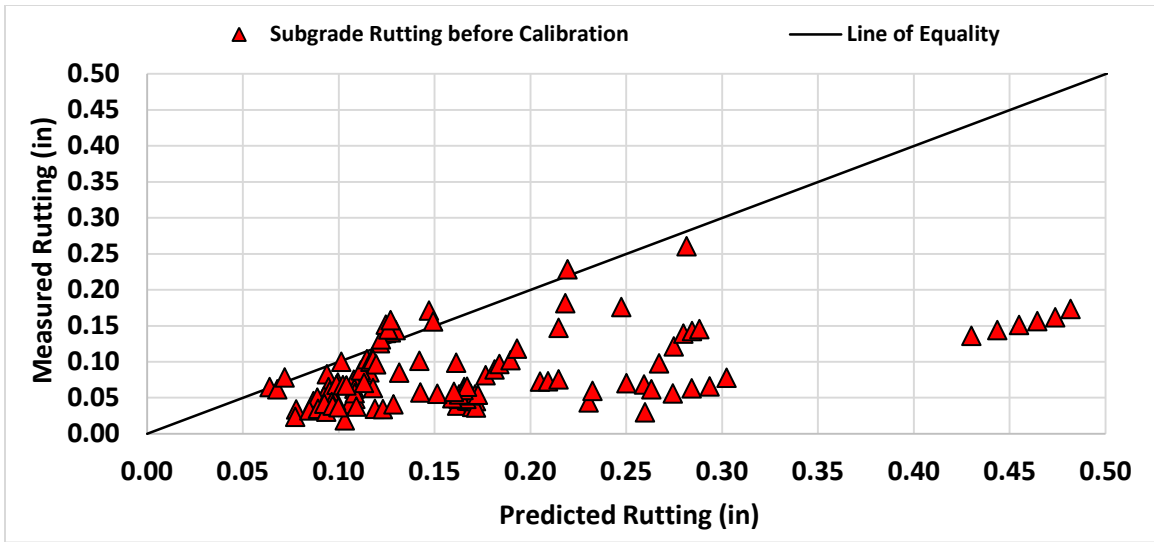


Figure 36 Measured vs. Predicted Subgrade Rutting Using Global Calibration Coefficients

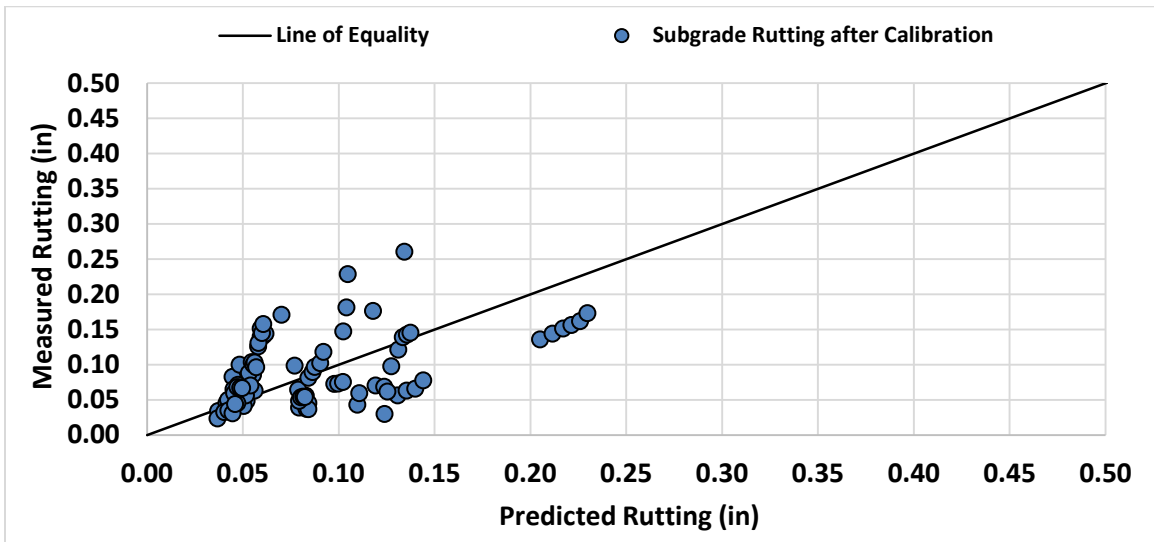


Figure 37 Measured vs. Predicted Subgrade Rutting Using Local Calibration Coefficients

Table 28 Calibration Coefficients for Subgrade Rutting

Calibration Coefficients	$\beta_{1s}$ (Fine)	N	Bias, $e_{r(\text{mean})}$	Standard Error, Se	Se/Sy	R <sup>2</sup> , %	p-value (Paired t-test)
Global	1.00	113	-0.18745	0.240	2.973	22.9	5.93E-22
Local	0.477	113	-0.00379	0.096	1.183	47.4	0.496



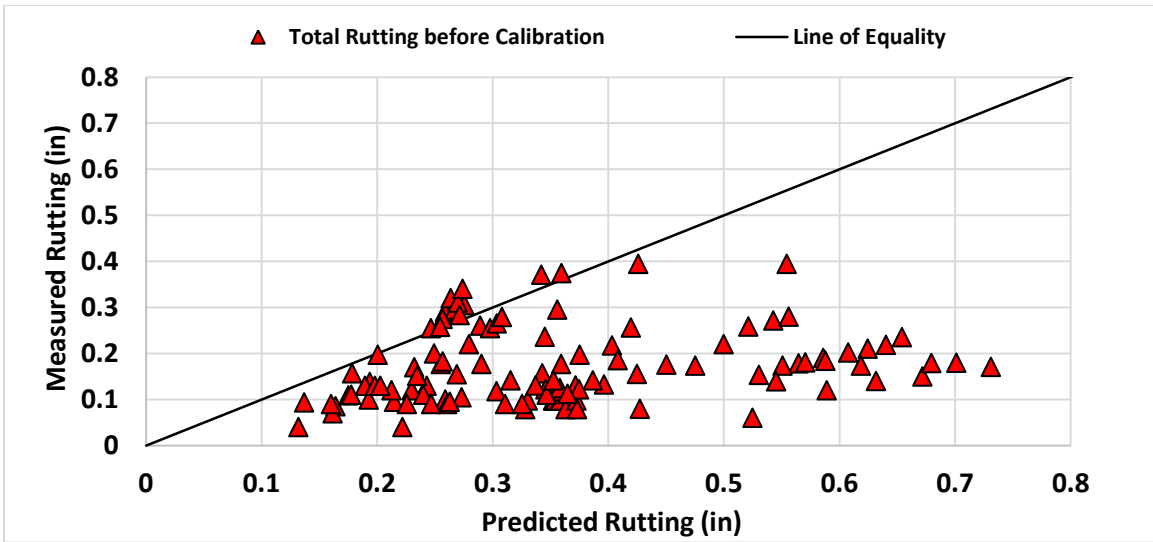


Figure 38 Measured vs. Predicted Total Rutting Using Global Calibration Coefficients

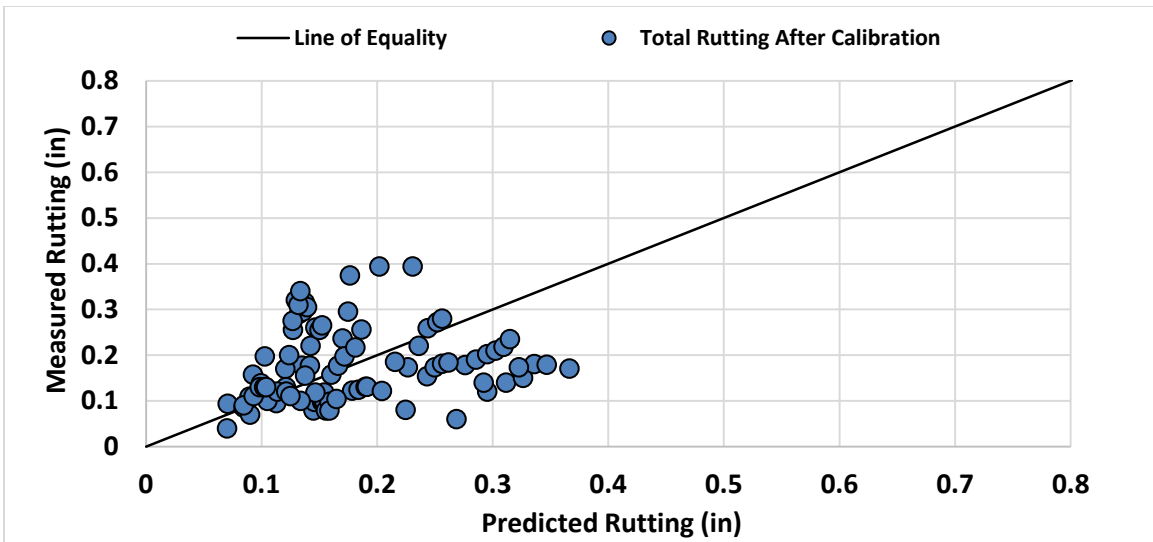


Figure 39 Measured vs. Predicted Total Rutting Using Local Calibration Coefficients

Table 29 Calibration Coefficients for Rutting

Calibration Coefficient	$\beta_{1r}$	$\beta_{2r}$	$\beta_{3r}$	$\beta_{1s}$ (Coarse)	$\beta_{1s}$ (Fine)	N	Bias, $e_{r(\text{mean})}$	Standard Error, Se	Se/Sy	$R^2$ , %	p-value (Paired t- test)
Global	1.00	1.00	1.00	1.00	1.00	113	-0.06858	0.093	2.783	3.7	8.27E-25
Local	3.000	1.000	0.661	0.530	0.477	113	-0.00365	0.035	1.034	17.6	0.338

### Longitudinal (Top-Down) Cracking Model

Figure 24 shows a comparison of measured and predicted longitudinal cracking using the globally-calibrated coefficients. The globally-calibrated model over-predicts the extent of longitudinal cracking. The researchers conducted several iterations and were unable to calibrate the model. The locally-calibrated coefficients that result in a lower bias are shown in Table 30. However, this improvement is not statistically significant. Some agencies have reported the same conclusion and recommend using the longitudinal crack prediction for informational and experimental purposes, and not for design at this time.<sup>(22,24,32)</sup> The longitudinal cracking prediction model is under development in NCHRP Project 1-52, A Mechanistic-Empirical Model for Top-Down Cracking of Asphalt Pavement Layers.

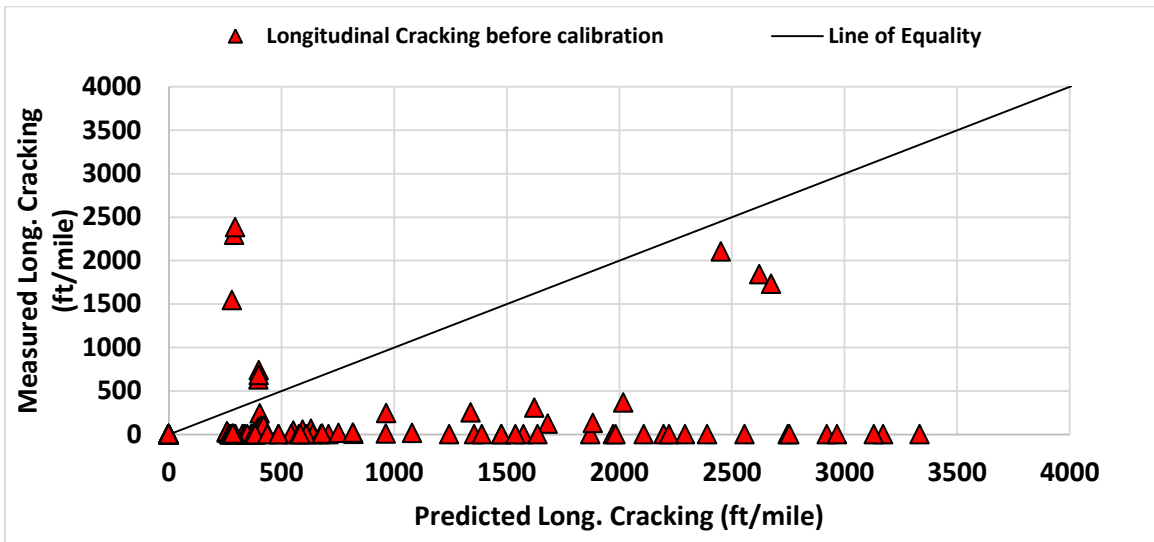


Figure 40 Measured vs. Predicted Longitudinal Cracking Using Global Calibration Coefficients

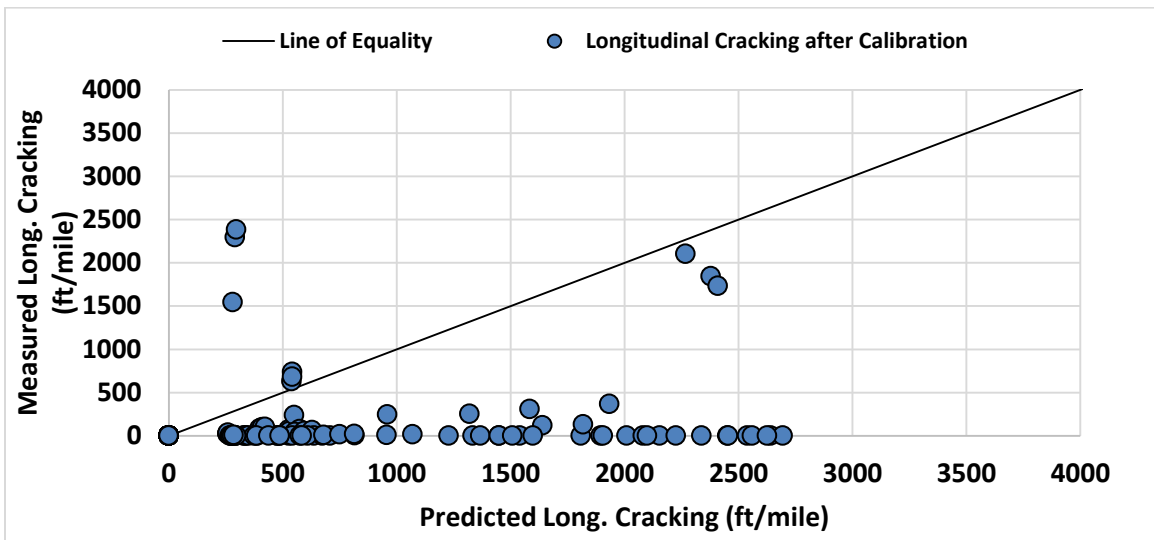


Figure 41 Measured vs. Predicted Longitudinal Cracking Using Local Calibration Coefficients

**Table 30 Calibration Coefficients for Longitudinal Cracking**

Calibration Coefficient	$B_{f1}$	$B_{f2}$	$B_{f3}$	$C_1$	$C_2$	N	Bias, $e_{r(\text{mean})}$	Standard Error, Se	Se/Sy	$R^2$ , %	p-value (Paired t-test)
Global	1.00	1.00	1.00	7.00	3.50	123	-634.56	1136.54	2.57	2.27	8.05E-12
Local	1.00	1.00	1.00	4.533	0.229	123	-602.78	1047.86	2.37	15.70	1.40E-12

### Alligator (Bottom-Up) Cracking Model

Figure 26 and 27 compare the AC alligator cracking measurements and corresponding predictions obtained using the nationally calibrated model, statistically there is no significant difference between predicted and measured alligator cracking. The research team was able to improve the model further by reducing the error. Table 31 shows the developed calibration coefficients.

### Thermal (Transverse) Cracking Model

Previous studies reported that little or no thermal cracking was predicted when using the appropriate PG binder for local climate conditions. As seen in Figure 28, the globally-calibrated thermal cracking model under predicts thermal cracking. Modification of calibration coefficients could not provide significant changes in PMED model predictions. In PMED v2.3.1, there is no input cell to change the thermal cracking model local calibration coefficient ( $\beta_{t1}$ ). Therefore, the research team adjusted the K value from the global calibration to compensate for the  $\beta_{t1}$  in thermal cracking model. Table 32 presents the statistical analysis of thermal cracking model using globally and locally coefficients.

### International Roughness Index Model

Figure 30 and 31 compares the predicted and measured IRI values using the global- and local calibrated coefficients, respectively. Both IRI models provide good estimation to field measurements. Further modification to the IRI model calibration coefficients were considered to improve prediction are shown in Table 33.

Interpretation of results and deciding on adequacy of the calibration coefficients is the last step in the calibration process. The standard error of the estimate for each distress and IRI prediction model should be evaluated to determine the impact on the resulting designs at different reliability levels. If the local calibration coefficients produce reasonable designs, the developed calibration coefficients can be implemented. If not, the calibration coefficients should be re-adjusted.

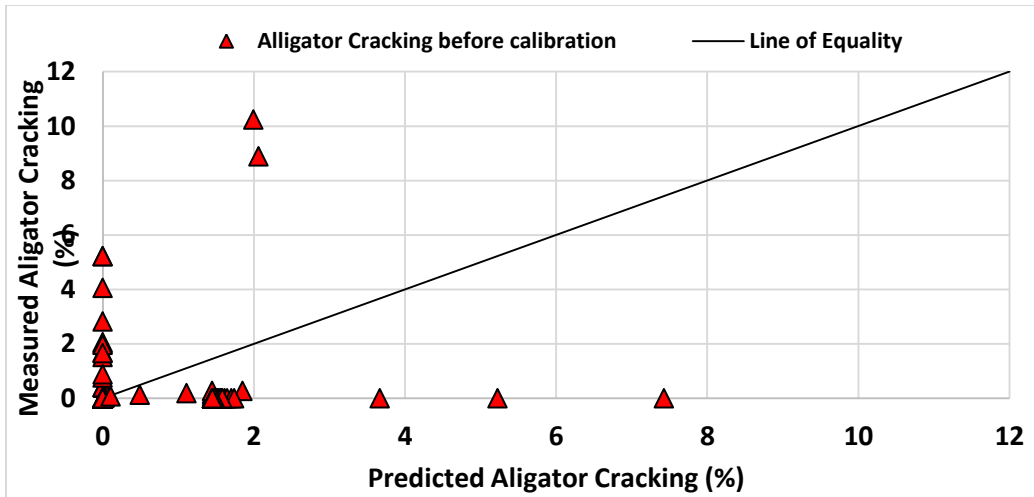


Figure 42 Measured vs. Predicted Alligator Cracking Using Global Calibration Coefficients

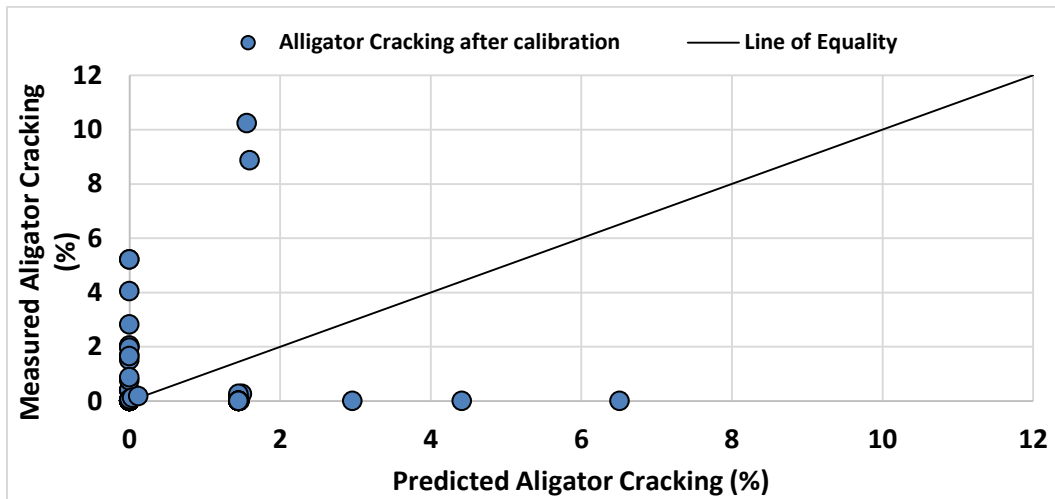


Figure 43 Measured vs. Predicted Alligator Cracking Using Local Calibration Coefficients

Table 31 Calibration Coefficients for Alligator Cracking

Calibration Coefficients	$B_{f1}$	$B_{f2}$	$B_{f3}$	$C_1$	$C_2$	N	Bias, $e_{r(\text{mean})}$	Standard Error, Se	Se/Sy	$R^2$ , %	p-value (Paired t-test)
Global	1.00	1.00	1.00	1.00	1.00	123	-0.216	1.742	1.213	0.22	0.0903
Local	1.00	1.00	1.00	1.00	0.824	123	-0.205	1.745	1.211	4.50	0.0956

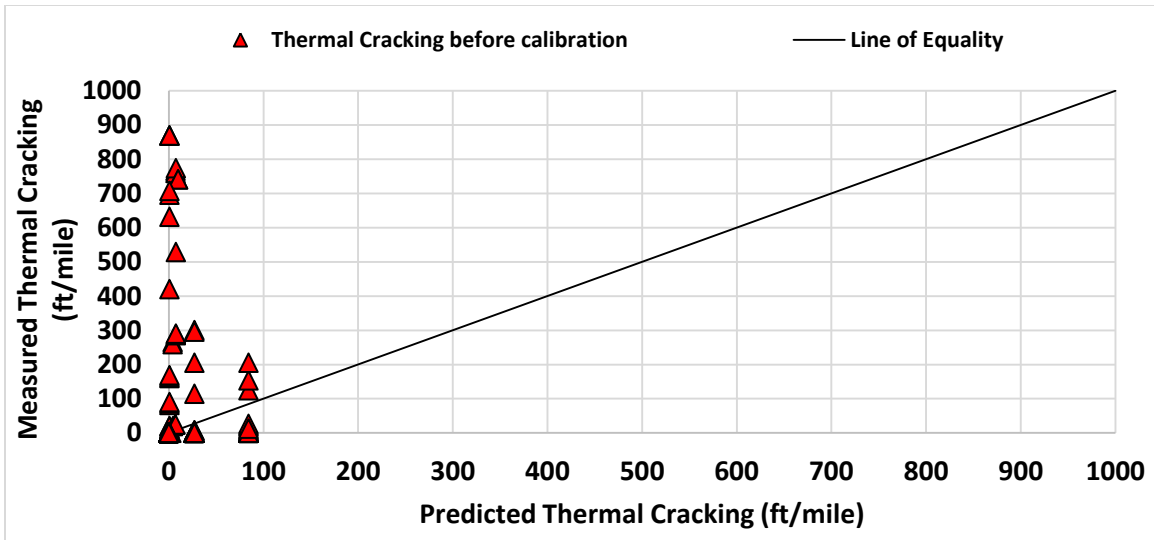


Figure 44 Measured vs. Predicted Transverse Cracking Using Global Calibration Coefficients

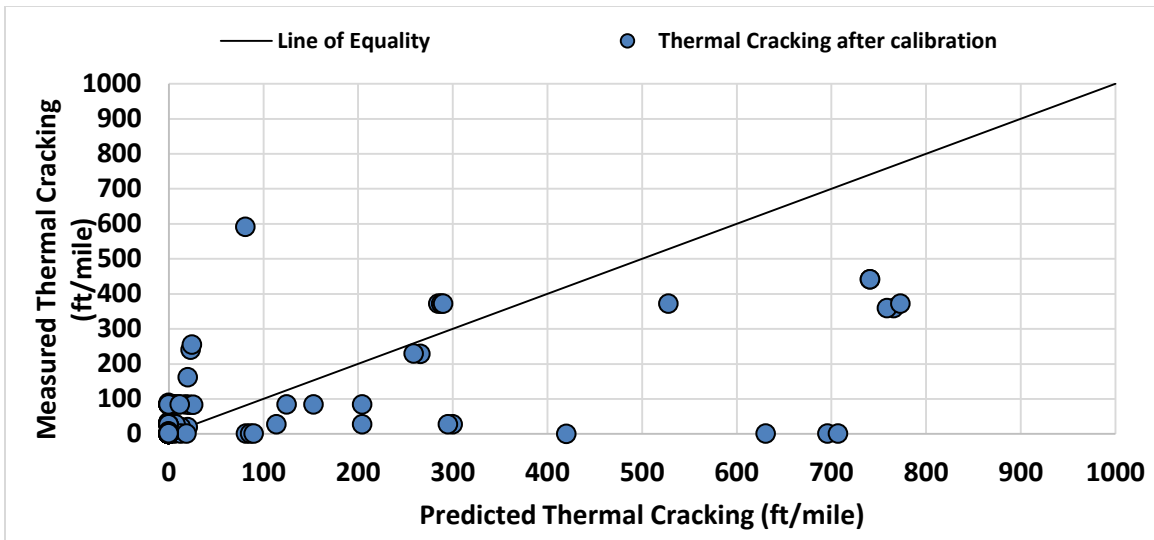


Figure 45 Measured vs. Predicted Transverse Cracking Using Local Calibration Coefficients

Table 32 Calibration Coefficients for Thermal Cracking

Calibration Coefficients	$K_{1,2,3}$	N	Bias, $e_{r(\text{mean})}$	Standard Error, Se	Se/Sy	$R^2$ , %	p-value (Paired t-test)
Global	1.5,0.5,1.5	118	63.559	207.160	1.050	1.95%	0.000495
Local	2.169,0.835,2.169	118	21.9495	155.251	0.787	59.81%	0.116

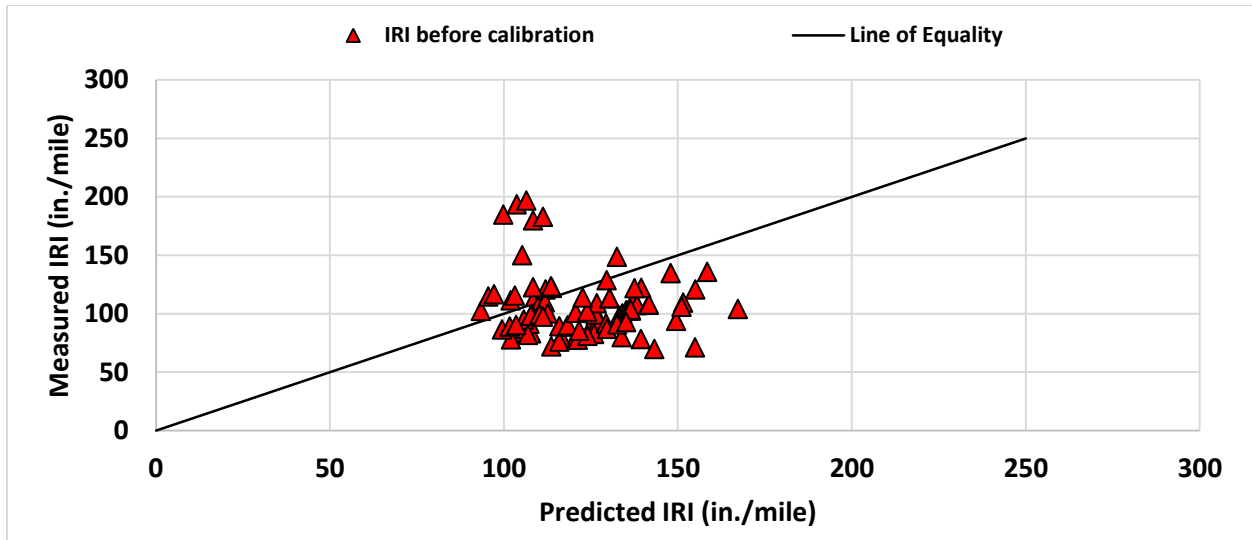


Figure 46 Measured vs. Predicted IRI Using Global Calibration Coefficients

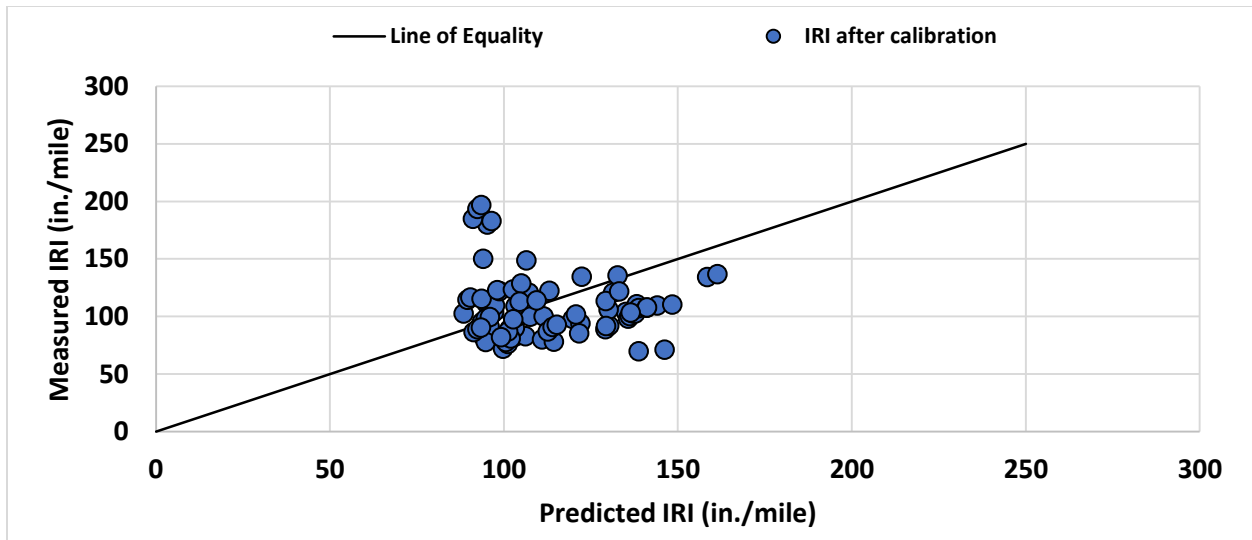


Figure 47 Measured vs. Predicted IRI using Local Calibration Coefficients

Table 33 Calibration Coefficients for IRI

Calibration Coefficients	C <sub>1</sub>	C <sub>2</sub>	C <sub>3</sub>	C <sub>4</sub>	N	Bias, e <sub>r(mean)</sub>	Standard Error, Se	Se/Sy	R <sup>2</sup> , %	p-value (Paired t-test)
Global	40	0.40	0.008	0.015	128	-16.805	34.310	0.670	0.35%	5.37E-07
Local	35	0.35	0.008	0.010	128	-8.0169	28.472	0.556	2.20%	0.0642

## Chapter 4

# Validation of the Developed Calibration Coefficients

The validation process is essential to illustrate that the calibrated models produce accurate predictions of pavement deterioration in the field. Validation usually requires an additional and independent set of pavement sections to confirm the calibration results. Successful model validation requires the bias and precision statistics of the validation data set to be similar to those obtained from the local calibration data set. Typically, two approaches are utilized to improve the accuracy of the prediction model; the traditional split-sample approach and an alternative jack-knifing approach for small sample sizes.

The split sample approach is usually employed in the statistical analysis. With an 80/20 split, 80 percent of the randomly chosen data is used during local calibration, while the remaining 20 percent used for validation. The lack of proper model validation is the most common mistake during model development, often resulting in misleading results. When all the available data are used for local calibration, the resulting goodness-of fit statistic only describes the model accuracy for the calibration data set, which may not indicate prediction accuracy for the full population. The split-sample testing for model validation solves this problem.

However, the traditional split-sample method has its limitations when it comes to small sample sizes (defined as a partial factorial with less than 25 percent of the cells filled with a project but without replication). Thus, the Jack-Knifing procedure is used as an alternative to the traditional approach to analyze small sample sizes. From the literature review, the only agency that used the Jack-Knifing method was Montana.

In this study, the calibrated models were validated using the split sample method. This was done by running the PMED on the remaining pavement sections that were not included in the local calibration process. Figures 48 through 55 show a comparison between the predicted and measured distresses. It is observed that the local calibration considerably reduced the difference between predicted and measured distresses/IRI as demonstrated by the statistical analysis shown in Tables 34 through 41.

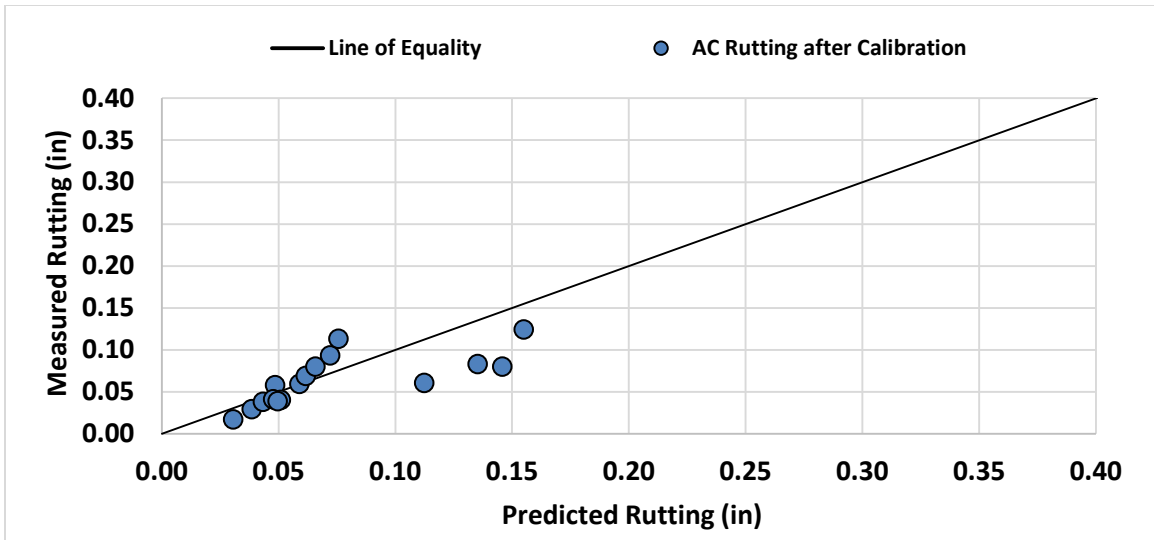


Figure 48 Measured vs. Predicted AC Using Local Calibration Coefficients

Table 34 Local Calibration Coefficients for AC Rutting

$\beta_{1r}$	$\beta_{2r}$	$\beta_{3r}$	N	Bias, $e_{r(\text{mean})}$	Standard Error, Se	Se/Sy	$R^2$ , %	p-value (Paired t-test)
3.000	1.000	0.661	26	-0.001	0.010	0.658	76.5	0.010

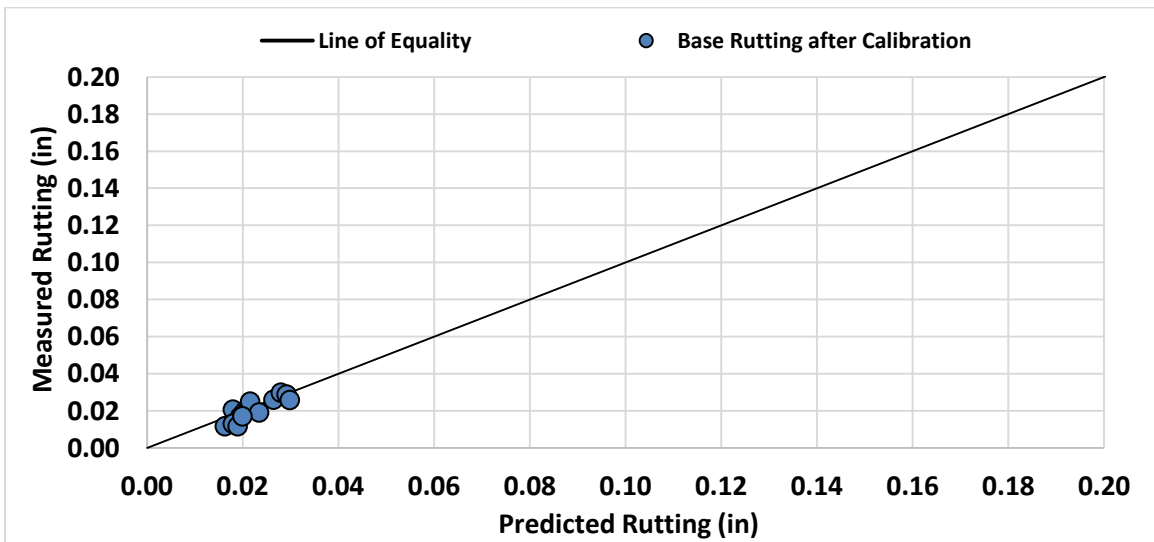
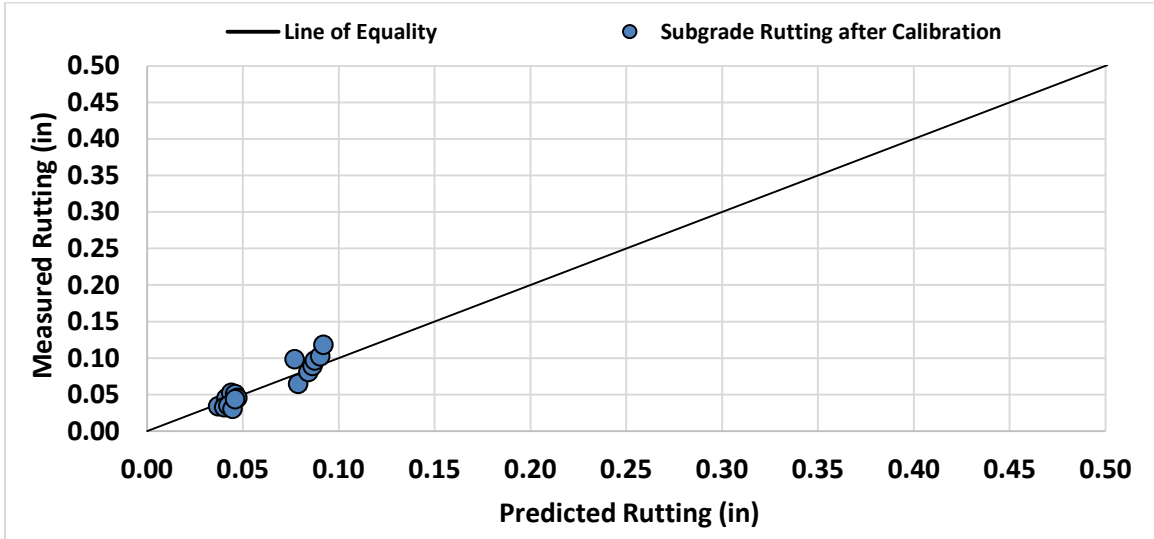


Figure 49 Measured vs. Predicted Base Layer Rutting Using Local Calibration Coefficients



**Table 35 Local Calibration Coefficients for Base Layer Rutting**

$\beta_{1s}$ (Coarse)	N	Bias, $e_{r(\text{mean})}$	Standard Error, Se	Se/Sy	R <sup>2</sup> , %	p-value (Paired t- test)
0.530	26	0.00251	0.022	0.697	80.0	0.299



**Figure 50 Measured vs. Predicted Subbase Layer Rutting Using Local Calibration Coefficients**

**Table 36 Local Calibration Coefficients for Subgrade Rutting**

$\beta_{1s}$ (Fine)	N	Bias, $e_{r(\text{mean})}$	Standard Error, Se	Se/Sy	R <sup>2</sup> , %	p-value (Paired t- test)
0.477	26	-0.01	0.050	1.024	71.8	0.287

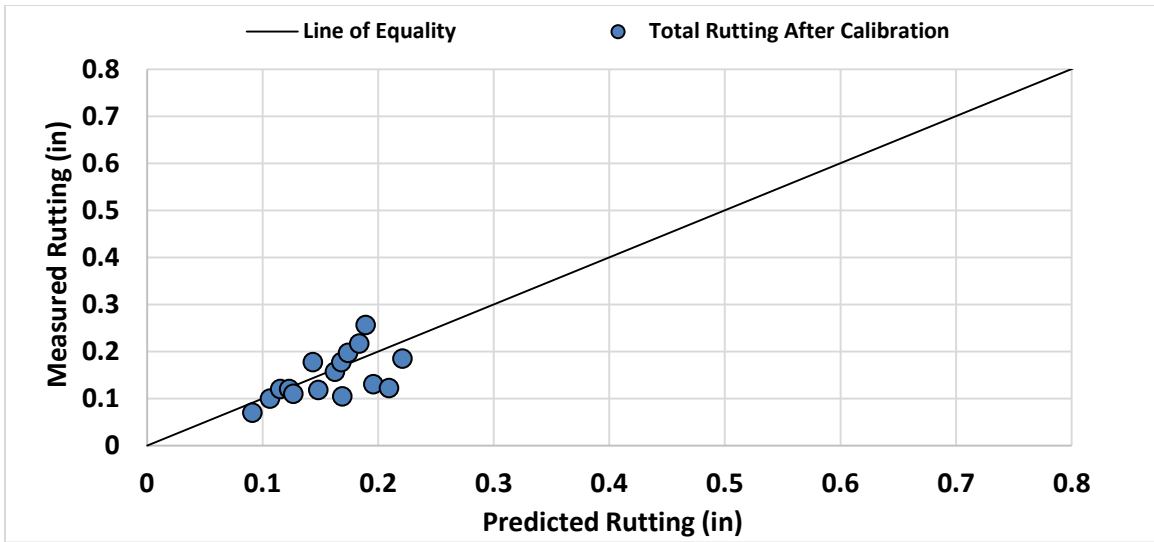


Figure 51 Measured vs. Predicted Total Rutting Using Local Calibration Coefficients

Table 37 Local Calibration Coefficients for Total Rutting

$\beta_{1r}$	$\beta_{2r}$	$\beta_{3r}$	$\beta_{1s}$ (Coarse)	$\beta_{1s}$ (Fine)	N	Bias, $e_{r(\text{mean})}$	Standard Error, Se	Se/Sy	R <sup>2</sup> , %	p-value (Paired t- test)
3.000	1.000	0.661	0.530	0.477	26	-0.0114	0.026	0.942	32.8	0.157

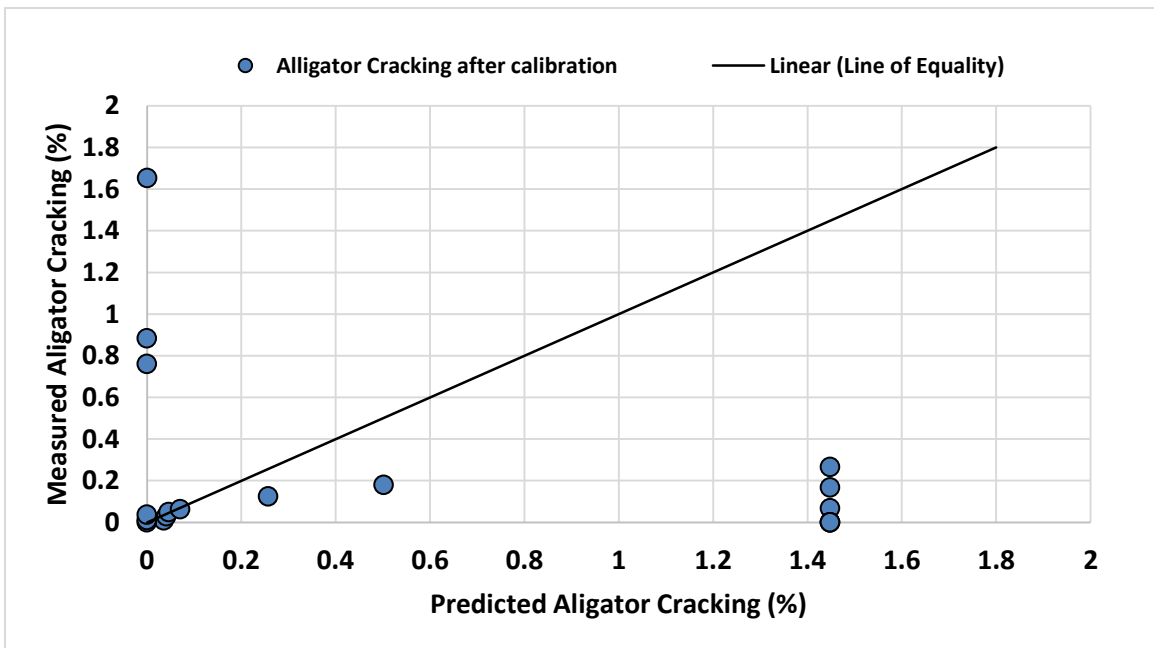
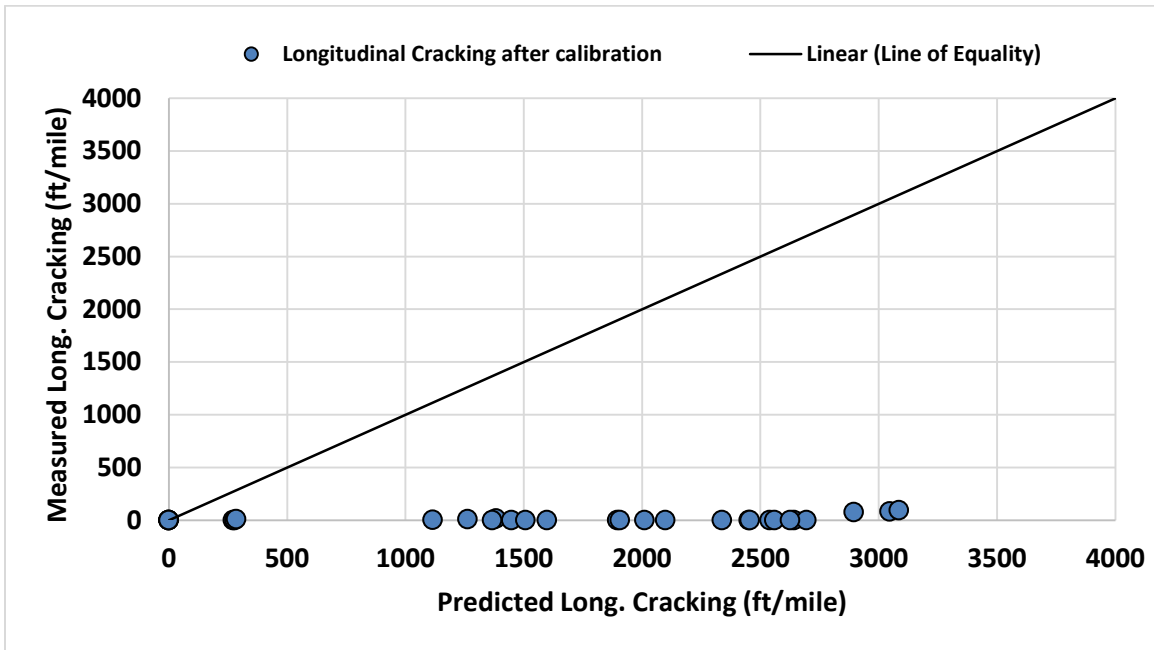


Figure 52 Measured vs. Predicted Alligator Cracking Using Local Calibration Coefficients

**Table 38 Local Calibration Coefficients for Alligator Cracking**

$B_{f1}$	$B_{f2}$	$B_{f3}$	$C_1$	$C_2$	N	Bias, $e_{r(\text{mean})}$	Standard Error, Se	Se/Sy	$R^2, \%$	p-value (Paired t-test)
1.00	1.00	1.00	1.00	0.824	18	-0.043	0.353	0.810	8.4	0.081



**Figure 53 Measured vs. Predicted Longitudinal Cracking Using Local Calibration Coefficients**

**Table 39 Local Calibration Coefficients for Longitudinal Cracking**

Calibration Coefficients	$B_{f1}$	$B_{f2}$	$B_{f3}$	$C_1$	$C_2$	N	Bias, $e_{r(\text{mean})}$	Standard Error, Se	Se/Sy	$R^2, \%$	p-value (Paired t-test)
LCF	1.00	1.00	1.00	4.533	0.229	29	-1636.9	1918.1	7.38	18.7	1.03E-09

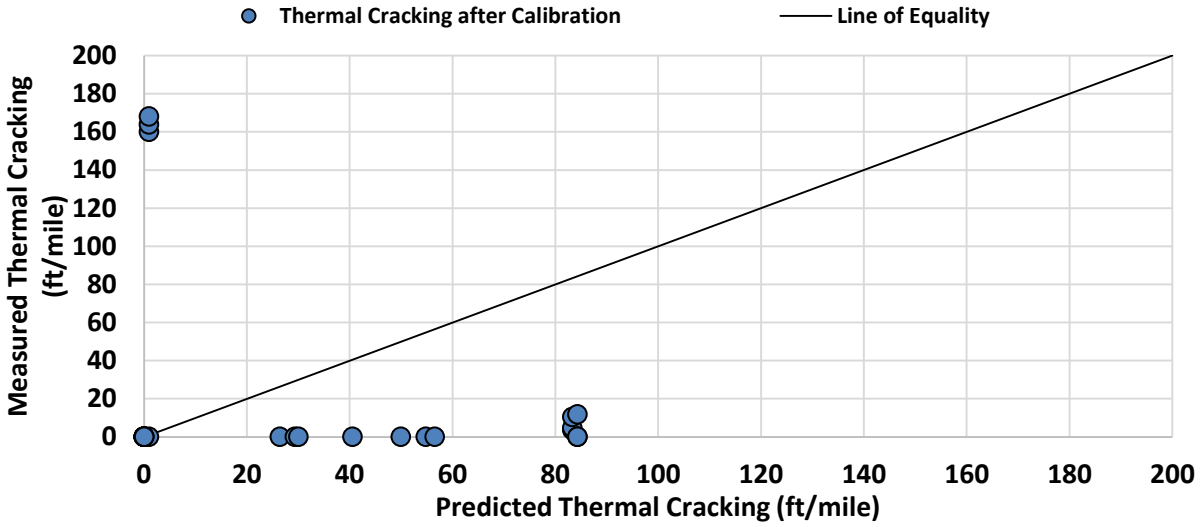


Figure 54 Measured vs. Predicted Thermal Cracking Using Local Calibration Coefficients

Table 40 Local Calibration Coefficients for Thermal Cracking

$K_{1,2,3}$	N	Bias, $e_{r(\text{mean})}$	Standard Error, Se	Se/Sy	$R^2$ , %	p-value (Paired t-test)
2.169,0.835,2.169	26	-10.493	70.679	1.331	0.77	0.229

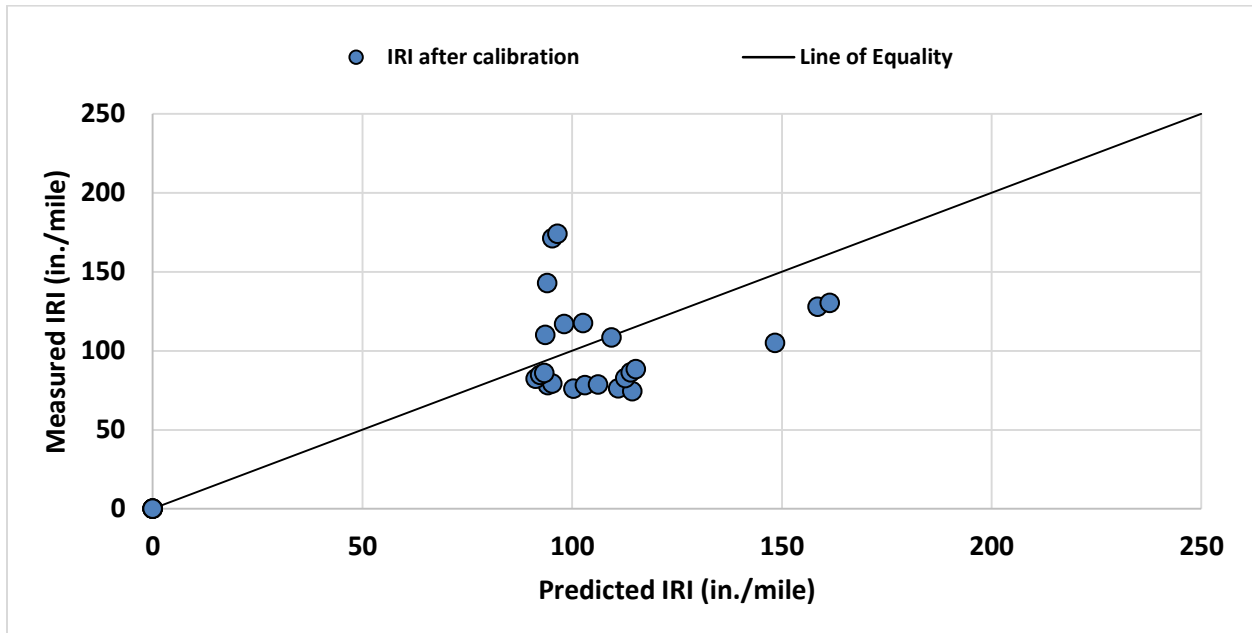


Figure 55 Measured vs. Predicted IRI Using Local Calibration Coefficients

**Table 41 Calibration Coefficients for IRI**

<b>C<sub>1</sub></b>	<b>C<sub>2</sub></b>	<b>C<sub>3</sub></b>	<b>C<sub>4</sub></b>	<b>N</b>	<b>Bias, er (mean)</b>	<b>Standard Error, Se</b>	<b>Se/Sy</b>	<b>R<sup>2</sup>, %</b>	<b>p-value (Paired t- test)</b>
35	0.35	0.008	0.010	27	-5.439	31.439	0.6807	56.92	0.189



## Chapter 5

### Summary, Conclusions, and Recommendations

#### Summary

This research aims to improve the accuracy of PMED performance predictions for Idaho pavements through local calibration. A total of 32 Asphalt Concrete pavement sections from different ITD districts were selected. The required PMED inputs for the selected pavement sections were primarily collected from material testing records, ITD phase reports, Job Mix Formula reports and the previous research report (RP193) as well as material testing results of creep compliance and indirect tensile testing performed in this project under Task4. A database of historical performance data for the selected pavement sections was prepared using data contained in the ITD Transportation Asset Management System (TAMS). The accuracy of the globally-calibrated PMED performance prediction models to Idaho conditions was evaluated. A statistical evaluation indicated that the global calibration coefficients did not accurately reflect Idaho in-service pavement performance. Therefore, a local calibration was conducted using a trial and error method, with multiple iterations, to improve the accuracy of model predictions.

The local calibration coefficients identified through this study are summarized in Table 42.

**Table 42 Summary of Calibration Coefficients Before and After Local Calibration**

Performance Model	Coefficients before Calibration	Coefficients after Calibration
Alligator Cracking	$\beta_{f1} = 1.00$	$\beta_{f1} = 1.00$
	$\beta_{f2} = 1.00$	$\beta_{f2} = 1.00$
	$\beta_{f3} = 1.00$	$\beta_{f3} = 1.00$
	C1= 1.00	C1= 1.00
	C2= 1.00	C2= 0.824
Longitudinal Cracking	$\beta_{f1} = 1.00$	$\beta_{f1} = 1.00$
	$\beta_{f2} = 1.00$	$\beta_{f2} = 1.00$
	$\beta_{f3} = 1.00$	$\beta_{f3} = 1.00$
	C1= 7.00	C1= 4.533
	C2 = 3.50	C2 = 0.229
Thermal Cracking	K1 = 1.50	K1 = 2.169
	K2 = 0.50	K2 = 0.835
	K3 = 1.50	K3 = 2.169

**Table 42 Summary of Calibration Coefficients Before and After Local Calibration (Cont.)**

Performance Model	Coefficients before Calibration	Coefficients after Calibration
AC Rutting	$\beta_{1r} = 1.00$	$\beta_{1r} = 3.00$
	$\beta_{2r} = 1.00$	$\beta_{2r} = 1.00$
	$\beta_{3r} = 1.00$	$\beta_{3r} = 0.661$
Unbound Base Rutting	$\beta_{s1} = 1.00$	$\beta_{s1} = 0.530$
Subgrade Rutting	$\beta_{s1} = 1.00$	$\beta_{s1} = 0.477$
IRI	C1 = 40	C1 = 35
	C2 = 0.4	C2 = 0.35
	C3 = 0.008	C3 = 0.008
	C4 = 0.015	C4 = 0.010

As part of the project tasks, the project team, in cooperation with Applied Research Associates (ARA) and ITD, conducted a training workshop for ITD engineers as well as other consultants' engineers who work on Idaho projects. The training workshop booklet was provided as a separate publication.

## Conclusions

- The globally-calibrated rutting models provide higher predictions of the total (accumulated) rutting than the measured values for new and rehabilitated AC pavements. This is the same trend observed from other agencies. However, the locally calibrated rutting models provide better predictions than the globally-calibrated models with less bias and errors.
- The globally-calibrated alligator (bottom-up) cracking model provides reasonable predictions for Idaho conditions. Minor change in the C2 factor improved the statistical results.
- The globally-calibrated longitudinal (top-down) cracking model provides poor prediction with high bias and standard errors. The statistical analysis showed significant difference between the measured and predicted performance, and the researchers were not able to calibrate the model. It is to be noted that researchers of AASHTO projects have confirmed that the model of Longitudinal cracking is being refined.
- Even though significant thermal cracking was observed on some pavement sections, the PMED predicted little to no thermal cracking. The model was calibrated to reduce bias and error.



- Good agreement is observed between predicted and measured IRI using the global calibration coefficients. More refinement to the calibration coefficients was conducted to reduce the error.
- ITD doesn't differentiate between the fatigue and reflective cracking during the pavement condition survey. Therefore, there was insufficient data to calibrate the reflective cracking model.
- The semi-rigid fatigue cracking model was not calibrated in this study due to the lack of observed fatigue cracking. None of the selected pavement sections for local calibration included AC over JPCP. Some selected pavement sections included a cement treated base; however, no fatigue cracking was observed in the field. As recommended in the Idaho PMED User Guide, all cement treated bases were simulated in the PMED as non-stabilized base. For those reasons, the research team was unable to calibrate the semi-rigid fatigue cracking model.

## Recommendations

- The calibration of the performance models is a continual process. Users need to allow reasonable bias between model prediction and field performance. The final design should fall within a reasonable range of expected values.
- Ongoing and future work that examines and assesses PMED models and the software function should continue to be monitored. The developed performance database for the selected pavement sections should be updated with additional years of performance data to improve the accuracy of the model prediction.
- The PMED longitudinal cracking model should only be used for experimental/informational purposes, until current model improvements are completed, validated, and local calibrated, if needed. The longitudinal cracking model is currently undergoing refinement as part of NCHRP Project 1-52.
- Some of the challenges identified in this study were the lack of observed distresses, limited ranges of distress values, and pavement service life. There were limited observation of alligator and longitudinal cracking in the selected pavement sections. Therefore, the research team recommends continued monitoring of these pavement sections until the next major rehabilitation activity. At that time, the alligator and longitudinal cracking models should be recalibrated.
- ITD, through preventive maintenance, applies seal coats to many major pavement sections. Such an application affects the observation of the distresses in the field, which may not necessary reflect the real performance of these sections. The research team identified two sections where seal coats were applied. These pavement sections should be excluded from any future calibration efforts.

- The PMED National Users Group, in their last meeting, discussed the tools to be added to the software, including the potential for tool to assist with local calibration. The local calibration tool is intended to “automate” the calibration process for reducing bias and error. Such a tool will require a database containing roadway section and performance data. The database developed in this study will play a vital role in providing accurate and precise data for future flexible pavement performance model validation and calibration. The database should be continually updated and maintained to support future PMED model calibration (or recalibration) efforts.

---

## References

1. **American Association of State Highways and Transportation Officials.** *AASHTO Guide for Design of Pavement Structures*. American Association of State Highways and Transportation Officials, Washington, DC. 1993.
2. **Applied Research Associates.** *Guide for the Mechanistic-Empirical Design of New & Rehabilitated Pavement Structures*. NCHRP Project 1-37A. Transportation Research Board, Washington, DC. 2004.
3. **American Association of State Highway and Transportation Officials.** *Guide for the Local Calibration of the Mechanistic-Empirical Pavement Design Guide*. American Association of State Highway and Transportation Officials, Washington, DC. 2010.
4. **Bayomy, F., S. El-Badawy, and A. Awed.** Implementation of the MEPDG for Flexible Pavements in Idaho. RP193. Idaho Transportation Department, Boise, ID. 2012.
5. **Mallela, J., H. Von Quintus, M. Darter, and B. Bhattacharya.** *Road Map for Implementing The AASHTO Pavement ME Design Software for the Idaho Transportation Department*. RP211A. Idaho Transportation Department, Boise, ID. 2014.
6. **Mallela, J., Glover, L., B. Bhattacharya, M. Darter, and H. Von Quintus,** *Idaho AASHTOWare Pavement ME Design User's Guide Version 1.1*. RP211B. Idaho Transportation Department, Boise, ID. 2014.
7. **Transportation Research Board.** *Facilitating the Implementation of the Guide for the Design of New and Rehabilitated Pavement Structures*, National Cooperative Highway Research Program 1-40. Washington, DC: Transportation Research Board, National Research Council. Last Accessed December 18, 2014.
8. **Transportation Research Board.** *Jackknife Testing—An Experimental Approach to Refine Model Calibration and Validation*. Research Results Digest 283. Transportation Research Board, Washington, DC. 2003.
9. **Transportation Research Board.** *Refining the Calibration and Validation of Hot Mix Asphalt Performance Models: An Experimental Plan and Database*. Research Results Digest 284. Transportation Research Board, Washington, DC. 2003.
10. **American Association of State Highway and Transportation Officials.** *Mechanistic-Empirical Pavement Design Guide: A Manual of Practice*. Interim Edition. American Association of State Highway and Transportation Officials, Washington, DC. 2008.

11. **American Association of State Highway and Transportation Officials.** *Mechanistic-Empirical Pavement Design Guide. A Manual of Practice.* American Association of State Highway and Transportation Officials, Washington, DC. 2015.
12. **Applied Pavement Technology.** *AASHTO Pavement ME User Group, Technical Report: First Annual Meeting – Indianapolis, IN Dec 14-15, 2016.* Federal Highway Administration, Washington, DC. 2017.
13. **Witczak, M. W.** *Development of Performance Related Specifications for Asphalt Pavements in the State of Arizona.* Final Report 402-2. Arizona Department of Transportation, Phoenix, AZ. 2008. [http://www.azdot.gov/TPD/ATRC/Publications/project\\_reports/PDF/AZ402-2.pdf](http://www.azdot.gov/TPD/ATRC/Publications/project_reports/PDF/AZ402-2.pdf) (Accessed in February 2017).
14. **Souliman, M.** *Calibration of the AASHTO MEPDG for Flexible Pavements for Arizona Conditions.* Master's Thesis. Arizona State University, Tempe, AZ. 2009.
15. **Lu, Q., Y. Zhang, and J. T. Harvey.** "Estimation of Truck Traffic Inputs for Mechanistic-Empirical Pavement Design in California," *Transportation Research Record No. 2095.* Transportation Research Board, Washington, DC. 2009.
16. **Von Quintus, H. L. and J. S. Moulthrop.** *Mechanistic-Empirical Pavement Design Guide Flexible Pavement Performance Prediction Models for Montana: Volume I - Executive Research Summary.* FHWA/MT-07-008/8158-1 Final Report. Montana Department of Transportation, Helena, MT. 2007. <http://www.archive.org/details/664B4642-A369-476C-BB5E-6196988FC74E> (Accessed in January 2016).
17. **Von Quintus, H. L. and J. S. Moulthrop.** *Mechanistic-Empirical Pavement Design Guide Flexible Pavement Performance Prediction Models for Montana: Volume II - Reference Manual.* Helena, MT: Montana Department of Transportation, FHWA/MT-07-008/8158-1 Final Report, 2007. <http://www.archive.org/details/664B4642-A369-476C-BB5E-6196988FC74E>, (Accessed in January 2016).
18. **Von Quintus, H. L. and J. S. Moulthrop.** *Mechanistic-Empirical Pavement Design Guide Flexible Pavement Performance Prediction Models for Montana: Volume III - Field Guide.* Helena, MT: Montana Department of Transportation, FHWA/MT-07-008/8158-1 Final Report, 2007. <http://www.archive.org/details/664B4642-A369-476C-BB5E-6196988FC74E>, (Accessed in January 2016).
19. **Karakouzian, M.,** *Characterization of Unbound Materials (Soils/Aggregates) for Mechanistic Empirical Pavement Design Guide (MEPDG).* Report No. 361-16-803, Nevada Department of Transportation, Carson, NV, 2018.
20. **Nabhan, P.,** *Calibration of the AASHTO MEPDG for Flexible Pavements to Fit Nevada's Conditions.* Reno, NV: University of Nevada, Master's Thesis, 2015.

21. **Williams, R. C. and R. Shaidur.** *Mechanistic-Empirical Pavement Design Guide Calibration for Pavement Rehabilitation*. 2013. Oregon Department of Transportation, Salem, OR. Retrieved from <http://hdl.handle.net/2060/19650075465>.
22. **Darter, M., L. Titus-Glover, and H. Von Quintus.** *Implementation of the Mechanistic-Empirical Pavement Design Guide in Utah: Validation, Calibration, and Development of the UDOT MEPDG User's Guide*. Report No. UT-09.11. Utah Department of Transportation, Salt Lake City, UT. 2009. <http://utah.ptfs.com/awweb/main.jsp?flag=browse&smd=1&awdid=1> (Accesses in January 2016).
23. **Li, J., L. Pierce, and J. Uhlmeyer.** "Calibration of Flexible Pavement in Mechanistic-Empirical Pavement Design Guide for Washington State." *Transportation Research Record 2095*. Transportation Research Board, Washington DC. 2009.
24. **Ng, K. W., H. L. Von Quintus, K. Ksaibati, D. Hellrung, and Z. Hutson.** *Characterization of Material Properties for Mechanistic-Empirical Pavement Design in Wyoming*. Wyoming Department of Transportation, Cheyenne, WY. 2013.
25. **Hutson, Z., K. Ng, and K. Ksaibati.** "Implementation in Wyoming through Comprehensive Testing Program and Wyoming MEPDG Database." *95<sup>th</sup> Annual TRB Meeting*. Transportation Research Board, Washington, DC. 2016.
26. **Federal Highway Administration.** *Local Calibration of the MEPDG Using Pavement Management Systems*. HIF-11-026. Federal Highway Administration. Washington, DC, 2010
27. **Von Quintus, H.L., J. Mallela, S. Sadasivam, and M. Darter.** *Literature Search and Synthesis Verification and Local Calibration/Validation of the MEPDG Performance Models for Use in Georgia*. GADOT-TO-01-Task 1. Georgia Department of Transportation, Atlanta, GA. 2013.
28. **Transportation Research Board.** *Independent Review of the Mechanistic-Empirical Pavement Design Guide and Software*. Research Results Digest 307. Transportation Research Board, Washington, DC. 2006.
29. **Hall, K. D., S. Beam, and M. Lee.** *AASHTO 2002 Pavement Design Guide Design Inputs Evaluation Study*. Little Rock, AR: Arkansas Highway and Transportation Department, TRC-0302, 2006.
30. **Romanoschi, S. A., and S. Bethu.** *Implementation of the 2002 AASHTO Design Guide for Pavement Structures in KDOT Part-II Asphalt Concrete Pavements*. Manhattan, KS: Kansas State University, K-TRAN: KSU-04-4 Part 2 Final Report, 2009.
31. **NCHRP. 2009.** Standard Practice for Conducting Local or Regional Calibration Parameters for the MEPDG. National Cooperative Highway Research Program Project 1- 40B Report (publication under review), Washington, DC: Transportation Research Board, National Research Council.

32. **Muthadi, N. R.**, *Local Calibration of the MEPDG for Flexible Pavement Design*. Raleigh, NC: North Carolina State University, Master's Thesis, 2007.
33. **Scott Fortmann-Roe**, the Bias-Variance Tradeoff, 2012 Retrieved from the World Wide Web:  
<http://scott.fortmann-roe.com/docs/BiasVariance.html>
34. **National Center for Asphalt Technology**, *Summary of ME Design Software Local Calibration Efforts*,  
<http://www.eng.auburn.edu/research/centers/ncat/newsroom/2016/local-calibration.html>.  
(Accessed in February 2018).
35. **Idaho Transportation Department**. *Standard Specification for Highway Construction*. Idaho Transportation Department, Boise, ID. 2012.  
<http://itd.idaho.gov/manuals/Manual%20Production/SpecBook/SpecHome.htm> Accessed in July 2015.
36. **Idaho Transportation Department**. *Idaho Transportation Department Pavement Rating Manual*. Boise, ID: Idaho Transportation Department. 2010.

## Appendix A

### Updated PMED Database to Include Creep Compliance and IDT Data (e-file)

**Creep Compliance and IDT Mix Selection Sheet**

Mix ID	PG	NMAS	Project ID	Key No.	Project No.
SP2-A	PG 64-28	1/2"	Swan Falls Rd. Dhoulder Widening	13518	A515-182
SP3-A	PG 58-34	1/2"	US95, Smith CR to MP 382 Benewah CO	9458	A516-423
SP3-B	PG 52-40	1/2"	Pancheri Dr. Bellin to SkylineTS 1 S1	11686	215001
SP3-C	PG 64-28	1/2"	State, Dist. Wide Turn Bays./ Red Rock	13823	BO1500507
SP3-D	PG 64-34	1/2"	US30 main street Soda Springs	13552	A405-435
SP3-E	PG 64-34	1/2"	Island Park, Pine Haven Dr to Buffalo Rv	18917	A018917
SP3-F	PG 70-28	1/2"	SH-44 W. State St. to JCT 55 North, Eagle	13923	A515-034
SP3-G	PG 70-28	1/2"	Karcher/Middleton	12046	BO1500218
SP3-H	PG 70-28	1/2"	STP-8423, Amity Rd	10541	BO1500237
SP5-A	PG 64-28	3/4"	US-95, Worley North, Kootenai Co. STG 2	12212	A515-113
SP5-B	PG 64-34	3/4"	I-15, Devils Cr to Marsh Valley Rd	12431	515-108
SP5-C	PG 70-28	3/4"	Fort Hall Boundary to Burns Rd	13079	A013-106
SP5-D	PG 70-28	3/4"	Cheyenne S. Valley Connector	7508	BO1500363
SP5-E	PG 70-34	3/4"	US20, MP 328.57 to MP 333.44	8454	A516-116
SP5-F	PG 76-28	1/2"	US-95, Lewiston Hill NB & SB lanes	13435	15011
SP5-G	PG 76-28	3/4"	I-84 Meridian RD I.C	10939	BO1400731
SP6-A	PG 76-28	1/2"	I-84, Snake RV Twin Bridges WB & EB	11239	BO1500206
SP6-B	PG 76-28	3/4"	I-84, Snake RV Twin Bridges WB & EB	11239	BO1500207

**Table A - 1 Asphalt Mix (KN13518) Creep Compliance (1/psi)**

<b>Loading Time (Sec)</b>	<b>Low Temp (-4 deg F)</b>	<b>Mid Temp (14 deg F)</b>	<b>High Temp (32 deg F)</b>
<b>1s</b>	4.46E-07	7.61E-07	1.56E-06
<b>2s</b>	4.64E-07	8.33E-07	1.86E-06
<b>5s</b>	4.98E-07	9.55E-07	2.46E-06
<b>10s</b>	5.37E-07	1.08E-06	3.08E-06
<b>20s</b>	5.93E-07	1.26E-06	3.95E-06
<b>50s</b>	6.76E-07	1.59E-06	5.52E-06
<b>100s</b>	7.48E-07	1.95E-06	7.14E-06

**Table A - 2 Asphalt Mix (KN13518) IDT (psi)**

<b>Sample #</b>	<b>1</b>	<b>2</b>	<b>3</b>	<b>Average</b>
<b>IDT (psi) @ 14°F</b>	708.30	759.46	719.79	<b>729.2</b>



**Table A - 3 Asphalt Mix (KN9458) Creep Compliance (1/psi)**

<b>Loading Time (Sec)</b>	<b>Low Temp (-4 deg F)</b>	<b>Mid Temp (14 deg F)</b>	<b>High Temp (32 deg F)</b>
<b>1s</b>	1.28E-08	1.16E-07	2.65E-07
<b>2s</b>	1.55E-08	2.52E-07	4.39E-07
<b>5s</b>	5.93E-08	5.29E-07	8.82E-07
<b>10s</b>	6.40E-08	9.31E-07	1.61E-06
<b>20s</b>	1.18E-07	1.49E-06	2.68E-06
<b>50s</b>	2.15E-07	2.76E-06	4.79E-06
<b>100s</b>	3.99E-07	4.43E-06	7.84E-06

**Table A - 4 Asphalt Mix (KN9458) IDT (psi)**

<b>Sample #</b>	<b>1</b>	<b>2</b>	<b>3</b>	<b>Average</b>
<b>IDT (psi) @ 14°F</b>	484.27	405.99	379.58	<b>423.3</b>

**Table A - 5 Asphalt Mix (KN 11686) Creep Compliance (1/psi)**

<b>Loading Time (Sec)</b>	<b>Low Temp (-4 deg F)</b>	<b>Mid Temp (14 deg F)</b>	<b>High Temp (32 deg F)</b>
<b>1s</b>	3.71E-07	6.93E-07	1.42E-06
<b>2s</b>	3.95E-07	7.88E-07	1.71E-06
<b>5s</b>	4.15E-07	9.41E-07	2.11E-06
<b>10s</b>	4.64E-07	1.11E-06	2.53E-06
<b>20s</b>	5.15E-07	1.32E-06	3.12E-06
<b>50s</b>	6.29E-07	1.61E-06	4.15E-06
<b>100s</b>	6.77E-07	1.85E-06	5.13E-06

**Table A - 6 Asphalt Mix (KN 11686) IDT (psi)**

<b>Sample #</b>	<b>1</b>	<b>2</b>	<b>3</b>	<b>Average</b>
<b>IDT (psi) @ 14°F</b>	959.78	869.73	861.18	<b>896.9</b>

**Table A - 7 Asphalt Mix (KN 13823) Creep Compliance (1/psi)**

<b>Loading Time (Sec)</b>	<b>Low Temp (-4 deg F)</b>	<b>Mid Temp (14 deg F)</b>	<b>High Temp (32 deg F)</b>
<b>1s</b>	2.44E-07	3.90E-07	5.27E-07
<b>2s</b>	2.46E-07	4.03E-07	5.97E-07
<b>5s</b>	2.68E-07	4.57E-07	7.21E-07
<b>10s</b>	3.07E-07	4.90E-07	8.63E-07
<b>20s</b>	3.08E-07	5.35E-07	1.09E-06
<b>50s</b>	3.52E-07	6.15E-07	1.57E-06
<b>100s</b>	3.83E-07	7.16E-07	2.08E-06

**Table A - 8 Asphalt Mix (KN 13823) IDT (psi)**

<b>Sample #</b>	<b>1</b>	<b>2</b>	<b>3</b>	<b>Average</b>
<b>IDT (psi) @ 14°F</b>	613.42	611.49	697.23	<b>640.7</b>

**Table A - 9 Asphalt Mix (KN 13552) Creep Compliance (1/psi)**

<b>Loading Time (Sec)</b>	<b>Low Temp (-4 deg F)</b>	<b>Mid Temp (14 deg F)</b>	<b>High Temp (32 deg F)</b>
<b>1s</b>	1.70E-08	3.74E-09	2.49E-08
<b>2s</b>	8.42E-09	2.00E-08	6.31E-09
<b>5s</b>	5.88E-10	2.07E-08	1.24E-08
<b>10s</b>	-1.28E-08	2.04E-09	5.57E-09
<b>20s</b>	8.38E-09	4.48E-09	2.14E-08
<b>50s</b>	4.39E-08	3.75E-08	1.41E-07
<b>100s</b>	6.54E-08	1.54E-07	4.41E-07

**Table A - 10 Asphalt Mix (KN 13552) IDT (psi)**

<b>Sample #</b>	<b>1</b>	<b>2</b>	<b>3</b>	<b>Average</b>
<b>IDT (psi) @ 14°F</b>	511.68	560.24	458.71	<b>510.2</b>

**Table A - 11 Asphalt Mix (KN 18917) Creep Compliance (1/psi)**

<b>Loading Time (Sec)</b>	<b>Low Temp (-4 deg F)</b>	<b>Mid Temp (14 deg F)</b>	<b>High Temp (32 deg F)</b>
<b>1s</b>	6.62E-08	2.05E-08	8.73E-08
<b>2s</b>	6.18E-08	2.73E-08	1.10E-07
<b>5s</b>	7.29E-08	1.10E-07	3.58E-07
<b>10s</b>	1.29E-07	1.51E-07	5.86E-07
<b>20s</b>	1.89E-07	3.69E-07	1.05E-06
<b>50s</b>	3.34E-07	7.46E-07	1.77E-06
<b>100s</b>	6.80E-07	1.22E-06	3.36E-06

**Table A - 12 Asphalt Mix (KN 18917) IDT (psi)**

<b>Sample #</b>	<b>1</b>	<b>2</b>	<b>3</b>	<b>Average</b>
<b>IDT (psi) @ 14°F</b>	0.00	600.87	540.25	<b>570.6</b>

**Table A - 13 Asphalt Mix (KN 13923) Creep Compliance (1/psi)**

<b>Loading Time (Sec)</b>	<b>Low Temp (-4 deg F)</b>	<b>Mid Temp (14 deg F)</b>	<b>High Temp (32 deg F)</b>
<b>1s</b>	4.53E-07	6.45E-07	1.39E-06
<b>2s</b>	4.84E-07	7.28E-07	1.63E-06
<b>5s</b>	5.13E-07	8.36E-07	2.10E-06
<b>10s</b>	5.78E-07	9.67E-07	2.64E-06
<b>20s</b>	6.11E-07	1.13E-06	3.36E-06
<b>50s</b>	6.75E-07	1.42E-06	4.79E-06
<b>100s</b>	7.74E-07	1.75E-06	6.25E-06

**Table A - 14 Asphalt Mix (KN 13923) IDT (psi)**

<b>Sample #</b>	<b>1</b>	<b>2</b>	<b>3</b>	<b>Average</b>
<b>IDT (psi) @ 14°F</b>	790.44	754.90	719.25	<b>754.9</b>

**Table A - 15 Asphalt Mix (KN 12046) Creep Compliance (1/psi)**

<b>Loading Time (Sec)</b>	<b>Low Temp (-4 deg F)</b>	<b>Mid Temp (14 deg F)</b>	<b>High Temp (32 deg F)</b>
<b>1s</b>	3.54E-07	4.91E-07	7.12E-07
<b>2s</b>	3.56E-07	5.21E-07	8.03E-07
<b>5s</b>	3.84E-07	5.81E-07	1.10E-06
<b>10s</b>	4.04E-07	6.25E-07	1.39E-06
<b>20s</b>	4.27E-07	6.94E-07	1.78E-06
<b>50s</b>	4.65E-07	8.62E-07	2.51E-06
<b>100s</b>	4.85E-07	1.01E-06	3.30E-06

**Table A - 16 Asphalt Mix (KN 12046) IDT (psi)**

<b>Sample #</b>	<b>1</b>	<b>2</b>	<b>3</b>	<b>Average</b>
<b>IDT (psi) @ 14°F</b>	573.80	511.63	621.72	<b>569.1</b>

**Table A - 17 Asphalt Mix (KN 10541) Creep Compliance (1/psi)**

<b>Loading Time (Sec)</b>	<b>Low Temp (-4 deg F)</b>	<b>Mid Temp (14 deg F)</b>	<b>High Temp (32 deg F)</b>
<b>1s</b>	4.42E-07	7.02E-07	1.23E-06
<b>2s</b>	4.57E-07	7.22E-07	1.37E-06
<b>5s</b>	4.92E-07	8.18E-07	1.69E-06
<b>10s</b>	5.13E-07	8.94E-07	1.99E-06
<b>20s</b>	5.85E-07	1.02E-06	2.45E-06
<b>50s</b>	6.34E-07	1.20E-06	3.24E-06
<b>100s</b>	6.84E-07	1.37E-06	4.19E-06

**Table A - 18 Asphalt Mix (KN 10541) IDT (psi)**

<b>Sample #</b>	<b>1</b>	<b>2</b>	<b>3</b>	<b>Average</b>
<b>IDT (psi) @ 14°F</b>	516.84	530.55	489.77	<b>512.4</b>



**Table A - 19 Asphalt Mix (KN 12212) Creep Compliance (1/psi)**

<b>Loading Time (Sec)</b>	<b>Low Temp (-4 deg F)</b>	<b>Mid Temp (14 deg F)</b>	<b>High Temp (32 deg F)</b>
<b>1s</b>	2.35E-07	3.71E-07	6.38E-07
<b>2s</b>	2.56E-07	3.85E-07	6.94E-07
<b>5s</b>	2.52E-07	4.34E-07	9.03E-07
<b>10s</b>	2.68E-07	4.98E-07	1.09E-06
<b>20s</b>	2.79E-07	5.68E-07	1.37E-06
<b>50s</b>	2.91E-07	7.11E-07	2.16E-06
<b>100s</b>	3.26E-07	8.10E-07	2.95E-06

**Table A - 20 Asphalt Mix (KN 12212) IDT (psi)**

<b>Sample #</b>	<b>1</b>	<b>2</b>	<b>3</b>	<b>Average</b>
<b>IDT (psi) @ 14°F</b>	720.34	667.50	688.28	<b>692.0</b>

**Table A - 21 Asphalt Mix (KN 12431) Creep Compliance (1/psi)**

<b>Loading Time (Sec)</b>	<b>Low Temp (-4 deg F)</b>	<b>Mid Temp (14 deg F)</b>	<b>High Temp (32 deg F)</b>
<b>1s</b>	4.01E-07	6.79E-07	1.66E-06
<b>2s</b>	4.33E-07	7.31E-07	1.99E-06
<b>5s</b>	4.74E-07	8.89E-07	2.72E-06
<b>10s</b>	5.10E-07	1.06E-06	3.59E-06
<b>20s</b>	5.62E-07	1.33E-06	4.77E-06
<b>50s</b>	6.62E-07	1.72E-06	7.00E-06
<b>100s</b>	7.70E-07	2.10E-06	9.20E-06

**Table A - 22 Asphalt Mix (KN 12431) IDT (psi)**

<b>Sample #</b>	<b>1</b>	<b>2</b>	<b>3</b>	<b>Average</b>
<b>IDT (psi) @ 14°F</b>	594.70	641.79	645.69	<b>627.4</b>

**Table A - 23 Asphalt Mix (KN 13079) Creep Compliance (1/psi)**

<b>Loading Time (Sec)</b>	<b>Low Temp (-4 deg F)</b>	<b>Mid Temp (14 deg F)</b>	<b>High Temp (32 deg F)</b>
<b>1s</b>	5.73E-09	8.69E-08	1.02E-07
<b>2s</b>	1.69E-08	1.65E-07	2.35E-07
<b>5s</b>	9.26E-08	4.00E-07	7.01E-07
<b>10s</b>	1.93E-07	6.88E-07	1.41E-06
<b>20s</b>	3.46E-07	1.00E-06	2.41E-06
<b>50s</b>	5.82E-07	1.81E-06	4.26E-06
<b>100s</b>	9.28E-07	3.01E-06	7.19E-06

**Table A - 24 Asphalt Mix (KN 13079) IDT (psi)**

<b>Sample #</b>	<b>1</b>	<b>2</b>	<b>3</b>	<b>Average</b>
<b>IDT (psi) @ 14°F</b>	406.84	493.99	504.53	<b>468.5</b>

**Table A - 25 Asphalt Mix (KN 7508) Creep Compliance (1/psi)**

<b>Loading Time (Sec)</b>	<b>Low Temp (-4 deg F)</b>	<b>Mid Temp (14 deg F)</b>	<b>High Temp (32 deg F)</b>
<b>1s</b>	2.75E-07	4.28E-07	8.37E-07
<b>2s</b>	2.54E-07	4.76E-07	9.29E-07
<b>5s</b>	2.66E-07	5.36E-07	1.11E-06
<b>10s</b>	2.78E-07	5.65E-07	1.31E-06
<b>20s</b>	2.87E-07	6.16E-07	1.58E-06
<b>50s</b>	2.99E-07	6.80E-07	2.10E-06
<b>100s</b>	3.34E-07	7.57E-07	2.68E-06

**Table A - 26 Asphalt Mix (KN 7508) IDT (psi)**

<b>Sample #</b>	<b>1</b>	<b>2</b>	<b>3</b>	<b>Average</b>
<b>IDT (psi) @ 14°F</b>	624.98	641.79	720.43	<b>662.4</b>

**Table A - 27 Asphalt Mix (KN 8454) Creep Compliance (1/psi)**

<b>Loading Time (Sec)</b>	<b>Low Temp (-4 deg F)</b>	<b>Mid Temp (14 deg F)</b>	<b>High Temp (32 deg F)</b>
<b>1s</b>	2.27E-08	6.48E-08	9.88E-08
<b>2s</b>	3.28E-08	1.72E-07	1.71E-07
<b>5s</b>	1.15E-07	3.88E-07	4.53E-07
<b>10s</b>	2.26E-07	6.39E-07	8.39E-07
<b>20s</b>	5.59E-07	1.10E-06	1.26E-06
<b>50s</b>	9.91E-07	1.93E-06	2.42E-06
<b>100s</b>	1.63E-06	3.05E-06	3.62E-06

**Table A - 28 Asphalt Mix (KN 8454) IDT (psi)**

<b>Sample #</b>	<b>1</b>	<b>2</b>	<b>3</b>	<b>Average</b>
<b>IDT (psi) @ 14°F</b>	544.40	411.36	380.03	<b>445.3</b>

**Table A - 29 Asphalt Mix (KN 13435) Creep Compliance (1/psi)**

<b>Loading Time (Sec)</b>	<b>Low Temp (-4 deg F)</b>	<b>Mid Temp (14 deg F)</b>	<b>High Temp (32 deg F)</b>
<b>1s</b>	2.82E-07	1.53E-07	2.88E-07
<b>2s</b>	2.99E-07	1.64E-07	3.69E-07
<b>5s</b>	3.17E-07	1.85E-07	4.91E-07
<b>10s</b>	3.39E-07	2.09E-07	5.25E-07
<b>20s</b>	3.50E-07	2.35E-07	6.33E-07
<b>50s</b>	3.89E-07	2.84E-07	8.36E-07
<b>100s</b>	4.07E-07	3.35E-07	1.14E-06

**Table A - 30 Asphalt Mix (KN 13435) IDT (psi)**

<b>Sample #</b>	<b>1</b>	<b>2</b>	<b>3</b>	<b>Average</b>
<b>IDT (psi) @ 14°F</b>	776.07	725.20	709.17	<b>736.8</b>

**Table A - 31 Asphalt Mix (KN 10939) Creep Compliance (1/psi)**

<b>Loading Time (Sec)</b>	<b>Low Temp (-4 deg F)</b>	<b>Mid Temp (14 deg F)</b>	<b>High Temp (32 deg F)</b>
<b>1s</b>	4.39E-07	6.93E-07	1.23E-06
<b>2s</b>	4.80E-07	7.48E-07	1.40E-06
<b>5s</b>	5.21E-07	8.37E-07	1.70E-06
<b>10s</b>	5.42E-07	9.30E-07	2.06E-06
<b>20s</b>	5.67E-07	1.07E-06	2.56E-06
<b>50s</b>	6.31E-07	1.29E-06	3.52E-06
<b>100s</b>	6.84E-07	1.56E-06	4.58E-06

**Table A - 32 Asphalt Mix (KN 10939) IDT (psi)**

<b>Sample #</b>	<b>1</b>	<b>2</b>	<b>3</b>	<b>Average</b>
<b>IDT (psi) @ 14°F</b>	522.37	542.41	533.74	<b>532.8</b>

**Table A - 33 Asphalt Mix (KN 11239-1/2") Creep Compliance (1/psi)**

<b>Loading Time (Sec)</b>	<b>Low Temp (-4 deg F)</b>	<b>Mid Temp (14 deg F)</b>	<b>High Temp (32 deg F)</b>
<b>1s</b>	3.89E-07	5.43E-07	8.04E-07
<b>2s</b>	4.08E-07	5.69E-07	9.05E-07
<b>5s</b>	4.35E-07	6.22E-07	1.14E-06
<b>10s</b>	4.65E-07	6.79E-07	1.38E-06
<b>20s</b>	5.10E-07	7.47E-07	1.67E-06
<b>50s</b>	5.74E-07	8.79E-07	2.27E-06
<b>100s</b>	6.37E-07	1.02E-06	2.88E-06

**Table A - 34 Asphalt Mix (KN11239-1/2") IDT (psi)**

<b>Sample #</b>	<b>1</b>	<b>2</b>	<b>3</b>	<b>Average</b>
<b>IDT (psi) @ 14°F</b>	549.37	611.25	562.62	<b>574.4</b>



**Table A - 35 Asphalt Mix (KN11239-3/4") Creep Compliance (1/psi)**

<b>Loading Time (Sec)</b>	<b>Low Temp (-4 deg F)</b>	<b>Mid Temp (14 deg F)</b>	<b>High Temp (32 deg F)</b>
<b>1s</b>	3.66E-07	6.05E-07	9.45E-07
<b>2s</b>	3.85E-07	6.58E-07	1.13E-06
<b>5s</b>	4.13E-07	7.52E-07	1.38E-06
<b>10s</b>	4.27E-07	8.50E-07	1.69E-06
<b>20s</b>	4.86E-07	9.49E-07	2.11E-06
<b>50s</b>	5.18E-07	1.17E-06	3.00E-06
<b>100s</b>	5.89E-07	1.42E-06	4.05E-06

**Table A - 36 Asphalt Mix (KN11239-3/4") IDT (psi)**

<b>Sample #</b>	<b>1</b>	<b>2</b>	<b>3</b>	<b>Average</b>
<b>IDT (psi) @ 14°F</b>	628.78	593.78	695.57	<b>639.4</b>



# Appendix B Performance Database

(e-file)

Calibration of the AASHTOWare Pavement ME Design Performance Models for Flexible Pavements in Idaho  
ITD Research Project RP235 - University of Idaho NIATT Project KLK572

*Performance Database Version 1.100*

Developed by:

**Fouad Bayomy (PI)**

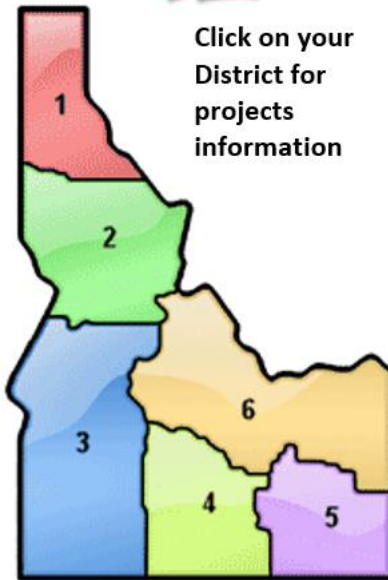
**Emad Kassem**

**Ahmed Muftah**

**Mumtahn Hasnat**



Click on your  
District for  
projects  
information



### District 1 Selected Projects

Section #	Route	Beg. MP	End MP	Location
<b>D1-1</b>	US-95	398.569	401.524	Benewah CL to Worley
<b>D1-2</b>	US-95	403.5	408.75	Worley North
<b>D1-3</b>	US-95	411.841	415.832	Setters to Bellgrove
<b>D1-4</b>	US-95	415.5	421.3	Bellgrove to Mica
<b>D1-5</b>	SH-3	76.822	84.201	St. Maries South
<b>D1-6</b>	SH-3	103.149	111.38	Swan Creek to CDA Rv Br
<b>D1-7</b>	US-95	477.098	486.362	Kootenai Cutoff to Samuels

**GO BACK TO MAIN SCREEN**

<b>District 1_Project 1</b>			
<b>Project Section: Benawah County Line to Worley</b>			
<b>Mile post 398.569 to 401.524</b>			
<b>DISTRICT 1 SELECTED PAVEMENT SECTIONS</b>			
<b>Construction time</b>	<b>2016</b>		
<b>Coordinates</b>	<b>47.3858</b>	<b>-116.878</b>	
<b>Elevation</b>	<b>2661 ft</b>		
<b>GO BACK TO MAIN SCREEN</b>			
<b>Performance Measurement</b>			
<b>Cracking</b>	<b>2016</b>	<b>2017</b>	<b>2018</b>
Aligator Cracking (%)	0.00		
Longitudinal Cracking (ft/mile)	0.00		
Thermal Cracking (ft/mile)	0.00		
<b>Structure</b>			
<b>Layer #</b>	<b>Layer type</b>	<b>Thickness</b>	<b>Property</b>
1	HMA	1.8 in	Class SP-3, 1/2" from JMF
2	HMA	6 in	Class I, 3/4"
3	rock cap	16.2 & 24 in	R =80, thickens after 399.68
4	subgrade	-	R > 7, class varies
<b>Traffic during the construction time</b>			<b>Binder Properties</b>
Passenger AADT on 2014	5824		<b>PG</b> 64-28
Commercial AADT on 2014	376		<b>AC</b> 5.1
Growth Factor	4		<b>Gb</b> 1.035
			<b>Gse</b> 2.684
			<b>Gsb</b> 2.651
			<b>Gmb</b> 2.375
			<b>vbe</b> 10.66
<b>WIM ID 148</b>			